Crosstalk of macrophages and endothelial cells in endothelial-to-mesenchymal transition and cardiac fibrosis

Doctoral Thesis

In partial fulfilment of the requirements for the degree

“Doctor of Philosophy (PhD)”

Division of Mathematics and Natural Sciences

In the Molecular Medicine Study Program

at the Georg-August University Göttingen

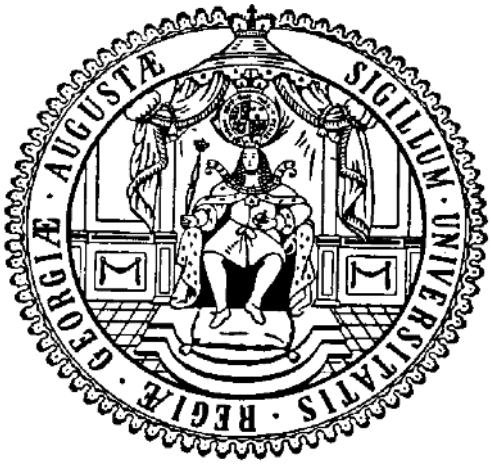

Submitted by

Elisa Sánchez Sendín

born in Salamanca, Spain

Göttingen 2017

Members of the Thesis Committee:

Prof. Dr. med. Elisabeth M Zeisberg (Supervisor)

Email: elisabeth.zeisberg@med.uni-goettingen.de

Phone: +49 551-39-20076

Postal Address: Institute of Cardiology and Pneumology
University Medical Center Goettingen
Georg-August University Göttingen
Robert-Koch-Str. 40
37075 Göttingen
Germany

Prof. Dr. rer. nat. Susanne Lutz (Second Supervisor)

Email: susanne.lutz@med.uni-goettingen.de

Phone: +49 551-39-10665

Postal Address: Institute of Cardiology and Pneumology
University Medical Center Goettingen
Georg-August University Göttingen
Robert-Koch-Str. 40
37075 Göttingen
Germany

Prof. Dr. Viacheslav O. Nikolaev (Third member of thesis committee)

Email: v.nikolaev@uke.de

Phone: +49 (0) 40 7410 51391

Postal Address: Institute of Experimental Cardiovascular Research
University Medical Centre Hamburg-Eppendorf
Martinistr. 52
20246, Hamburg
Germany

Date of Disputation: June 26th, 2017.

AFFIDAVIT

Here I declare that my doctoral thesis entitled:

"Crosstalk of macrophages and endothelial cells in endothelial-to-mesenchymal transition and cardiac fibrosis"

has been written independently with no other sources and aids than quoted.

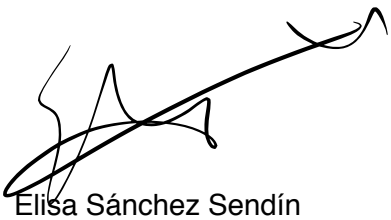

Elisa Sánchez Sendín

Göttingen, April 27, 2017

You have to finish things — that's what you learn from, you learn by finishing things.

Neil Gaiman

to Alex Johnston.

List of publications:

Xu X, Tan X, Tampe B, **Sanchez E**, Zeisberg M, Zeisberg EM. Snail Is a Direct Target of Hypoxia-inducible Factor 1α (HIF1α) in Hypoxia-induced Endothelial to Mesenchymal Transition of Human Coronary Endothelial Cells. The Journal of Biological Chemistry. 2015;290(27):16653-16664.

List of poster presentations:

Sanchez E, Otsu K, Zeisberg EM (2017). Macrophage-induced Endothelial-to-Mesenchymal Transition. IRTG 1816 Alumni meeting & On-site visit

Sanchez E, Rinkleff S, Zeisberg EM (2016).The role of macrophages in endothelial-to-mesenchymal transition and cardiac fibrosis. BHF annual symposium, London, UK.

Sanchez E, Rinkleff S, Zeisberg EM (2015). Role of Macrophages in cardiac EndMT. IRTG annual symposium, Wernigerode, Germany

Sanchez E, Rinkleff S, Zeisberg EM (2015). Resident peritoneal macrophages promote Endothelial-to-Mesenchymal Transition in Mouse Cardiac Endothelial Cells. BHF annual symposium, London, UK

Sanchez E, Xu X, Brewer AC, Ridley AJ, Zeisberg EM (2014). RASAL1 promoter methylation and Ras activity in cardiac fibrosis.IRTG summer symposium, Goettingen, Germany

Table of contents

Acknowledgements

I want to thank first and foremost my supervisor, Prof. Elisabeth Zeisberg, for the extraordinary opportunity of working and learning within her group, for her understanding, her support and patience.

I would like to express my gratitude to the core of the IRTG program, Prof. Dörthe Katschinski, Prof. Susanne Lutz and Dr. Christina Würtz, for being always there to help in every possible way.

I want to thank Dr. Erik Meskauskas, because without him it wouldn't have been possible to go through the PhD bureaucratic process.

I want to deeply thank all the Zeisberg lab members, Nephro and Cardio, that taught me so much through the PhD path. Specially, I want to thank Sarah and Gungee for their friendship through the roughest times, and Dr. Björn Tampe for the insightful scientific conversations and extremely practical help. Also, I thank Melanie Hulshoff for taking the time to go through this thesis.

Huge thanks to my parents, my brothers and my friends.

Summary

Abstract

Cardiac fibrosis (CF) is an integral component of virtually all forms of chronic cardiac disease. CF manifests as an accumulation of excessive extracellular matrix (ECM) components throughout the myocardium. Aberrant deposition of fibres through the interstitium and perivascular areas have structural and functional deleterious consequences for the heart: it stiffens the cardiac muscle and causes progressive adverse myocardial remodelling; a pathological hallmark of the failing heart irrespective of its etiologic origin. Cells in charge of ECM homeostasis are cardiac fibroblasts, which directly contribute to cardiac fibrosis due to their activation and transformation to cardiac myofibroblasts upon injury. Cardiac myofibroblasts are therefore key mediators that actively divide and produce excessive ECM. Cardiac fibroblasts are a heterogenous population, known to be derived from the epicardium and the endocardium in the developing heart. Endothelial-to-Mesenchymal Transition (EndMT) describes the process of endothelial cell transformation to a mesenchymal phenotype, a process that occurs during cardiac development in order to give rise to the mesenchymal cells that form the primordia of the valves. In the adult diseased heart, EndMT is activated and contributes to the total pool of fibroblasts that are responsible for fibrotic disease. Thus, diverse models of murine cardiac fibrosis such as Angiotensin II infusion, aortic banding and myocardial infarction (MI) develop fibrosis and exhibit newly activated fibroblasts with endothelial origin, as shown by several groups. Injury signals such as hypoxia, TGF-beta and inflammatory cytokines are known inducers of *in vitro* EndMT. Cellular sources of such signals are not well characterised.

Inflammation is another facet of disease that that consistently coexists with fibrosis. Every tissue injury triggers an inflammatory response by the innate immune system that aims to heal and re-establish homeostasis. Macrophages are myeloid cells present at the steady-state heart and are highly recruited upon pathological insult. Their specialised functions are critical for the healing heart: they phagocyte cardiomyocyte debris and modulate inflammation by secreting inflammatory cytokines; but also, they drive inflammation resolution by releasing anti-inflammatory cytokines and fibrotic factors. Macrophages are able to display a wide range of features and therefore can be subdivided in a spectrum of phenotypes. A simplification of this spectrum relies on two main groups, pro-inflammatory macrophages, able to amplify the inflammatory immune response and anti-inflammatory macrophages, able to mitigate the inflammatory reaction.

Due to their critical role in both cardiac inflammatory and reparative activities, we hypothesised that macrophages had a role in contributing to cardiac EndMT. Indeed, we identified an increase in macrophages in fibrotic regions of human myocardial infarction hearts, aortic stenosis and diabetic myocardiopathy. Increased macrophage populations were also identified in murine fibrotic models of aortic banding and AngII infusion. Moreover, it was found that macrophages were closely associated with endothelial cells undergoing EndMT in a murine model of atherosclerosis. We therefore established the tools to investigate a direct link between macrophages and EndMT. We generated distinct murine macrophage lines and characterised resident peritoneal macrophages, polarised bone marrow-derived macrophages and the polarised RAW264.7 macrophage cell line.

Three different *in vitro* cell culture systems were then established to analyse unidirectional paracrine signalling, bidirectional paracrine signalling, and juxtacrine signalling between endothelial cells and macrophages. As a control, EndMT was induced in mouse cardiac endothelial cells with TGF-Beta and inflammatory cytokines. These results demonstrated that indeed macrophages alone induce EndMT via a juxtacrine cell-cell contact manner but not under paracrine conditions. Interestingly, we found that pro-inflammatory TLR-stimulated bone marrow-derived macrophages showed enhanced induction of EndMT compared with anti-inflammatory bone marrow-derived macrophages. Moreover, pro-inflammatory TLR-stimulated RAW 264.7 cells, but neither native nor anti-inflammatory RAW 264.7 cells, induced EndMT. We additionally found that pro-inflammatory RAW 264.7 cells induced-EndMT and were associated with induction of the Notch signalling pathway; a juxtacrine signalling pathway known to induce EndMT during embryonic development.

Next the vice versa impact of EndMT on macrophage polarisation phenotype was investigated. We found that EndMT cells hindered the macrophage activation phenotype by down-regulation of pro-inflammatory markers TNF-alpha, MHCII and CCL2 in a paracrine related manner. EndMT also inhibited anti-inflammatory and pro-fibrotic macrophage markers.

In summary, this PhD thesis describes the crosstalk between macrophages and cardiac endothelial cells undergoing EndMT.

Zusammenfassung

Die kardiale Fibrose ist eine zentrale Komponente nahezu aller chronischer Herzerkrankungen. Diese manifestiert sich als eine Akkumulation von Extrazellulärmatrix im Myokard. Diese Deposition extrazellulärer Matrix im Interstitium und perivaskulären Arealen hat ungünstige Konsequenzen für das Herz: es versteift den Herzmuskel und verursacht ein progressives myokardiales Remodelling als wichtiges Phänomen des Herzversagens unabhängig von dessen Ursache. Extrazellulärmatrix wird hierbei insbesondere von kardialen Fibroblasten gebildet, welches direkt zur kardialen Fibrose durch deren Aktivierung und Transdifferenzierung zu Myofibroblasten beiträgt. Diese kardialen Myofibroblasten nehmen somit eine Schlüsselrolle bei Herzfibrose ein und sind durch vermehrte proliferative Aktivität charakterisiert. Kardiale Fibroblasten sind eine heterogene Population, welche in der Herzentwicklung vom Epikard und Endokard abstammen. Die sog. endothelial-mesenchymale Transition (EndMT) beschreibt hierbei einen Prozess der Transdifferenzierung von endothelialen Zellen hin zu Zellen mit mesenchymalem Phänotyp, ein Prozess der in der Herzentwicklung mesenchymale Zellen zur Anlage der Herzklappen generiert. Im adulten Herzen spielt EndMT bei Herzerkrankungen ein Rolle und trägt durch dessen Aktivierung zum Fibroblastenpool und Fibrose bei. Somit kann eine Aktivierung von EndMT in multiplen murinen Modellen der Herzfibrose wie Angiotensin II-Infusion, Aortenstenose und myokardialer Ischämie beobachtet werden und produziert neue aktivierte Myofibroblasten mit endothelialem Ursprung, wie von zahlreichen Arbeitsgruppen gezeigt werden konnte. Stimuli wie Hypoxie, TGF-beta und inflammatorische Zytokine, welche im kranken Herzen induziert werden, sind bekannte Mediatoren von EndMT *in vitro*. Dagegen sind die zellulären Ursachen solcher Stimuli nur wenig charakterisiert.

Eine weitere Komponente von Fibrose ist die assoziierte Inflammation. Jeder Organschaden vermittelt eine inflammatorische Antwort des Immunsystems, um Heilung zu vermitteln und

Homöostase wiederherzustellen. Makrophagen sind Zellen myeloischen Ursprungs, welche im Herzen präsent sind und bei pathologischen Insulten vermehrt rekrutiert werden. Deren spezialisierte Funktionen sind kritische Komponenten für Heilungsprozesse im Herzen: diese phagozytieren Zellschrott und modulieren die inflammatorische Antwort durch Sekretion von Zytokinen; Makrophagen können aber auch Inflammation durch anti-inflammatorische und fibrotische Wachstumsfaktoren auflösen. Aufgrund der zahlreichen Funktionen von Makrophagen lassen sich diese in Subtypen unterteilen. Eine einfache Unterteilung ist hierbei die Trennung in die beiden Hauptgruppen "M1" als pro-inflammatorische und "M2" als anti-inflammatorische Makrophagen.

Aufgrund derer kritischen Funktionen bei sowohl Inflammation und Reparaturprozessen vermuteten wir, dass Makrophagen eine Rolle auch bei EndMT im Herzen spielen könnten. Wir konnten zeigen, dass Makrophagen in fibrotischen Arealen humaner Herzen nach myokardialer Ischämie, bei Aortenstenose und diabetischer Kardiomyopathie akkumulieren. Dies konnte in den Mausmodellen der Aortenstenose und der Angiotensin II-Infusion bestätigt werden. Zudem konnten wir etablieren, dass Makrophagen mit EndMT Zellen räumlich assoziiert sind. Um einen direkten Zusammenhang zwischen Makrophagen und EndMT zu etablieren, generierten wir murine Makrophagenzelllinien, charakterisierten residente Peritonealmakrophagen und polarisierten Makrophagen aus dem Knochenmark bzw. die Makrophagen Zelllinie RAW264.7. Zudem etablierten wir 3 *in vitro* Zellkultursysteme, um unidirektionale bzw. bidirektionale parakrine sowie juxtakrine Effekte zwischen endothelialen Zellen und Makrophagen zu untersuchen. Als Kontrolle wurde EndMT in murinen kardialen Endothelzellen mit TGF-beta und inflammatorischen Zytokinen induziert. Wir konnten zeigen, dass Makrophagen tatsächlich EndMT in Endothelzellen durch juxtakrine Zellinteraktion vermitteln können, allerdings nicht unter parakrinen Konditionen. Interessanterweise konnten wir zudem etablieren, dass pro-inflammatorische Makrophagen aus dem Knochenmark verglichen mit nativen und anti-inflammatorischen Makrophagen aus dem Knochenmark nach TLR-Stimulation vermehrt EndMT induzieren. Dies konnte auch für pro-inflammatorische RAW264.7-Zellen gezeigt werden. Zudem war EndMT durch inflammatorische RAW264.7-Zellen mit einer Induktion der Notch-Signalkaskade, die auch in EndMT-Induktion in der Embryonalentwicklung involviert ist, assoziiert. Umgekehrt konnte gezeigt werden, dass EndMT-Zellen die Aktivierung von Makrophagen durch Repression der pro-inflammatorischen Marker TNF-alpha, MHCII und CCL2 in parakriner Weise hemmen. Zudem hemmte EndMT auch anti-inflammatorische und pro-fibrotische Marker in Makrophagen.

Zusammenfassend beschreibt diese PhD-Arbeit die Wechselwirkung zwischen Makrophagen und kardialen Endothelzellen, welche EndMT durchlaufen.

Abbreviations

α-SMA = alpha - smooth muscle actin

AAC = ascending aortic constriction

ADAM = a disintegrin and metalloproteinase

AS = aortic stenosis

Ang II = angiotensin II

ApoE = apolipoprotein E

AV = atrioventricular

BMP = bone morphogenic protein (family)

BSA = bovine serum albumin

CCL2 = chemokine ligand 2

CCR2 = C-C chemokine receptor type 2

CF = cardiac fibrosis

CM = conditioned medium

COL1A1 = collagen, type I, alpha 1

COL3A1 = collagen type III Alpha 1

COX-2 = inducible cyclooxygenase

D = diabetes

DAMPS = danger-associated molecular patterns

ECM = extracellular matrix

LDL = low-density lipoprotein

EMT = epithelial-to-mesenchymal transition

EndMT = endothelial-to-mesenchymal transition

eNOS = endothelial nitric oxide synthase

ET-1 = endothelin 1

Fap = Fibroblast activation protein

FGFs = fibroblast growth factors

FSP1 = fibroblast specific protein 1

GM-CSF = Granulocyte-macrophage colony-stimulating factor

HFD = high fat diet

HSCs = hematopoietic stem cells

IFN-γ = interferon gamma

IL-1ß = interleukin 1 beta

IL-4 = interleukin 4

IL-10 = interleukin 10

IP-10 = interferon gamma-induced protein 10

L = lumen

LAD = left anterior descending (coronary artery)

LDLR = low-density lipoprotein receptor

LLC = large latent complex

LPS = lipopolysaccharides

M-CSF = macrophage colony-stimulating factor

MCECs = mouse cardiac endothelial cells

MCFs = murine cardiac fibroblasts

MCP-1 = monocyte chemoattractant protein-1

MHC II = major histocompatibility complex II

MPS = mononuclear phagocyte system

MI = myocardial infarction

MIP-2 = macrophage inflammatory protein 2-alpha

MMP = matrix metalloproteinase

MTS = Masson's trichrome stain

NICD = notch intracellular domain

PAH = pulmonary arterial hypertensive

PAMPs = pathogen-associated molecular patterns

PBS = phosphate buffered saline

PDGF = platelet derived growth factor

PECAM1 = Platelet endothelial cell adhesion molecule 1

PH = pulmonary hypertension

PMs = peritoneal macrophages

SDS-PAGE = sodium dodecyl sulfate polyacrylamide gel electrophoresis

SOD = manganese-dependent superoxide dismutase

SMCs = smooth muscle cell

Stat3 = signal transducer and activator of transcription 3

TAC = transverse aortic constriction

TGF-ß = transforming growth factor - beta

TIE1= Tyrosine kinase with immunoglobulin-like and EGF-like domains 1

TIE2 = Tyrosine kinase with immunoglobulin-like and EGF-like domains 1

TIMP = Tissue inhibitor of metalloproteinase

TLR = toll-like receptor

TNF-α = tumor necrosis factor alpha

TNFR1 = tumor necrosis factor alpha receptor 1

TNFR2 = tumor necrosis factor alpha receptor 2

VECs = valve aortic endothelial cells

VEGF = vascular endothelial growth factor

VICs = valve aortic interstitial cells

VCAM-1 = vascular cell adhesion protein 1

YS = yolk sac

Introduction

1.Cardiac fibrosis

Fibrosis appears in the body as a chronic signature of major organ diseases that worsens with age (1-3). In the heart, cardiac fibrosis (CF) is an integral component of virtually all forms of chronic heart disease and it is characterised by an excess of extracellular matrix (ECM) deposition in the cardiac interstitium, generated by fibroblasts (4). ECM in the heart is the structural protein network between cardiomyocytes. It is composed of a majority of fibrillar collagen I, which confers tensile strength, and collagen III, which confers relative elasticity (4,5). Cardiac ECM fundamentally provides structural support, aligning cardiac myofibrils in a laminar structure that prevents them from detrimental sarcomere stretching. But as well, ECM is equally important in providing mechano-electrical conduction and serving as a homeostatic buffer, by its storage of latent growth factors (6,7,82). Increased accumulation of ECM causes stiffening of the heart muscle and impedes its normal physiological function of effectively pumping the blood to the body (3).

Cardiac fibrosis occurs in heart disease of various underlying causes such as local ischemia (induced e.g. by instability of atherosclerotic plaques), systemic disease (such as diabetes or chronic kidney disease) or as a result of chronic pressure overload (induced by aortic stenosis or arterial hypertension). While organs like skin, liver or intestine have a strong capacity to de-differentiate and transdifferentiate their tissues as means of regeneration when needed, cardiac potential for regeneration is negligible (8). For example, myocardial ischemia results in permanent damage at the infarcted site, which compromises the tissue's capacity for efficient contractile and electrical function. This is caused in part by the heart's inability to replace ischemic tissue with new cardiomyocytes. Instead, damaged tissue is "healed" with a network of newly formed vessels and mesenchymal progenitors. Cardiomyocytes depend on aerobic oxidative metabolism, thus requiring steady energy supply. Therefore when necrotic injury occurs, muscle cells are replaced with connective tissue, in an attempt to preserve structural integrity, resulting in adverse cardiac remodelling.

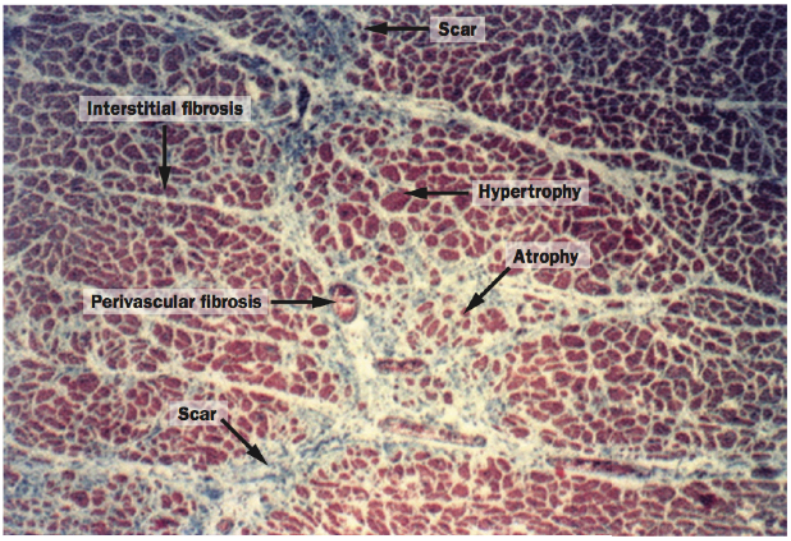

Figure 1.1. Adverse cardiac remodelling. Histology image shows fibrotic features of fibrotic adverse remodelling: hypertrophic or atrophic cardiomyocytes, perivascular fibrosis surrounding a vessel, scattered interstitial fibrosis surrounding cardiomyocytes, and accumulation of fibre forming scars. Adapted from Weber et al 2012 (6).

Extensive fibrotic remodelling is thus found in diseases with aggressive cardiomyocyte death. After acute ischemic damage, also known as myocardial infarction (MI), the obstruction of coronary arteries generally due to atherosclerotic instability leads to rapid cardiomyocyte death. Necrotic cells trigger an inflammatory reaction that activates reparative pathways that lead to debris removal and replacement with granulation tissue (an unorganised cellular structure formed by myeloid cells, fibroblasts, endothelial cells and ECM). Ultimately, a collagen-based scar is formed (Figure 1.1.). This fibrous replacement, termed replacement fibrosis, is adaptive at first although in the long term is detrimental, as the heart cannot work as efficiently as it did previously.

When CF does not involve macroscopic cardiomyocyte death, the fibrotic remodelling is gradual and insidious. Sublethal ischemic insults cause transient inflammation and disposal of ECM, predominantly scattered throughout the interstitium and around vessels, referred to as reactive interstitial fibrosis and perivascular fibrosis, respectively (Figure 1.1.). Pressure overload in the heart is generated in patients with conditions such as hypertension or aortic stenosis, and contributes to the development of extensive cardiac fibrosis, resulting in diastolic and systolic dysfunction. Volume overload due to valvular lesions also develops CF characterised with deposition of excessive non-collagenous ECM, formed by non-collagenous proteins such as laminins, tenascins, and fibronectin (3,9). Hypertrophic cardiomyopathy and post-viral dilated cardiomyopathy are also often associated with the development of significant cardiac fibrosis

(10,11). Furthermore, metabolic disturbances such as diabetes and obesity also manifest themselves in progressive fibrosis (12,13).

Regardless of the aetiology of fibrosis, cardiac fibroblasts are the central cellular effectors in the pathogenesis of CF. Cardiac fibroblasts are mesenchymal cells whose physiological function relies not only on the maintenance and ECM turnover and physical support of the muscle, but also on their contribution to homeostasis of the interstitial space and provision of an efficient communication between cardiomyocytes, as they may contribute to correct electromechanical coupling. They reside in the myocardial interstitium, epicardium and in the perivascular regions (14,15). While for years, fibroblasts were thought to be the largest non-myocyte contribution, this statement was revisited by Pinto *et al* in 2016, lowering this contribution to less than 20% of the total cardiac cell population. Instead endothelial cells are now believed to constitute the majority of non-cardiomyocyte cells in the heart and are likely to play a greater role in physiologic function and response to injury than previously anticipated (16).

Under stress stimuli, cardiac fibroblasts undergo a phenotypical and functional change and become activated myo-fibroblasts (15,17). Activated myofibroblasts are actively dividing, ECM-producing cells that express alpha-smooth muscle protein (α-SMA), contractile stress fibres and an extensive endoplasmic reticulum. In the injured heart, alterations in mechanical stress, interstitial environment and expression of cytokines and growth factors dramatically impact fibroblast phenotype. It has been hypothesised that a subset of activated myofibroblasts fail to return to a quiescent state or to undergo apoptosis, therefore causing excessive cell accumulation and ECM production.

Resident fibroblasts in the heart represent a heterogeneous population due to the different sources they arise from at the embryonic development. Fibroblasts located in the interstitium are reported to arise from the developmental epicardium. Epicardial cells forming the epithelial outer layer of the heart, undergo epithelial-to-mesenchymal transition (EMT), a process tightly regulated by the expression of factors like fibroblast growth factors (FGFs) and transforming growth factor-beta (TGF-ß) signalling. During EMT process, platelet derived growth factor (PDGF) and TGF-ß contribute to the acquirement of the cardiac fibroblast phenotype. Furthermore, approximately 20%

of the adult cardiac fibroblasts distributed at the interventricular septum and left-ventricular free wall are reported to have an endothelial origin, as indicated by several studies through a process called endothelial-to-mesenchymal transition (EndMT). Furthermore, cardiac fibroblasts may arise from circulating cells and bone marrow derived progenitors (18-20).

2. EndMT is a central hallmark of endothelial plasticity

Endothelial cells exhibit a vast degree of plasticity during development and adulthood. If we consider endothelial cells as a whole, the extent of their network becomes vast: the endothelium lines both blood and lymphatic vessels which provide nutrients and oxygen to virtually all parts of the mammalian organism (21). Therefore it is logical, and true, to think of the endothelium as highly heterogeneous as it is directly exposed to a broad spectrum of biochemical components carried by the bloodstream. Furthermore, it lines both capillary and central vessels as well as straight and branched segments, whose hemodynamics and shear stress generation vary greatly due to diameter, bloodstream speed and anatomical structures. Thus, throughout embryonic development endothelial cells are able to respond to diverse biochemical and haemodynamic stimuli and change their composition in response to the prerequisites of each location (22). Such extensive heterogeneity therefore requires significant plasticity. For example vessel regions that are exposed to different biomechanical forces exhibit different patterns of expression of genes pathophysiologically relevant in atherosclerosis (23). It is generally accepted, based on human swine and mouse models, that specific non-random focal sections of the endothelium are athero-prone or athero-susceptible. In fact they differentially express genes like V-CAM1, eNOS (the endothelial isoform of nitric oxide synthase), COX-2 (the inducible isoform of cyclooxygenase), and SOD (manganese-dependent superoxide dismutase). Furthermore, these areas also have different epigenetic marks, including site-specific differentially methylated regions of swine and mouse endothelial methylomes, histone marks regulating chromatin conformation, microRNAs and long noncoding RNAs (23,24).

Interestingly, failure of cardiomyocytes to successfully regenerate contrasts with remarkable cardiac endothelial plasticity. Cardiac endothelial regenerative capacity manifests after infarction in neonatal and adult hearts. This is thought to occur via a tyrosine-protein kinase kit (c-kit, also known as CD117) induction dependent process, as cell tracking studies show that endothelial cells generated post-infarction are c-kit positive. Thus, while c-kit is normally associated with cardiomyocyte precursors, a recent study has shown that although there is a strong induction of c-kit at the infarcted area after injury, this induction is “overwhelmingly” associated with neovasculogenesis rather than myogenesis (25,26). That is, whereas c-kit positive cells give rise to

cardiomyocytes and endothelial cells in neonatal hearts, c-kit progenitors only give rise to endothelial cells in adulthood after injury. Somehow, adult cardiomyocytes seem to loose their plasticity during adulthood whereas endothelial cells maintain it.

A central hallmark of endothelial plasticity that manifests during development and adulthood is EndMT (27-31). EndMT is a special type of cell fate conversion that involves the transformation of differentiated endothelial cells into mesenchymal cells. There is an evident disparity, almost direct opposition, between these two cell types (Figure 1.2); while endothelial cells form a monolayer, display apical-basal polarity, exhibit gap junctions and stay immobile; mesenchymal cells are loosely associated, have front-rear polarity, are less interconnected and exhibit migratory and invasive properties. During EndMT endothelial cells delaminate from the monolayer, lose cell-cell junction proteins such as CD31 (also known as PECAM1), VE-Cadherin, markers like TIE1 and Von Willebrand factor proteins, and gain mesenchymal markers such as fibroblast specific protein 1 (FSP1, also known as S100A4), alpha-smooth muscle actin (α-SMA) and collagen proteins (COL1A1, COL3A1) (28,29). This transition may be reversible via a mechanism known as mesenchymal-endothelial transition, which is important in the context of cardiac neovascularization (30).

Canonical transcription factors that drive EndMT are zinc-finger containing proteins Snail and Slug, encoded by Snai1 and Snai2 genes (32-34). Snail is activated upon inducers such as TGF-ß, Notch and hypoxia signalling, and binds to conserved E-box elements at the promoter regions of VE-cadherin, directly transcriptionally repressing endothelial cell adhesion transcription (36). Snail alone is able to induce epithelial to-mesenchymal transition (EMT) (37), therefore is thought to have several molecular targets. Snail induces vimentin, known to be involved in stimulation of stress fibre expression and inducing changes in the cytoskeleton to facilitate mobility and cell migration (37). Furthermore, Snail is upstream of mesenchymal molecules such as matrix metalloproteinase 2 (MMP-2) (38) and fibronectin (39). One interesting feature in Snail biological function is its potential to protect cells from death and provide resistance to DNA damage, according to studies in epithelial cells (40,41). This is consistent with the fact that endothelial cells show apoptotic resistance as they undergo EndMT when they encounter apoptotic signals such as TGF-ß and hypoxia. Slug is also up-regulated in developmental EndMT and known to be a direct target of TGF-ß 2. Twist is another recurrent inducer of EndMT. The expression of Twist, a basic helix-loop-helix transcription factor, is as well linked to cancer-EMT and endocardial EndMT (42). It is reported to be regulated by BMP2 (42), a member of the TGFβ family that has been implicated

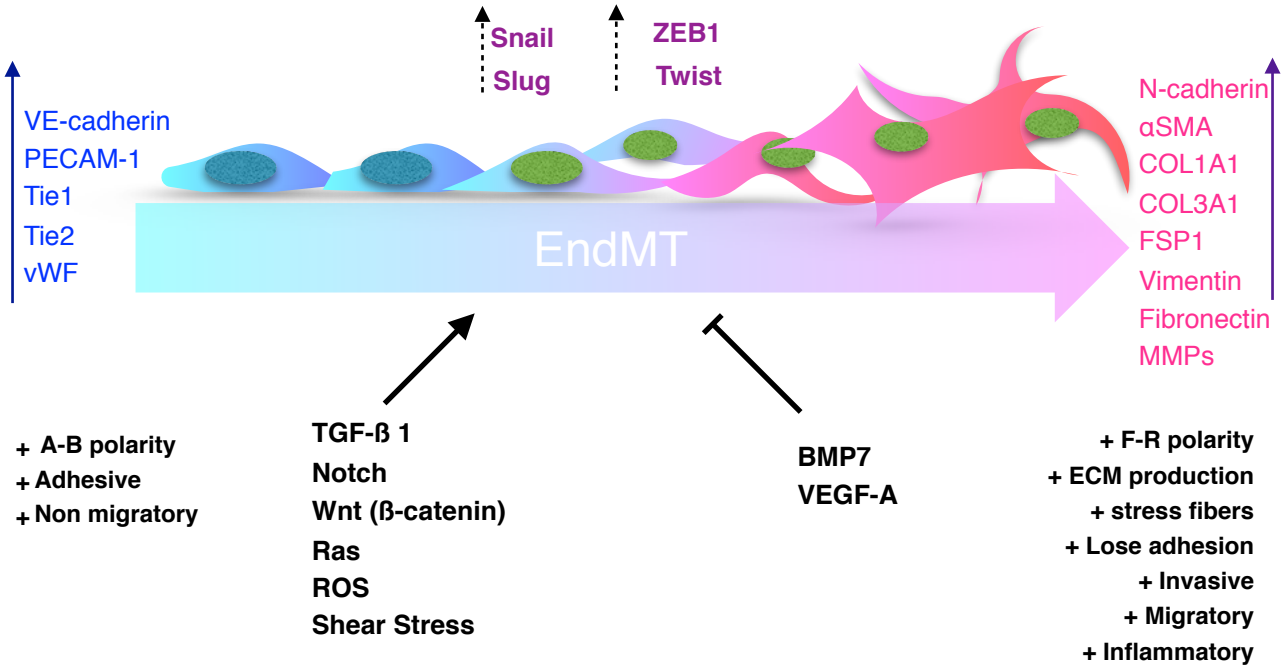

Figure 1.2. Endothelial-to-mesenchymal transition (EndMT). Endothelial cells form a monolayer, exhibit apical-basal polarity (A-B polarity) and express cell-cell adhesion proteins such as vascular endothelial cadherin (VE-cadherin), platelet endothelial cell adhesion molecule 1 (PECAM 1) and typical proteins Tie1, Tie2 and Von Willebrand factor (vWF). EndMT is induced by diverse external and internal stimuli, including transforming growth factor beta (TGF-ß) proteins, Notch signalling ligands, canonical Wnt pathway ligands, ras hyperactivity, reactive oxygen species (ROS) generated by hypoxic conditions, shear stress, high glucose levels, and others. EndMT is modulated by the transient expression of EndMT transcriptional factors such as Snail, Slug, Twist, and ZEB1, which are involved in repressing endothelial proteins and activating the expression of mesenchymal-related genes. Mesenchymal-like cells derived from EndMT acquire migratory and invasive capacities, exhibit front-rear polarity (F-R polarity), are loosely associated and express mesenchymal typical proteins such as alpha-smooth muscle actin (αSMA), Collagens I and III (COL1A1 and COL3A1), Vimentin, Fibronectin, fibroblast specific protein 1 (FSP1) and extracellular matrix (ECM) regulatory proteins such as matrix metalloproteinases (MMPs). The process may be inhibited via bone morphogenic protein 7 (BMP 7) and vascular endothelial growth factor A (VEGF-A) (27-43).

in cardiac cushion EndMT. Twist is also induced by hypoxia in cancer and by TGF-ß-induced EndMT (43, 44, 103). Thus Snail and similar EMT-inducing transcription factors coordinate reprogramming of endothelial cells towards a mesenchymal phenotype.

3. Developmental EndMT

EndMT has been first and best described in embryonic development during heart formation (45,18,46). During cardiac valve and septa formation a subset of endothelial cells of the primitive endocardium expressing Tie-1, Tie-2, VEGFRI/II and CD31 undergo EndMT to give rise to primordial septa and valves in a spatiotemporally restricted manner. In murine heart this process has been accurately described (18). At embryonic day 8.5 the mouse heart is a tube composed by three layers: i) the inner endocardium, ii) the cardiac jelly, formed by ECM secreted primarily by the

outer layer, iii) the primitive myocardium. At day 9.5, signals from the myocardium activate a subset of endocardial cells from regions of the outflow tract and atrioventricular (AV) canal undergoing EndMT. These selected EndMT-cells acquire a migratory phenotype and invade the cardiac jelly, forming the endocardial cushions. This then contributes to cardiac valve formation and heart septation.

Functional studies in mouse and chicken prove that TGF-ß signalling factors TGF-β 2 and TGF-β 3 are essential for endocardial cushion formation (47). Moreover, Ras signalling plays as well a critical role in cushion formation as indicated by studies in NF1 deficient embryos, a model where Ras activity is activated as a consequence of the loss of Ras activator NF1 (48).

Developmental EndMT also contributes to the thickening of vessels as shown in studies in chick swine and cow in which endothelial cells undergo EndMT and acquire a smooth muscle cell (SMCs)-like phenotype accumulating at the intima (the outer layer of the vessel in direct contact with the endothelium) (49,50). Similar processes of intimal thickening have been found in pulmonary development (51). As such, the contribution of EndMT as a source of mural cells during development makes it particularly important in angiogenesis and arteriogenesis processes as EndMT may provide the necessary support to trigger the advancement of vessel formation. Moreover it has been reported that EndMT-derived pericytes and SMCs exhibit proliferative capacity (49), and therefore angiogenic potential. Interestingly tip cells, during angiogenic sprouting are endothelial cells lacking in lumen with the capacity for migration (54), a phenotype consistent with an EndMT phenotype. It has been speculated that endothelial tip cells may acquire an EndMT phenotype and thereafter remain with a mesenchymal phenotype indefinitely (52,53).

4. EndMT in disease

It is commonly accepted that re-activation of developmental processes in adulthood often has pathological consequences (55). EndMT is no exception to this phenomenon. Indeed, EndMT is a recurrent mechanism after tissue injury, although its pathological contributions differs between studies. The first reports of EndMT in adulthood only appeared in the last decade and the majority of such studies categorise EndMT as a deleterious mechanism, thus portraying the link between EndMT and pathologies involving different organs.

4.1. EndMT in cardiac fibrosis

Cardiac fibrosis was the first pathology where EndMT was described in the adult organism in a study by EM Zeisberg and colleagues a decade ago (56). Using lineage tracing studies they showed for the first time that a significant percentage of fibrotic cells in a mouse model of cardiac fibrosis had an endothelial origin. In the *in vivo* study, using a Cre-loxP recombinase system under Tie-1 promoter, cells with endothelial origin expressed LacZ regardless of subsequent phenotypic conversions. Furthermore FSP1-GFP reporter mice could show cells double expressing CD-31 and FSP-1, indicating cells in an intermediate EndMT state (expressing of both mesenchymal protein FSP1 and endothelial CD31 protein). Importantly, evidence of EndMT was reported only in fibrotic mice and not in sham control models. Similarly, experiments using murine models of MI in which mice undergo ligation of the left ascending coronary artery (LAD) and subsequent ischemia, together with cell lineage tracing studies have reported evidence of EndMT in scars produced after experimental MI. They linked EndMT-derived α-SMA positive cells to canonical Wnt signalling activation (57).

Recently the role of EndMT in diabetes mellitus-induced cardiac fibrosis was also investigated. High levels of plasma endothelin-1 (ET-1) in diabetic patients were linked to cardiac fibrosis and EndMT (58). Widyantoro and colleagues found that in diabetes mellitus cardiac ET-1 expression is up-regulated *in vivo* and the diabetic phenotype is ameliorated in a vascular endothelial cell-specific ET-1 knockout mice, highlighting the importance of an endothelial-related regulatory process. In the study, fibrotic areas exhibited endothelial cells co-expressing CD31 and FSP1 markers, indicating EndMT. Moreover, high glucose alone has been identified as an inducer of EndMT in human cardiac endothelial cells, an effect that has been replicated *in vivo* and ameliorated by using a glucagon analog drug, thus reducing EndMT and cardiac fibrosis (59, 60).

Endocardial fibroelastosis (EFE) is a severe cardiac fibrotic condition in which the ventricular endocardium undergoes a fibro-elastic thickening causing left ventricular hypoplasia and obstruction of left ventricular outflow. In a study by Xu et al, human patient samples from EFE tissue were analysed and it was found that every patient sample contained endothelial cells co-expressing alpha-SMA and FSP-1 mesenchymal markers, indicative of EndMT (44). Further analysis of patient tissue vs control showed that EFE samples exhibited bone morphogenic protein-7 (BMP-7) signalling differentially and epigenetically suppressed. BMP signalling is

antagonistic to TGF-ß signalling which is a known inducer of EndMT and will be subsequently addressed in this thesis.

4.2. EndMT in fibrotic pathologies

EndMT has been meanwhile also directly implicated in the pathophysiology of fibrogenesis of numerous other organs such as the kidney, the lung and the gut (61-70).

In pulmonary fibrosis the occurrence of EndMT is well established; EndMT orchestrates bleomycin- and radiation-induced pulmonary fibrosis (63,64). Recently several studies have also demonstrated the involvement of EndMT in pulmonary hypertension (PH). In a model of PH, endothelial lineage studies revealed endothelial cells at neointima expressing smooth muscle phenotype-like markers. This has also been detected in human pulmonary arterial hypertensive (PAH) neointimal lesions (65), and in patients of sclerosis-associated pulmonary artery hypertension (66). In a parallel study Ranchoux et al identified EndMT in PAH patients and then using transmission electron microscopy, correlative light and electron microscopy the study provided unequivocal ultrastructural-level evidence of ongoing dynamic EndMT in pulmonary hypertension samples (67). Furthermore EndMT also plays a role in non small cell lung cancer (68).

The substantial contribution of EndMT to the pathophysiology of renal fibrosis has also been largely demonstrated. Together with its closely related mechanism epithelial-to-mesenchymal transition (EMT), EndMT contributes significantly to the accumulation of fibroblasts. This has been shown by EM Zeisberg and colleagues in murine fibrotic models of different sources, including unilateral ureteral obstruction (UOO), a model that depicts progressive tubulointerstitial fibrosis, streptozotocin-induced diabetic nephropathy, and α3 chain of collagen type 4 knockout mice (a model for Alport syndrome, with an acute fibrotic phenotype). Their findings show co-localisation of CD31 and α-SMA of stromal cells in all models (62). These studies have been further corroborated in early development of interstitial kidney fibrosis in STZ-induced diabetic nephropathy by Li and colleagues, in which lineage tracing analysis using Tie2-cre recombinase was used to find a significant number of fibroblasts of endothelial origin (69).

EndMT has been also detected in models of fibrotic bowel pathologies such as inflammatory bowel disease and colonic fibrosis (70) using Tie2–green fluorescent protein (GFP) reporter–expressing

mice. Furthermore, induction of EndMT has an important role as a source of cancer associated fibroblasts (CAFs) in solid tumor progression and pancreatic cancer (53).

4.3. EndMT in atherosclerosis

EndMT has only recently been linked with atherosclerosis (71,72). Atherosclerosis is a vascular immuno-inflammatory disease that appears in focal localised regions of large and medium-sized arteries in which disturbed laminar flow, such as at branch sites and bifurcations, is present. Proximal parts to the heart at the aortic root are also greatly affected. Atherosclerosis is the leading cause of death in Western countries, a statement which is shortly anticipated to be globally applicable (73). The pathophysiology of atherogenesis involves decades-long expansion of the arterial intima due to the accumulation of lipids, cells, and ECM. Whereas atherosclerosis alone is not per se fatal and generally the process does not lead to major symptoms when the lumen of the artery is preserved, in a few cases focal lesions of the intima lead to necrotic development (atherosclerotic plaques). These complications may lead to acute, occlusive thrombosis in coronary arteries, leading to the fatal consequences of myocardial infarction, unstable angina and sudden cardiac death or to stroke when cerebral arteries are affected (74). Endothelial cells at athero-prone sites suffer severe damage and develop a dysfunctional phenotype characterised by altered nitric oxide metabolism and vascular reactivity, increased lipoprotein permeability and oxidation, increased monocyte adhesion, altered ECM metabolism and dysregulation of hemostatic-thrombotic balance (23). Often, these areas even become de-endothelialized (denuded) on advanced lesions, raising the question of whether these endothelial cells have died or transitioned to a mesenchymal fate.

In vitro and *in vivo* studies in porcine and human tissues have shown that laminar flow inhibits EndMT whilst disturbed flow activates EndMT in valvular aortic endothelial cells, contributing to fibroproliferative vascular damage. More importantly, EndMT has been identified in atherosclerotic lesions (71,72). Using Tie1- and Tie2- cre recombinase mice to trace mesenchymal cells of endothelial origin, positive cells have been identified directly at the intima and adventitia of atherosclerotic plaques. It has been speculated that EndMT is induced by TGFß-1 expression and high oxidative stress conditions. Moreover, EndMT has been associated with unstable human plaques, by co-localisation of CD31 and mesenchymal markers Fap (Fibroblast activation protein)

and FSP1.It has been hypothesised that the reason EndMT leads to plaque instability is because EndMT derived-fibroblasts have deleterious MMP activity; that is they aberrantly produce more extracellular MMPs and TIMPs, which decreases the quality of the fibrous cap and damage ECM homeostasis (72).

5. EndMT inducing signals

EndMT program can be activated by several diverse but connected external and intrinsic signals. EndMT's regulation is controlled by tight regulatory mechanisms. A tight regulation is critical to maintain the integrity of the endothelium and avoid aberrant fibrotic processes. As such, signalling pathways involved in regulating EndMT are, not surprisingly, well established pathways already known for their essential role in controlling other critical cellular fate decisions such as division, migration, senescence or apoptosis. Subsequently, we are providing an overview of the best-studied signalling pathways and microenvironmental factors known to induce EndMT. We are aware, however, that it is far from complete, as the regulation of EndMT is an active field of research and mechanistic insight into EndMT is growing rapidly.

5.1. TGF-β signalling

TGF-ß is a multifunctional growth factor that belongs to the large TGF-ß superfamily of pleiotropic growth factors. TGF-ßs are involved in critical cellular processes such as growth, cell division, apoptosis, senescence and migration (75-77). The members of the TGF-β superfamily include two major branches, bone morphogenetic proteins (BMPs) and TGF-β/activin A subfamilies. All TGF-β family members are homodimeric proteins that interact with transmembrane TGF-β receptors.

In the adult organism TGF-ß is released to extracellular space by a variety of cell types, including fibroblasts, macrophages and cells from the parenchyma, contributing to tissue homeostasis and tissue repair. TGF-ß can be found in 3 isoforms, TGF-beta 1, TGF-beta 2 and TGF-beta 3, which share high similarity and homology but are coded by three separated genes (78). The three isoforms are multifunctional and can act in autocrine, paracrine and endocrine manner (80) and are believed to have overlapping and distinct effects, depending on the cell context. For example, while having growth inhibitory effects in a subset of epithelial cells and myeloid cells, they cause

proliferation of fibroblasts (76,79). TGF-ß is synthesised as a precursor protein that is proteolytically processed. TGF-ß is released to the extracellular space as an inactive latent complex, the LLC (large latent complex), that after a series of proteolytic steps regulated by proteins from the ECM, and processed by BMP1 and some MMPs in a tightly regulated process, is converted into the mature TGF-ß form. Mature TGF-ß acts as an extracellular ligand that binds to a complex of receptors at the cell membrane (81,82).

The TGF-β signals are transmitted through specific transmembrane type I and type II serine/ threonine kinase receptors (83,84). In endothelial cells, TGF-β binds two distinct type I receptors, ALK1 and ALK5, to activate ALK1/Smad1/5/8 and ALK5/Smad2/3 signaling pathways. ALK1 induces Smad1/5 phosphorylation, leading to increased endothelial cell proliferation and migration and cytoskeleton reorganisation, while ALK5 promotes Smad2/3 activation and promotes quiescence and permeability (86). These two pathways regulate different genes and exhibit antagonistic biological functions in endothelial cells. Interestingly, endothelial ALK5 activity is necessary for ALK1 signalling (87). Nevertheless, it seems that the effect of ALK1 is also dependent on cellular context (85).

TGF-ß regulates endothelial cell plasticity and is one of the greatest inducers of developmental EndMT (89). Studies from knockout mice have shown that signals activating EndMT in the heart development include multiple TGF-ß isoforms and downstream signalling proteins and receptors. TGF-ß co-receptor Endoglin, is required for successful formation of the endocardial cushions. *In vitro* and *in vivo* studies have shown that TGF-β efficiently induces EndMT in different types of endothelial cells, including human, swine and mouse. The molecular mechanism behind TGF-β induced EndMT involves Snail signalling activation. In mouse embryonic stem cell-derived endothelial cells TGF-β 2 induces EndMT and expression of Snail. Importantly, activation of Snail is essential for TGF-β to induce EndMT. Finally, TGF-β -induced EndMT has been achieved via Smad-dependent and independent ways (90-92).

5.2. Notch signalling pathway

Various studies have identified a critical role for Notch signalling in EndMT (93,112). The evolutionarily conserved Notch regulates cell fate specification through local cell interactions in

both vertebrates and invertebrates. Notch signalling is known to regulate multiple cellular processes and is essential to endothelial development. In adulthood, Notch regulates stem cell maintenance and tissue homeostasis (94). Notch multiple homolog genes are expressed at many sites in the developing organism and code for transmembrane receptors whose typical structure contains an extracellular segment comprised of a variable number of epidermal growth factors (EGF)-like repeats, a transmembrane fragment and an internal cytosolic region termed the NICD (notch-intracellular domain) that contains nuclear localisation signals. Notch receptors interact specifically with canonical membrane-bound DSL ligands Delta, Serrate and Lag2, found in Drosophila. The mammalian DSL ligands counterparts account for Delta-like (Dll1, Dll3 and Dll4) and Serrate-like (Jagged1 and Jagged2) ligands. Notch ligands are type 1 cell-surface proteins that, similarly to Notch, contain EGF repeats at the extracellular domain together with the so-called DSL domain, which is thought to be required for Notch binding. Jagged ligands have a longer structure than Delta-like ligands, and contain almost double the number of EGF-repeats and other sequences of so far unknown function. The intracellular region of DSL ligands have 2 distinct domains that serve for ligand intracellular signalling and interactions with the cytoskeleton (95).

To activate Notch signalling, an interaction of DSL ligand of one cell (the signal-sending cell) and the extracellular part of Notch receptor of an adjacent cell (signal receiving-cell) is needed. Ligand binding triggers additional proteolytic cleavages of Notch, first by a disintegrin and metalloprotease (ADAM) within the juxtamembrane region followed by γ-secretase within the transmembrane domain resulting in the release of the Notch intracellular domain (NICD) from the membrane. NICD translocates to the nucleus where it directly interacts with the CSL (CBF1, Su(H), LAG1) transcription factor and recruits co-activators including Mastermind to turn on expression of Notch target genes such as hairy and enhancer of split related proteins (Hes and Hey) (95-99).

Notch is directly involved in inducing endothelial EndMT in the context of murine fibrosis (112). NICD overexpression in zebrafish embryos leads to hyper cellular cardiac valves, whereas inhibition of Notch signalling leads to detrimental valve development (100). Notch induces EndMT by directly targeting transcriptional factors Snail and Slug (101,102). Accordingly, activation of Notch in the context of TGF-β stimulation results in synergistic up-regulation of Snail in endothelial cells. Furthermore, Jagged1 ligand can also induce EndMT (103). Unpublished experiments made

in our lab showed that EndMT was induced in human cardiac endothelial cells by application of exogenous Jagged1 recombinant protein ligand (data not shown).

5.3. Canonical Wnt signalling

Canonical Wnt signalling is an autocrine and paracrine transduction signalling pathway that, similarly to Notch, activates gene transcription by extracellular receptor activation. Briefly, Wnt canonical pathway activates downstream gene expression by nuclear accumulation of protein ß-catenin, which otherwise localises at the inner site of plasma membrane and is rapidly degraded by a degradation complex formed by AXIN2 and others. Soluble Wnt ligands bind to Frizzled receptors, activating the pathway by halting ß-catenin degradation and consequent accumulation at the nucleus, which leads to activation of targeted genes (104,105). In the context of diabetic kidney disease, blockage of canonical Wnt signalling reduces EndMT and fibrosis (106). Moreover, in MI murine samples, mesenchymal cells of endothelial origin show activation of Wnt by accumulation of nuclear ß-catenin (57). Furthermore, *in vitro* pharmacological accumulation of ß-catenin induced mesenchymal phenotype in bovine aortic endothelial cells (57,107).

5.4. Ras

Ras GTPase activity is known to regulate a myriad of biological processes, widely acknowledged for its critical role in malignant transformation and cancer. Ras activation's ultimate cellular effects depend essentially of the cell context (109). In kidney fibroblasts, TGF-ß induces fibroblast to myoblast transformation in a Ras-related mechanism (101). In pulmonary fibrosis, Hashimoto and colleagues demonstrated that Ras and TGF-beta cooperation is necessary in order to induce *in vitro*-EndMT (63). Furthermore, loss of Ras activity inhibitor RASAL1 is known to be significantly down-regulated by epigenetic silencing in EndMT cells in a model of murine cardiac fibrosis and *in in vitro* experimental EndMT in human endothelial cells (111).

5.5. Hypoxia

EndMT is induced under hypoxic conditions *in vivo* and *in vitro* (113,115,116). Developmental angiogenesis is known to be triggered by hypoxia, as hypoxia inducible factor 1-alpha (HIF-1alpha) induces VEGF which promotes endothelial tip formation and sprouting angiogenesis. *In vitro*, EndMT is induced when exposing human cardiac endothelial cells (HCAEC) to hypoxia conditions

(1% oxygen) during 4 days, as cells show a decrease in CD31 expression, VE-cadherin and increase of a-SMA, COL1A1, and EndMT transcription factors Snail, Slug and Twist. HIF1-alpha is a direct target of Snail, by binding to Snail promoter region and inducing Snail expression (22,36).

5.6. Inflammation

Inflammatory mechanisms are activated in every context of cardiac fibrosis (114). After MI, cell death triggers an acute inflammatory reaction to initiate the reparatory fibrotic process, inducing infiltration of leukocytes and myeloid cells to the infarcted myocardium, followed by activation of inhibitory mediators such as TGF-ß, whose function in that context is to promote inflammatory cell death whilst promoting fibrosis (4,79). Inflammatory cytokines TNF-α, IL1-ß, and IL-6 are first released post-MI. Models of progressive cardiac fibrosis caused by hypertension or aortic stenosis exhibit significant induction of inflammatory cytokines TNF-α and IL1-ß, inflammatory CXC chemokines MIP-2 and IP-10, and CC chemokine MCP-1 in pressure overload murine models (113,79) .

In vitro studies with exogenous application of inflammatory cytokines IL-6 and TNF-α have shown successful induction of EndMT in porcine aortic valve endothelial cells and cytokines IL-1ß and TNF-α in embryonic and adult human valvular endothelial cells (117,120). Another study found that TGF-ß 2 and IL1-ß had an additive effect in EndMT induction in HUVECs, in a manner dependent of NFκB signalling (118). Additionally, complement cascade antagonists have been shown to reduce EndMT (119). However, detailed mechanisms of how inflammatory signals regulate EndMT *in vivo* are still only incompletely understood.

6. Macrophages

Macrophages are known for their integral role in innate immunity as first line defenders against pathogens and tissue damage. However, macrophage functionality goes far beyond defence, and macrophages are nowadays increasingly considered as essential regulators of vertebrate biology, therefore representing a powerful target for an expansive list of pathologies (121-124).

For decades, it was believed that adult tissue-resident macrophages were continuously replenished by blood-circulating monocytes, in a concept described by Van Furth and colleagues in the 1970s known as the “mononuclear phagocyte system” (MPS). The foundational concept stated that macrophages terminally differentiate within their fate tissue without capacity to proliferate,

therefore requiring continuous replacement from blood derived monocytes (125). However, the knowledge of macrophage ontogeny has dramatically changed and concepts are currently being rewritten. Nowadays it is known that the MPS paradigm is true for only a number of murine tissues under homeostasis, such as gut, dermis, pancreas and peritoneum, whereas resident macrophages in other tissues like the brain and heart have an embryonic origin and are able to proliferate (126-129).

During development, macrophages are derived from two sources. In mice, yolk sac (YS) derived-macrophages appear from day 8 (E8.5), and a second wave of macrophages is produced via definite hematopoiesis in the liver, in a process where hematopoietic stem cells (HSCs) appear within the hematogenic endothelium at E10.5 and migrate to the fetal liver where they expand and differentiate starting from E12.5., where the liver becomes the main hematopoietic organ and generates all hematopoietic lineages, including monocytes (130,131).

Nevertheless, the MPS system still applies to inflammatory conditions. Massive recruitment of monocytes to tissues occurs upon tissue injury or infection, a process that takes place simultaneously with the proliferation of resident macrophages. Once inflammation has been contained, resident macrophages may rebuild the total macrophage pool by local proliferation or newly recruited cells may take up residence by acquiring self-renewal capabilities and tissue-resident effector functions. These processes may depend on the nature of the insult and the tissue and organ where inflammation takes place (132,133).

7. Macrophages in inflammation

Macrophages are myeloid cells of the innate immune system that are primarily considered as “homeostasis keepers” due to their ability to sense any perturbation and to respond with a broad range of activities (from tissue-dependent tasks to general immune effector functions) (123,124). In fact, inflammation caused by either pathogens or injury may be considered as an extreme disruption of homeostasis, that calls macrophages into action to restore tissue integrity and functionality.

Macrophages continuously survey their surroundings to detect anomalies, such as foreign invaders or tissue damage, and respond accordingly by initiating inflammation and by eliminating the threat

by phagocytosis and production of enzymes, anti-microbial peptides and reactive oxygen species. In addition, as major cytokine and chemokine producers, macrophages orchestrate inflammation and regulate the recruitment of other leukocyte populations. Moreover, macrophages participate in the adaptive immune response by presenting antigen via major histocompatibility complexes (MHCI and MHCII) to T and B lymphocytes, and by clearing pathogenic agents in the humoral response of B lymphocytes. Furthermore, macrophages are essential regulators of resolution of inflammation and are involved in wound healing processes by secreting anti-inflammatory mediators, remodelling of extracellular matrix and promoting angiogenesis. In line with their critical role in tissue homeostasis, deregulation of the macrophage effector functions results in numerous pathologies (133-140).

8. Macrophage activation

Another aspect of macrophage functional specialisation manifests when a macrophage encounters endogenous or exogenous pathogenic insults. Over the last several years in macrophage literature, the terms polarisation and activation have been, often mistakenly, widely interchangeable. A macrophage is activated when a stimulus, a perturbation of the steady state, such as a cytokine or toll-like receptor (TLR) agonist produces a response, which generates distinct patterns of gene and protein expression in the macrophage. Thus, the specific features of the macrophage reaction towards the stimulus is critically dependent on the surrounding environment at the moment of the insult and on previous instructions received during the macrophage's lifetime. Therefore, macrophage activation relies on the integration of signals derived from their ontogeny, differentiating factors, cytokines, metabolites and ligands for pathogen-/danger-associated molecular patterns (PAMPs/DAMPs). As a consequence, macrophages can acquire an almost infinite number of polarisation states, which has led to the hypothesis of the "spectrum model" of macrophage activation (135) (Table 1.1). In this context, macrophages are classified according to the factors which they have been primed with (polarisation) and to the type of response they carry out upon a pathogenic challenge (activation) (141). For example, macrophages primed with cytokine IL-4 may be classified as M-(IL-4), and so on. For the sake of simplicity, this classification has been classically divided in two main groups according to the macrophage's response to the pathogenic insult. Thus, macrophages can either be pro-inflammatory (also found in literature as "M1" or "M1-like" macrophages) or anti-

Activator	M(IL-4)	M(IL-10)	M(-)	M(LPS)	M(IFNγ+LPS)	M(IFNγ)
Transcription factors, SOCS proteins	pStat6+++ pStat1-ve *Ifr4, Socr2*	pStat3+ Nfil3 Sbno2,Socs3	Baseline gene expression dependent of culture variables	pStat1+ pStat6 -ve	pStat1+ pStat6 -ve *Socs1,Nfkbiz,Irf 5*	pStat1+++ *Socs1*
Cytokines	*Il10*	*Il10*		*Tnf,Il6,Il27*	*Tnf,Il6,Il27 il23a, il12a*	
Chemokines	*Ccl17,Ccl24, Ccl22*	*Cxcl13,Ccl1,Ccl20*				
Scavenger receptors					Marco	Marco
Aminoacid metabolism	*Arg1+++*	*Nos2*		*Arg1 +*	*Arg1 +*	*Nos2*
Others	*Rentla,Chi3l3*	*il4ra*				

Table 1.1. Marker systems for activated macrophages. This schematic shows functional subdivisions according to stimulation of mouse CSF-1 macrophages with the existing M1-M2 spectrum concept (Martinez and Gordon, 2014; Mosser and Edwards, 2008; Stout and Suttles, 2004). Stimulation conditions are IL-4, LPS, LPS and IFN-g, and IFN-g alone. Marker data were drawn from a wide range of published and unpublished data from the authors' laboratories and represent a starting consensus (Edwards et al., 2006; Fleetwood et al., 2009; Gratchev et al., 2008; Gundra et al., 2014; Krausgruber et al., 2011; Lang et al., 2002; Shirey et al., 2008; Shirey et al., 2014; Shirey et al., 2010; Xue et al., 2014). Adapted from reference 141

inflammatory ("M2" or "M2-like"). M1-like, pro-inflammatory macrophages secrete TNF-α, IL-12, IL-6 and IL-23 upon activation with PAMPs and DAMPs and exhibit high antigen-presenting capabilities, whereas anti-inflammatory, "M2-like" macrophages produce IL-10 and are highly phagocytic and pro-fibrotic. Macrophages can be further classified according to the differentiating and/or activating cytokines and factors. Therefore macrophages exposed to IFNγ or GM-CSF become pro-inflammatory, whereas macrophages treated with IL-10, IL-4, IL-13, glucocorticoids or M-CSF preferentially display anti-inflammatory functions. Needless to say, these *in vitro* derived macrophage populations are a simplification that reflect only discrete aspects of *in vivo* macrophages (142). Nevertheless, *in vitro*-polarised macrophages have proven very useful in the study of macrophage biology since many of their specific responses and behaviours have been confirmed *in vivo* (143).

9. Cardiac Macrophages

Macrophages are present in the healthy heart and are the main population after myocytes, fibroblasts and endothelial cells. The concept that cardiac macrophages are continuously replenished by haematopoietic stem cells has remained elusive for long, and was recently examined by several studies that characterised cardiac macrophage ontogeny in homeostasis and stress (144-146). Now evidence suggests that macrophages are present in the murine myocardium as early as day E9.5 of embryonic development, which indicates that they originate from the embryonic yolk sac (YS) as fetal liver haematopoiesis occurs from day E11.5. However, a second wave of macrophages derived from fetal liver does invade the myocardium later. Interestingly, YS macrophages in the heart are maintained through adulthood and are not substantially replaced by fetal liver or bone marrow-derived monocytes, unlike in other tissues such as skin macrophages. Embryonic cardiac macrophages form different subsets and exhibit differential functions. YS-macrophages are CCR2-negative and exhibit angiogenic potential, in contrast with the macrophage subset derived from fetal monocyte haematopoiesis, which is CCR2-positive and exhibit a pro-inflammatory gene expression profile. Adult cardiac macrophages are self-renewing during homeostasis and benefit from circulating monocytes as a source of cell maintenance. Still, when resident macrophages are experimentally depleted, bone marrow stem cells are able to

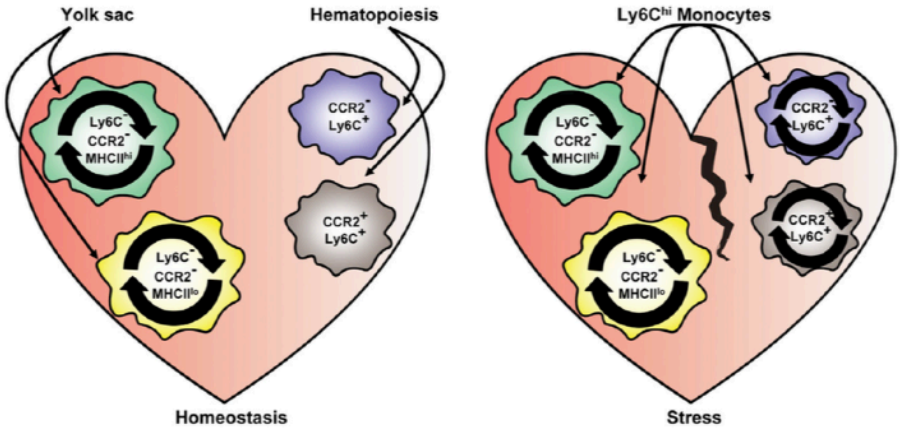

Figure 1.3. Resident macrophage heterogeneity in the heart. The most abundant populations originate from YS progenitors, are able to self-renew, and are CCR2$^-$ Ly6C$^-$. This population can be further dissected into MHCII^{hi} (shown in green) and MHCII^{lo} (shown in yellow). The second, smaller pool of resident cardiac macrophages is developmentally dependent on embryonic haematopoietic stem cells precursors, which are maintained from circulating monocytes under steady state conditions. These cells can be further subdivided into CCR2$^-$ (shown in violet) and CCR2$^+$ (shown in brown) populations. Although, LyC$^-$ resident macrophages do not depend on circulating monocytes for maintenance under homeostatic conditions (left), during cardiac stress (right), recruited Ly6C$^+$ blood monocytes can differentiate into all resident cardiac macrophage subsets, which can subsequently expand and proliferate, thus restoring homeostasis within the heart by local proliferation and HSC-derived recruitment. (Adapted from B. Cohen and M. Mosser, Cell 2015).

repopulate the myocardium, and re-establish all subsets identified in normal healthy hearts. During angiotensin II injection, macrophage numbers are increased substantially via both monocyte recruitment and proliferation of resident macrophages (Figure 1.4.) (144,146).

This is corroborated by Epelman et al, who identified adult-derived macrophages derived from monocytes but also from local proliferation and reported the additional nuance that monocyte derived macrophages are involved in coordinating cardiac inflammation, while having a less important role in functions like antigen sampling and efferocytosis (126). Furthermore, it has been revealed that embryonic origin-derived macrophages in the adult heart have a protective, wound reparative role, whereas monocyte recruited macrophages lack such repair properties (145).

10. Objectives

EndMT is a process that contributes to the mesenchymal phenotype in fibrotic diseases, and even though biochemical inducers of EndMT have been delineated, cellular sources and effectors that impact EndMT are not well established. Macrophages have a critical role in modulation of cardiac inflammation, healing and fibrosis and as knowledge on the vast variety of functions that macrophages have upon other cell types and their microenvironment is increasing, the impact of macrophages on endothelial cells in context of EndMT has not yet been addressed. Based on this, we aimed to explore if a potential crosstalk between macrophages and endothelial could impact EndMT and/or macrophage polarisation. More specifically we aimed to test if cardiac macrophages are involved in inducing EndMT in the context of cardiac fibrosis and atherosclerosis and also if endothelial cells undergoing EndMT impact macrophage polarisation. The aims of the present thesis were therefore the following:

i) to evaluate macrophage and EndMT load in human tissue and in mouse models of cardiac fibrosis and cardiovascular atherosclerotic disease

ii) to explore whether macrophages induce EndMT *in vitro.*

- ii a) to elucidate which macrophage phenotype is responsible for EndMT induction
- ii b) to investigate the putative cellular and molecular mechanisms involved in macrophage-induced EndMT

iii) to analyse the impact of EndMT on macrophage phenotype

Materials and Methods

2.1. Materials

2.1.1. Biological material

2.1.1.1. Cell lines

The cell lines used in this study are listed in table 2.1.

cell line	cell type	characteristics	Obtained from	reference
C2C12	murine skeletal muscle cells		Prof Lehnart UMG Göttingen	(151)
HeLa	human epithelial	adenocarcinoma	UMG Göttingen	(149)
MCEC	murine neonatal cardiac endothelial cells	immortalised with sv40 and telomerase	Cellutions Byosystems,#clu510	(152)
MCF	mouse cardiac fibroblasts	neonatal	Sciencell, #M6300-57	(148)
MCT	murine renal tubular epithelial cell line	transformed with sv40	Prof M Zeisberg UMG Göttingen	(150)
RAW 254.7	murine acrophages	Abelson murine leukemia virus transformed,biosafety level S2	Prof Uwe Raaz UMG Göttingen Prof Dr Katschinski UMG Göttingen	(147)

Table 2.1: cell lines

2.1.1.2. Primary cells

Peritoneal macrophages and bone marrow-derived macrophages were harvested from 10 weeks old C57BL/6N mice purchased from Charles River Company.

2.1.1.3. Patient samples

Human heart tissues from cardiac infarction, aortic stenosis and diabetic cardiomyopathy patients were obtained from autopsy samples obtained from the Department of Pathology at UMG (Göttingen Medical Center).

2.1.2. Cell culture media and additives

All media and additives used for the culture of cells lines and primary cell s are listed in Table 2.2.

name	provider	order number
DMEM	Sigma-Aldrich	D5796
Fetal calf serum	Sigma-Aldrich	F4135-500ML
HEPES 1M	Sigma-Aldrich	15630080
Penicillin/Strepromycin Solution	Gibco	15140-122
Phosphate buffered saline	Gibco	14190-094
Piruvate	Sigma-Aldrich	28374849
Beta-Mercaptoethanol for cell culture 50 mM	Gibco	31350-010
L-Glutamine (200 mM)	Gibco	25030081
ACK Lysing Buffer	ThermoScientific	A1049201
Accutase® Solution	Sigma-Aldrich	A6964-100ML
FM2 medium	ScienCell	2331b
FM2 basal medium	ScienCell	2331
CellTracker™ orange CMTMR Dye	ThermoScientific	C2927
Trysin-EDTA 0,25%	Sigma-Aldrich	T4049-100ML
Glutamax TM	Sigma-Aldrich	3345-100ML

Table 2.2: cell culture materials

2.1.3. Chemicals and reagents

All chemical reagents used are presented in Table 2.3.

name	provider	ordering number
Ethanol	ROTH	5054.1
Fast SYBR green	Applied Biosystems	4385612
Glycin	MERCK	1.04201.0100
20X LumiGLO and 20X Peroxide	Cell Signaling	7003
2-Mercaptoethanol	ROTH	4227.3

Isoflurane	Abbvie	B506
Isopropanol	ROTH	6752.2
Magnesium Chloride Solution 25mM	Sigma-Aldrich	M8787-1.5ML
Nuclease-Free Water	QIAGEN	129114
OligodT 12-18 Primers	Invitrogen	58862
Non fat powdered milk	ROTH	T145.2
Trizol	Ambion	15596-026
Tween20	Sigma-Aldrich	P1379-500ML
Weigert's iron hematoxylin solution	Sigma-Aldrich	HT1079
Xylol	ROTH	9713.3
Lipopolysaccharides from Escherichia Coli O55:B5 (LPS)	Sigma-Aldrich	L6529-1MG
Ponceau reagent	ROTH	3469.1
SDS loading buffer	Novex	96868
NP-40 Lysis buffer	Invitrogen	FNN0021
NuPAGE LDS Sample buffer (4x)	Novex	NP0007
Pierce Fast Semi-Dry Transfer Buffer	ThermoScientific	35045
MOPS Running Buffer	Invitrogen	3324
10x PBS	Invitrogen	7757R
4% PFA	Roth	664666
Blocking buffer	Roth	33285
Target retrieval solution 10x pH6	Dako	S1699
Dimethyl sulfoxide	Sigma-Aldrich	D8418-50ML
cOmplete ULTRA Tablets, Mini, EDTA-free,EASYpack	Roche	5892791001
SEA BLOCK Blocking Buffer	ThermoScientific	37527
RNaseZap	Ambion	AM9782
Superscript® II Reverse Transcriptase	Invitrogen	100004925
dNTP mix	Invitrogen	18427-013
5X First Strand Buffer	Invitrogen	y02321
0,1M DTT	Invitrogen	y00147
Rnase OUT	Invitrogen	100000840

Table 2.3: chemicals

2.1.4. Cytokines and recombinant proteins

Cytokines used in this study are listed in table 2.4.

name	company	order number
human recombinant TGF-Beta 1	R&D Systems	240-B-010/CF
mM-CSF	R&D Systems	416-ML
mGM-CSF	R&D Systems	415-ML
IL4	Immunotools	77675
IFN-gamma	R&D Systems	240-B-01890
TNF-alpha	R&D Systems	240-B-010CF
IL1-Beta	R&D Systems	240-B-0798A

Table 2.4: cytokines

2.1.5. Antibodies

Antibodies used in this study are listed in table 2.5.a and 2.5.b

2.1.5.a Primary Antibodies

epitope	company	Order number	use
Actin	abcam	ab8227	WB
CD31	abcam	ab28364	WB, IF
a-SMA	Sigma Aldrich	A5228-200UL	WB, IF
PECAM1	DB Pharmingen	553370	IF
Snail	Cell Signalling	ab180714	WB
iNOS	Thermoscientific	PA3-030A	WB
MHCII	abcam	ab25259	(WB, IF)
Notch 1	abcam	ab52627	WB
NICD	abcam	ab8925	(WB, IF)
Jagged 1	abcam	ab7771	WB
CD11b	abcam	ab8878	IHC
F4/80	Cell Signalling	MCA497R	IHC,IF,IcF,FACS
Col1A1	abcam	ab34710	IF
CD68	Bioss	bs-0649R	IF
CD11b	Biolegend		FACS

ß-catenin (carboxy-terminal)	Cell Signalling	9587S	IF
Twist	Millipore	ABD29	IF
PE anti-mouse F4/80	Biolegend	123110	FACS
Pacific Blue™ anti-mouse/ human CD11b	Biolegend	101223	FACS

Table 2.5.a: primary antibodies

2.1.5.b Secondary Antibodies

epitope	company	Order number	use
Alexa Fluor ® 488 donkey anti-rabbit	Life technologies	A21206	IF
Alexa Fluor ® 488 donkey anti-rat	Life technologies	A21208	IF
Alexa Fluor ® 647 goat anti-mouse	Life technologies	A21235	IF
Alexa Fluor ® 568 donkey anti-rabbit	Life technologies	A11042	IF
Alexa Fluor ® 488 donkey anti-mouse	Life technologies	A21202	IF
Polyclonal Rabbit Anti-Rat Immunoglobulins	DAKO	P0450	WB
Polyclonal Rabbit Anti-Mouse Immunoglobulins	DAKO	P0161	WB
Polyclonal Goat Anti-Rabbit Immunoglobulins	DAKO	P0448	WB

Table 2.5.b: secondary antibodies

2.1.6. Primers

Primers pairs used in this thesis in real time quantitative PCR (qRT-PCR) experiments are listed in table 2.6.

Gene	Sequence	Source
mSnailF	CCACGCTAATGTGTCAACACGA	Primer Design
mSnailR	AATCGATGCCTGGATTCCAAG	Primer Design
mSlugF	GCTGTGTACCAGGTAGCTGAC	Primer Design
mSlugR	GGCCTCCCATCTCCTTCAAT	Primer Design

Gene	Sequence	Source
mTwistF	GGTCTGCACAGATGAGCTTGCC	Primer Design
mTwistR	ATCAATCGGCATCGTGAACGAGGTAC	Primer Design
mActa2F	CACTATTGGCAACGAGCGC	Primer Design
mActa2R	CCAATGAAGGAAGGCTGGAA	Primer Design
mCol1a1F	ATGGATTCCCGTTCGAGTACG	Primer Design
mCol1a1R	TCAGCTGGATAGCGACATCG	Primer Design
ms100a4F	CATGCCTTGAGTAGCATCTATGC	Primer Design
ms100A4R	CAAGTTGTTCAGACTCTCTCGCCTA	Primer Design
mNotch1F	CCGCGTGAACTTAGCCCTGTATG	Dr Fouzi Alnour
mNotch1R	TGACTACGCCTAGAGTGGCCTGTCTA	Dr Fouzi Alnour
mNotch2F	TGATACAAGCCTGAGTGCGCTGTTTT	Dr Fouzi Alnour
mNotch2R	AGGTCGACTTGTGAACGGATTTG	Dr Fouzi Alnour
mNotch4F	TTGTTGGATCCCTCCTACAGACTGG	Dr Fouzi Alnour
mNotch4R	CTGTTGTTCGTTACCACTACTCCCT	Dr Fouzi Alnour
mHey1F	GCGCGGACGAGAATGGAAA	Primerbank
mHey1R	TCAGGTGATCCACAGTCATCTG	Primerbank
mHes1F	CCAGCCAGTGTCAACACGA	Primerbank
mHes1R	AATGCCGGGAGCTATCTTTCT	Primerbank
mHes5F	AGTCCCAAGGAGAAAAACCGA	Primerbank
mHes5R	GCTGTGTTTCAGGTAGCTGAC	Primerbank
mTNFaF	GACGTGGAACTGGCAGAAGAG	Primerbank
mTNFaR	TTGGTGGTTTGTGAGTGTGAG	Primerbank
mIL6F	CCAAGAGGTGAGTGCTTCCC	Primerbank
mIL6R	CTGTTGTTCAGACTCTCTCCCT	Primerbank
mIL12p35F	CTGTGCCTTGGTAGCATCTATG	
mIL12p35R	GCAGAGTCTCGCCATTATGATTC	Primerbank
IL23p19F	ATGCTGGATTGCAGAGCAGTA	Primerbank
IL23p19R	ACGGGGCACATTATTTTTAGTCT	Primerbank
IL12p40F	TGGTTTGCCATCGTTTTGCTG	Primerbank

Gene	Sequence	Source
IL12p40R	ACAGGTGAGGTTCACTGTTTCT	Primerbank
mIL10F	GCTCTTACTGACTGGCATGAG	Primerbank
mIL10R	CGCAGCTCTAGGAGCATGTG	Primerbank
mCCL2F	TTAAAAACCTGGATCGGAACCAA	Primerbank
mCCL2R	GCATTAGCTTCAGATTTACGGGT	Primerbank
mCTGF_F	TGCGAAGCTGACCTGGAGGAAA	Origene
mCTGF_R	CCGCAGAACTTAGCCCTGTATG	Origene
mTGFB1_F	TGATACGCCTGAGTGGCTGTCT	Origene
mTGFB1_R	CACAAGAGCAGTGAGCGCTGAA	Origene
mTGFB2_F	TTGTTGCCCTCCTACAGACTGG	Origene
mTGFB2_R	GTAAAGAGGGCGAAGGCAGCAA	Origene
mstat6_F	ACGACAACAGCCTCAGTGTGGA	Origene
mstat6_R	CAGGACACCATCAAACCACTGC	Origene
mIL4_F	ATCATCGGCATTTTGAACGAGGTC	Origene
mIL4_R	ACCTTGGAAGCCCTACAGACGA	Origene
mCCL17_F	CGAGAGTGCTGCCTGGATTACT	Origene
mCCL17_R	GGTCTGCACAGATGAGCTTGCC	Origene
mCCL22_F	GTGGAAGACAGTATCTGCTGCC	Origene
mCCL22_R	AGGCTTGCGGCAGGATTTTGAG	Origene
mHPRT_F	GGCCTCCCATCTCCTTCATG	Genebank
mHPRT_R	CAGTCCCAGCGTCGTGATTA	Genebank
MGAPDH_F	TGTAGACCATGTAGTTGAGGTCA	Dr. Fouzi Alnour
mGAPDH_R	AGGTCGGTGTGAACGGATTTG	Dr. Fouzi Alnour

Table 2.6: primers

2.1.7. Commercial kits

The commercial kits used in this thesis are listed below in Table 2.7.

Kit	Provider	order number
Pierce BCA Protein Assay Kit	Thermo Scientific	23225
PureLink RNA mini Kit	Ambion (Life Sciences)	12183025
Vectastain Universal Elite ABC kit	Vector Laboratories	99585
ELISA Kit for TGF-Beta	Cloud-Clone Corp	CEA218Mu

Table 2.7: kits

2.1.8. Equipment

The equipment utilised in this study is listed in table 2.8.

Function	Instrument	Company
Cell line tissue culture S1	BIOWIZARD	KOJAIR
Cell Culture Centrifugation	ROTOFIX 32 A	Hettich
RNA concentration measurement	NanoDrop 2000	ThermoScientific
Heating Block	Thermomixer Comfort	Eppendorf
Cell Culture Incubator S1	InCu safe	EWALD
Primary Cell Culture Incubator S1	NU-543-400E	tecnomara
Cell Culture Incubator S2		EWALD
Bright Light Microscopy	BX43	OLYMPUS
Protein Electrophoresis	Xcell SureLock Electrophoresis Cell	Invitrogen
Protein Semi Dry Blotting	Fastblot B44	Biometra
RealTime Q-PCR	StepONePlus Real-Time PCR System	Applied Biosystems
Vortexing	Vortex Genie	Bender & Hobein AG
FACS	FACS Aria II	Becton Dickinson,

Table 2.8: equipment

2.2. Methods

2.2.1. Cell culture experiments

2.2.1.1. Culture of MCECs

Immortalised Mouse Cardiac Endothelial Cells (MCEC) were purchased from Cedarlane Labs. MCECs consist of microvascular endothelial cells derived from neonatal murine hearts, that have been immortalised by lentiviral infection with large sv40 antigen and human telomerase. MCECs retain typical endothelial properties by showing contact inhibition, growing on a monolayer and LDL uptake, and expressing endothelial cell specific proteins such as VE-cadherin, PECAM-1, Willenbrand factor and others like Laminin and ß-catenin in intercellular regions. Cells were generally cultured in Endothelial Growth medium, consisting of DMEM supplemented with 1% of HEPES and 5% of Fetal Calf Serum. Cells were cultured under 21% of O2 and 5% of CO2 conditions (152).

2.2.1.2. Generation of macrophage cell lines

2.2.1.2.1. Murine peritoneal Macrophages (PMs)

PMs were harvested from the peritoneal cavity of 10-12 weeks old wild type BL6/N mice (Charles River). The adapted protocol, kindly provided by Prof. Von Vietinghoff, consisted of euthanising the mice by cervical dislocation of anaesthetised animals and opening a small incision on ethanol-disinfected skin on the centre of the abdomen, followed by an injection of 5 ml of ice-cold PBS inside the peritoneal cavity. After applying a gentle abdominal massage to detach cells, PBS was collected with a syringe. Thereafter, PBS containing peritoneal cells was handled under cell culture sterile conditions and centrifuged at 100g for 10 min. Cell pellets were resuspended in DMEM supplied with 10% of Fetal Call Serum (FCS) and 1% of antibiotics Streptomycin and Penicillin. Cell suspension was counted using a Neubauer chamber and cells were typically seeded in 12-well plates at approximately 1 x 10^6 cells per ml of medium. Typically, total of cells harvested from PBS peritoneal lavages have a composition of B cells (60 %), macrophages (40%) and T cells (less than 10 %). In order to enrich macrophages titre, total cell suspension is allowed to adhere on

plate for 1 hour at 37ºC, and non adherent cells are removed by gently washing three times with culture medium, increasing macrophage count by 90% (153).

2.2.1.2.2. Murine Bone Marrow Derived Macrophages (BMDMs)

Bone marrow cells were flushed in basal DMEM media from tibias and femurs of 10-12 weeks old wild type BL6/N mice, following standard procedures. To avoid clumps, DMEM containing cells were collected through a 70 μm strainer and in order to get rid of erythrocytes, all cells were treated with blood cell lysing buffer for 3 minutes at room temperature. Next, remaining cells were plated in 10 % FCS DMEM supplemented with L-Glutamine (2 mM) and beta-mercaptoethanol (50 µM) overnight in standard tissue culture treated dishes. Following overnight incubation, supernatants were collected and mesenchymal cells attached to tissue culture plates were discarded. Supernatants containing macrophage progenitors were counted and spread in suitable amount of plates (5-8 x 10^6 cells per plate) for differentiation in plastic bacteriologic dishes in growth medium DMEM supplemented with 10% FCS, L-glutamine and beta-mercaptoethanol and in the presence of differentiating cytokines GM-CSF (1000 U/ml) or M-CSF (25 ng/ml) to generate GM-BMDM and M-BMDM, respectively. Fresh cytokines were added every 3 days. At day 7, differentiated macrophages could be re-plated at a concentration of 5 x 10^5 cells per ml of medium

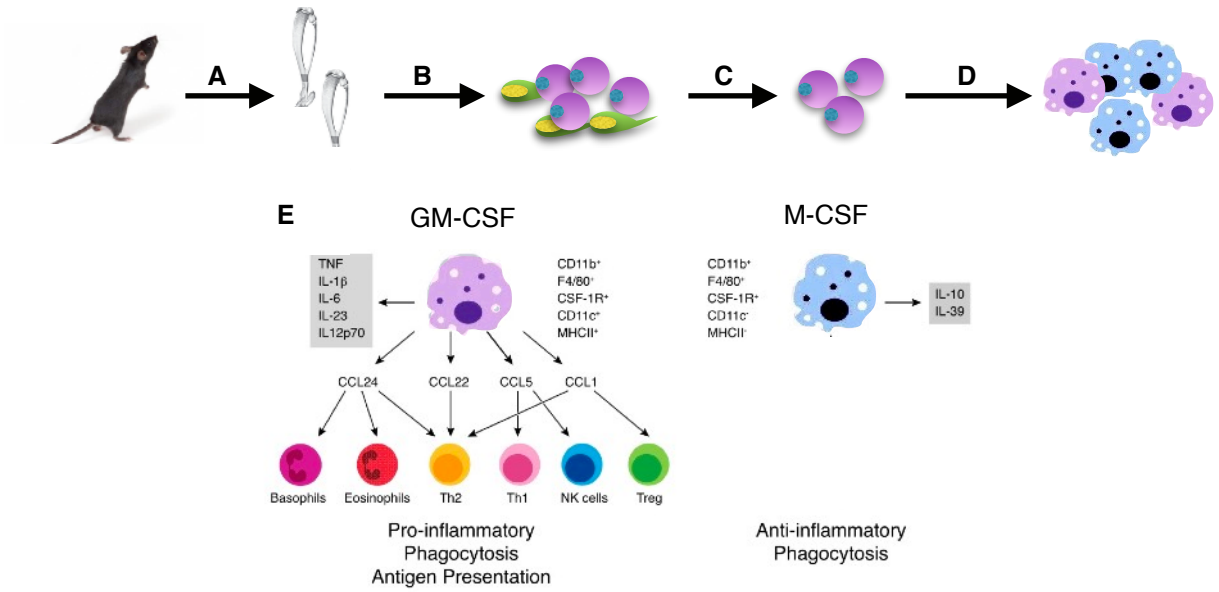

Figure 2.1. Depiction of BMDMs differentiation protocol. Femurs and tibias are extracted from euthanised BL6/N mice (A). Whole bone marrow cells are flushed and kept in culture in bacteriological dishes overnight (B). Non adherent cells are collected (in purple), while proliferating fibroblast-like cells, mature mononuclear phagocytes, and other stromal cells adhering to the flask (in green) are discarded (C). Macrophage progenitors are cultured for 7 days in GM-CSF and M-CSF (D). At the 7, they have acquired spread and spindle shape morphology and differential expression of pro-inflammatory and anti-inflammatory mediators (E). Adapted from reference 205.

for assay. Cells were cultured in 21 % O_2 and 5 % CO_2. Cells were subcultured using Accutase. For macrophage activation, 50 ng/ml of E.Coli derived lipopolysaccharide (LPS) was added to growth medium for at least 6 hours.

2.2.1.2.3. RAW 264.7 cell line

RAW 264.7 cells were a kind gift from Prof. Dr. Katschinski and Prof. Dr. Raaz. RAW 264.7 cells are immortalised murine cells derived from Abelson virus leucemic mice. RAW were grown in 10 % FCS DMEM and were subcultured by scraping. Cells were cultured in 21 % O_2 and 5 % CO_2. For polarisation, RAW 264.7 cells were treated in growth medium with IL-4 (20 ng/ml), IFNγ (100 ng/ml) or IFN-γ (100 ng/ml) and LPS (50 ng/ml) combined for the indicated times in normal growth culture. Native controls were treated with PBS.

2.2.1.3. Culture of control cell lines

2.2.1.3.1. Mouse Cardiac Fibroblasts (MCFs)

MCFs were purchased from ScienCell (#M6300-57). MCFs are neonatal murine cardiac fibroblasts and were used at passage number 5-10. Cells were subcultured in growth FM2 medium according to the manufacturer instructions on poly-Lysine coated tissue culture plates at 5 % CO_2 and 21% O_2 conditions. To activate fibroblasts, MCFs were first starved overnight in basal FM2 medium and then treated with human recombinant TGF-ß 1 at 10 ng/ml in basal FM2 medium.

2.2.1.3.2. HeLa

HeLa cells were a gift from Prof. M. Zeisberg. HeLa cells are adenocarcinoma epithelial cells that divide indefinitely and are widely used for mechanistic assays and cancer research due to their straight forward handling. HeLa cells were grown in 10 % FCS, low glucose DMEM at 5 % CO_2 and 21% O_2 conditions.

2.2.1.3.3. C2C12 cells

C2C12 cells were a kind gift from Prof. S. Lehnart. C2C12 cell line is a murine skeletal myoblast cell line derived from satellite cells from the thigh muscle of C3H mouse strain. It divides indefinitely and differentiates rapidly to myocytes, forming contractile tubes and muscle proteins (151). Although differentiation protocol requires horse serum and insulin supplements, C2C12 cells

can differentiate easily upon cell-cell contact (154). Cells were maintained in DMEM supplemented with 10 % FCS and Glutamax™ and subcultured by trypsinizing followed by dilution in a 1:30-1:60 factor. For co-cultures, cells were seeded at minimum density of 5x10^3 cells/ml, termed as “low-C2C12” or at high density of 5x10^5 cells/ml, termed as “high-C2C12”.

2.2.1.3.4. MCT cells

MCT cells were a kind gift from Prof. M. Zeisberg. MCT cells are a differentiated, SV40 transformed cell line originally derived from SJL mice. MCT cells are well characterised functional proximal tubular epithelial cells. Cells were grown under standard conditions in 10 % FCS DMEM and at a cell culture chamber at 5 % CO_2 and 21% O_2.

2.2.1.3. TGF-ß induced EndMT

To induce classical EndMT, MCECs were subcultured and plated at a density of 30-40 % confluence in endothelial growth medium. When attached to plate and after acquiring normal morphology, growth medium was replaced by reduced serum medium, containing 1 % FCS, and cells were incubated overnight. At the following day and until experiments were finished and unless otherwise indicated, human recombinant TGF-ß 1 was added to serum reduced medium every day at a concentration of 10 ng/ml of medium.

2.2.1.3. Conditioned medium (CM) experiments

2.2.1.3. 1. Macrophage-derived CM

Conditioned medium (CM) from GM-BMDM and M-BMDM was generated by plating differentiated macrophages at a density of $1x10^6$ cells/ml on standard tissue culture wells. For activated macrophages, LPS was added to GM-BMDMs and M-BMDMs at 50 ng/ml and allowed to incubate for 1 hour. For control unstimulated cells, equivalent amount of vehicle (PBS) was added. After stimulation, medium containing LPS was discarded and cells were washed extensively by washing three times with PBS and two times with basal DMEM medium. Thereafter, basal medium was added and remained in incubation with cells for at least 48 hours. After incubation, CMs were collected, centrifuged and filtered through a 0,22 μm filter to remove debris and either were immediately used for assay or were snap frozen in liquid nitrogen and stored at -80ºC. CMs were

applied on MCECs cells that were previously serum starved in DMEM overnight at 1:1 (v/v) with basal DMEM or grown in complete CM. Negative control was assayed using basal DMEM. Positive control was tested using basal DMEM and TGF-ß 1 at 10 ng/ml. When indicated, CMs were supplied with TGF-ß 1 at a final concentration of 10 ng/ml for further analysis.

2.2.1.3. 2. Endothelial-derived CM

Native endothelial derived CM were generated by plating MCECs at 60-70 % confluence and incubating cells for 24 hours in basal DMEM supplemented with 1 % of HEPES. After incubation, CM was collected and filtered as previously described.

EndMT-derived CM was generated by inducing EndMT in MCECs with TGF-ß1 as indicated earlier. After 48 hours of TGF-ß 1 treatment, cells were extensively washed, three times with PBS and two times with basal DMEM, and basal serum supplemented with 1 % of HEPES was applied. After 24 hours of incubation, EndMT-CM was collected, filtered, and used for assay or stored at -80ºC.

native-MCEC and EndMT-MCEC derived CMs were applied to RAW 264.7 macrophages at 1:1 (v/v) with RAW growth medium for 24 hours. Negative controls consisted of endothelial basal DMEM (1 % FCS) mixed with RAW 264.7 growth medium.

2.2.1.3. 3. Co-culture-derived CM

Conditioned medium from co-cultures was collected by recovering supernatants from co-cultures of BMDMS and MCECs after 48 hours of cell co-culture (procedure explained below). CMs were harvested and filtered and stored or applied to serum-starved MCECs following the same protocol than macrophage-derived CM application.

2.2.1.4. Bidirectional paracrine co-culture experiments

MCECs were plated in serum reduced DMEM on Transwell® (Costar®, #3460) porous inserts at 40 % confluence. BM-BMDMs and M-BMDMs were plated at a density of 5 x 10^5 cells/ml beneath transwell® inserts containing MCECs. Macrophages were allowed to attach overnight before applying MCECs on co-culture insert. Co-cultures were allowed to grow for 48 hours. In parallel, mono-cultures (negative controls) of MCECs, M-BMDMs and GM-BMDMs were plated under the same conditions in serum reduced endothelial medium. A positive control was added in which MCECs were treated in mono-culture with TGF-ß 1.

2.2.1.5. Juxtacrine co-culture experiments

In order to study contact dependent cell-cell interactions, MCECs and macrophages were co-cultured together in the same culture plates. An orange fluorescent live cell tracker CMTMR was utilised to track one of the cell populations, to be able to sort them conveniently on downstream operations through fluorescence activated cell sorting (FACS). According to manufacturers instructions, CMTMR fluorophore remain vividly fluorescent for at least 72 hours after incubation in fresh medium at 37ºC and through at least four cell divisions. In our hands, cells lost fluorescence at 72 hours of co-culture (Figure 2.2. A), which hindered the efficient separation process of distinct populations. For this reason, co-cultures were collected 48 hours after tracker application. No detrimental effects on proliferation and plating efficiency of stained cells were observed, and leakage from one cell population to the other was never observed, consistent with previous reports (155,156). No significant changes upon TGF-ß stimulation were found in MCECs treated with CMTMR (Figure 2.1 B). Our FACS sorting isolated a 97-99 % pure population (assessed by BC FACS Diva 5.0 software) which was checked by FACS and fluorescence microscopy (Figure 2.1 C).

MCECs were loaded with CMTMR tracker by incubating confluent adherent cells with 10 μM of CMTMR diluted in basal DMEM for 45 min at 37 ºC in a cell culture incubator. After tracker loading, tracker solution was discarded and cells were washed, trypsinized and subcultured for experiments. Generally, MCECs were plated at 40 % confluence on standard 6-well plates. After 1 hour, unstained cells (either macrophages or control cells) were added to stained cells. For mature BMDMs, M-BMDM and GM-BMDM were either vehicle treated or LPS-stimulated. 1 hour after stimulation, BMDMs were extensively washed and subcultured at $5x10^5$ cells/ml on plates containing CellTracker stained MCEC cells. Contact co-cultures were sustained for 48 hours. After incubation, cells were detached and prepared for FACS sorting. For RAW 264.7 co-cultures, similar procedures was followed. RAW 264.7 cells were stimulated with polarisation cytokines 6h prior to co-culture.

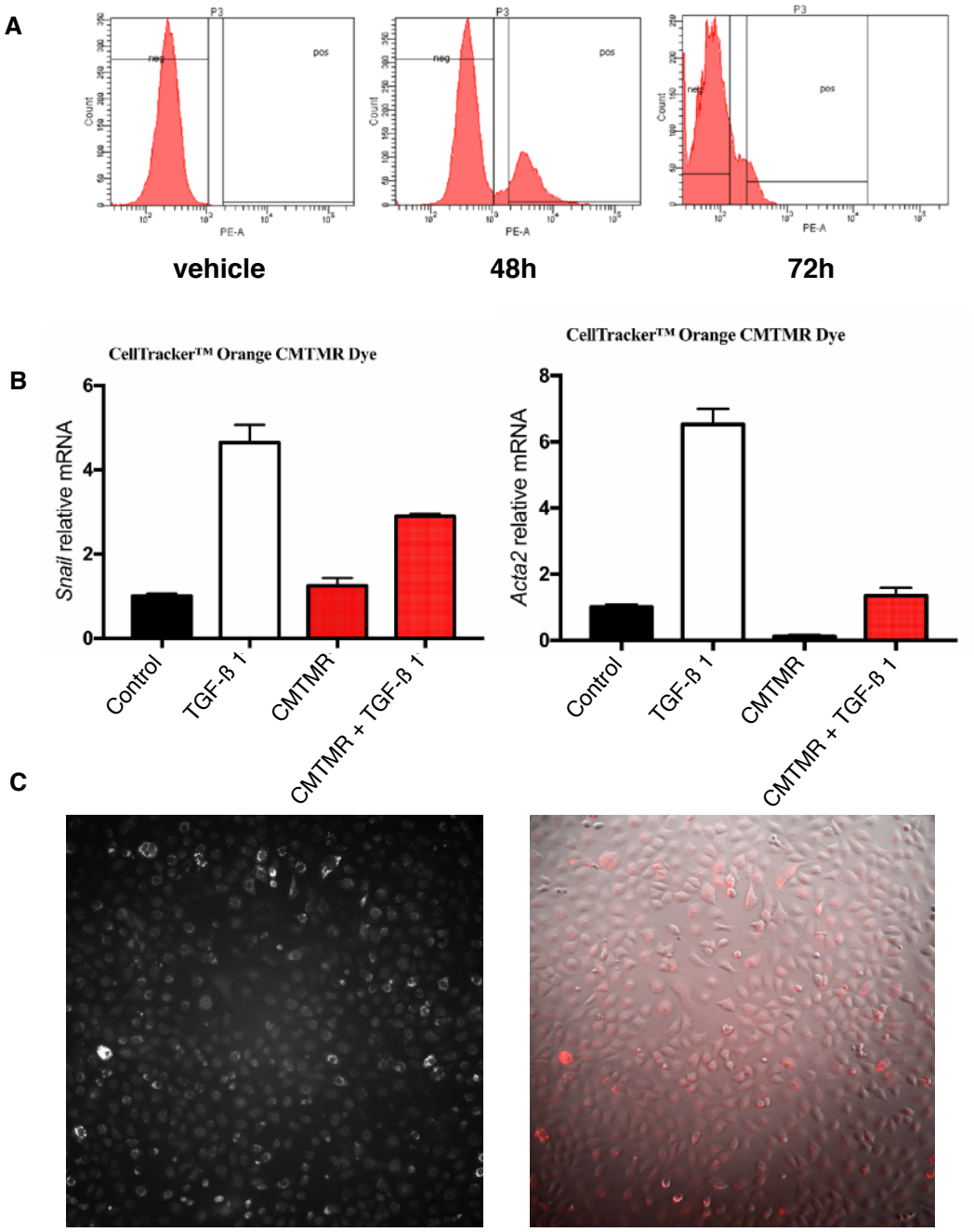

Figure 2.2. CMTMR live fluorescent staining. A) Representative cytometry analysis of unstained cells (left), cells stained after 48h (middle) and cells stained for 72h (right). B) RT-qPCR analysis of EndMT marker genes in unstained MCEC cells ("control", "TGF-ß1") and stained ("CMTMR", "CMTMR +TGF-ß1"). C) Left, fluorescent microscopy of stained MCEC cells. Right, bright field microscopy and fluoresce microscopy merged image (magnification is 200x).

2.2.2. Animal models

All experimental animal studies were performed with the approval of the Institutional Animal Care and Use Committee of the University Medical Center Göttingen. All surgical animal procedures were performed by specifically trained staff of the Zeisberg group.

2.2.2.1. AAC model

Ascending aortic constriction was performed in 12-week-old mice under anesthesia with a mixture of ketamine (100 mg/kg) and xylazine (10 mg/kg) given at 0.1 ml intraperitoneally as described previously (56). Adequacy of anesthesia was monitored by observing muscle twitch and by tail pinch as well as documenting heart rate and body temperature. As postoperative analgesia, Buprenex (0.1 mg/kg) was given intraperitoneally every 6–8 h for the first 48 h. All mice used weighed 25–30 g. For sham control operated mice, the chest was surgically opened under the same conditions as banded mice except that no aortic banding was performed. 4 weeks after operation, mice were sacrificed with a lethal intraperitoneal dose of pentobarbital sodium (100 mg/kg) followed by cervical dislocation.

2.2.2.2. Ang II model

Angiotensin II model was performed as described (156). Briefly, 2 mg/kg per day of Ang II was administered by implantation of osmotic minipumps (ALZET osmotic minipumps; type 2ML4) for 14 days. At the end of the experiment, echocardiography was performed under 2-4 % of isofluorane anaesthesia.

2.2.2.3. ApoE -/- model

Frozen sections of aortas from Apolipoprotein E deficient mice were used in collaboration with Prof. Von Vietinghoff (Hannover University) and PhD student Alexandra Helmke. Apo E Mice were generated as described (157). Both wild type and ApoE-/- strains (both with C57BL/6 background) were fed during 12 weeks with high-fat diet (HFD) containing 40 % kcal from fat and 1.5 % cholesterol. Animal experiments were approved by the Animal Care Committee at La Jolla Institute for Allergy and Immunology and Landesamt für Verbraucherschutz und Lebensmittelsicherheit, Lower Saxony, Germany.

2.2.3. Molecular Biology techniques

2.2.3.1. RNA isolation and Real Time Quantitative-PCR

Total RNA was extracted from cells using PureLink RNA kit following the manufacturer's protocol. 1µg of total RNA was digested with DNase I (Sigma) and used for cDNA synthesis using the SuperScript II system (Life Technologies). Diluted cDNA (1/10) was used as a template in Fast SYBR Master Mix (Life Technologies) and run on a StepOne Plus realtime PCR system with the real-time specific PCR primers (sequences are listed in Table 2.6.). Measurements were standardised to GAPDH or HPRT using delta delta Ct standard methodology.

2.2.3.2. Immunoblotting

2.2.3.2.1. Protein extraction

Proteins were extracted from cells using NP40 lysis buffer (Life technologies), containing protease inhibitor cocktail (Roche). Cell were lysed by resuspending cell pellet in adequate amount of lysis buffer (usually 100 µl per 6-well plate dish), and cell suspensions were incubated at 4 ºC per 30 min in a rotating system. Thereafter, lysate suspension was centrifuged at maximum speed in a tabletop centrifuge at 4 ºC. After centrifugation, supernatant was collected and assayed for protein content measurement using BCA Kit (ThermoScientific). After protein concentration determination, samples were stored at -80 ºC or used for sodium dodecyl sulfate polyacrylamide gel (SDS-PAGE) electrophoresis.

2.2.3.2.2. SDS-PAGE electrophoresis

Protein samples were diluted till concentration of 1µg/µl and 15-20 µl were used per sample in a mixture with SDS-loading buffer (25%) and beta-mercaptoethanol (10%) in a SDS-PAGE gel pocket. Equal amounts of protein were loaded in each pocket. Samples were then resolved on 4-12 % SDS-PAGE (Novex, Invitrogen) at 80-120 mV.

2.2.3.2.3. Western Blot

After proteins were resolved, proteins contained in gel were transferred onto a nitrocellulose membrane (Amersham Biosciences) using a semi-dry protein transfer system (Biometra). Protein transfer was efficiently accomplished by using 150 mA for 15 min followed by 250 mA for 45 min. Thereafter, membrane was blocked by incubating it for 1 hour at room temperature with a blocking buffer of tris-buffered saline (TBS), Tween 20 (0,1%) and non-fat milk (5%) at pH 7.2. After

blocking, the membrane was incubated overnight at 4ºC with primary antibodies in an adequate dilution (1:500-1:5000) of antibody (primary antibodies are listed in table 2.5. a) in TBST buffer supplemented with 2% non-fat milk.

2.2.3.2.4. Protein detection

On the second day, after washing three times for 10 min with TBST, the membrane was incubated with secondary HRP-conjugated antibodies (listed in table 2.5.b) diluted in TBST and 2% non-fat milk during 45 min at room temperature. Secondary antibody excess was removed by washing 3 times for 10 min with TBST . Finally, antibody signals were detected using a chemiluminescent kit and visualisation was made in a Bio-rad camera system.

2.2.4 Immunostaining techniques

2.2.4.1. Immunohistochemistry

Paraffin embedded cardiac tissue sections were prepared by technical assistance employees Annika Faust and Sarah Rinkleff. Paraffin embedded tissue sections were deparaffinized by incubation with Xylol for 10 min, two times. Next, gradual dilutions of ethanol (100%-30% ethanol) were applied to sections for 30 min until final incubation with distilled H_2O at room temperature. After washing with PBS two times, sections were treated with pH 6 citrate buffer for 40 min in a steam bath. Afterwards, sections were blocked with 0.3 % peroxidase buffer for 30 min at room temperature. Thereafter, samples were blocked with bovine serum albumin (BSA) 2 % in phosphate buffered saline (PBS) and primary antibody was applied and let overnight for incubation at 4 ºC. The next day, excesses of antibody were removed by gently washing three times with PBS. After washing, a specific secondary antibody from Vectastain Universal Elite ABC commercial kit was applied following the manufacturer's protocol. Sections were then analysed at a bright field microscope.

2.2.4.2. Immunofluorescence of Paraffin sections

Paraffin embedded cardiac tissue sections were prepared by technical assistance employees Annika Faust and Sarah Rinkleff. Sections were deparaffinized as explained previously. Thereafter, antigen retrieving was accomplished by using citrate buffer in a warm steam bath for 40 min.

Afterwards sections were blocked with a PBS buffer containing BSA 2 % for 30 min and first antibody was applied in blocking solution overnight at 4 ºC. The day after, sections were washed 3 times with PBS and secondary antibody was applied in blocking solution at a dilution of 1:400 and incubated for 45 min. Next, secondary antibody excess was removed by washing with PBS 3 times for 5 mins, and DAPI staining was applied. Sections were then mounted and dried for one hour. Samples were then ready to visualise in confocal or conventional fluorescence microscope.

2.2.4.3. Immunofluorescence frozen sections (aortas)

Frozen aortic tissue sections were prepared by AG Von Vietinghoff group at Hannover Medicine University. Frozen tissue sections were air dried for 10 mins and fixed with 100 % methanol for 9 minutes. Thereafter, equal immunofluorescence protocol than paraffin-embedded sections was applied.

2.2.4.4. Immunocytofluorescence

For immunofluorescence analysis, cells were grown in polystyrene chamber slides (Falcon). When experiment was finished, chambers were removed from slides and slides were washed in PBS briefly. Next, cells were fixed by using ice-cold methanol (100%) for 9 min. Thereafter, for intracellular protein detection, cells were permeabilised by using PBS containing Triton 0, 1% for 10 min at room temperature. Next, blocking step was followed by incubating slides with 2% BSA in PBS or using sea blocking buffer for 30 min at room temperature. After blocking, primary antibody was added in blocking solution and allowed to incubate overnight at 4 ºC. The next day, the same protocol as for immunofluorescence tissue sections was followed.

2.2.5. Fluorescence-activated cell sorting (FACS)

For immunostaining of adherent cells, cells were trypsinized, centrifuged and resuspended in 2 % BSA in PBS to a final concentration of 10^6 cells/ml. After blocking in 2 % BSA for 10 minutes, fluorescence-labelled antibody was applied to cell suspension and incubated for 60 min at 37 ºC in a cell incubator. Thereafter, cells were washed three times by adding blocking buffer and centrifuging the cell suspension. Afterwards, cells were resuspended in adequate amount of blocking buffer and loaded at BD sorting machine for analysis.

2.2.6. Statistical Analysis

Analysis of variance was used for multiple comparisons of groups to determine significance. A Student t test analysis was used for the single-parameter comparisons. Statistical significance was defined as P values less than 0.05. Prism 5 and 7 software (GraphPad, La Jolla, CA) were used for statistical analysis.

Results

3.1. Cardiac macrophages are increased in cardiac disease

3.1.1. Macrophage numbers are increased in human myocardial fibrosis

Macrophages have not been of great interest for cardiologists in the past, probably due to an only small incidence of infective diseases in the heart. The increasing knowledge unveiling that pathogenesis of atherosclerosis involves a complex maladaptive immune response brought the attention of immunology to the cardiology field. Still, although progress has been made, data of macrophage abundance in human cardiac disease is quite limited to myocardial infarction (160). Because cardiac fibrotic onset and progression extend beyond fibrotic remodelling as a result of acute cardiac ischemia and nowadays we know that extensive fibrosis occurs in a wider range of cardiac pathologies, we examined macrophage content in patients with cardiac fibrosis of different backgrounds. We examined macrophage specific marker CD68 in cardiac tissue samples from patients with aortic stenosis, diabetic cardiomyopathy and myocardial infarction, and we compared these to healthy controls derived from individuals that had suffered sudden death (meaning that they were allegedly healthy individuals before time of death) (Figure 3.1). Human CD68 is a heavy glycosilated transmembrane protein that is expressed in the endosomal-lysosomal system in the cytoplasms of the monocyte/macrophage myeloid lineage. CD68 is widely used as a broad pan-macrophage marker, and there is extensive literature of its use for identification of macrophages in diverse cardiovascular pathologies such as atherosclerosis, chronic inflammation, and also in the ischemic heart (161-163). CD68 antibody stained elongated and rounded cells with a granular and sometimes defused red cytoplasm staining in the examined cardiac tissue specimens (Figure 3.1 A-D). CD68-positive cells localised around the vessels and scattered through the myocardium in the intercellular space between cardiomyocytes. In diseased patients, numerous CD68-positive cells accumulated in fibrotic regions, encapsulated within, and accumulated in perivascular areas. Importantly, the macrophage number was significantly higher in diabetic cardiomyopathy, aortic stenosis, and myocardial infarction derived tissue samples than in healthy control samples (Figure 3.1, I) . Aortic stenosis (AS) is a condition that as a result of age, calcification or congenital disease, leads to aortic valve constriction that eventually results in left ventricle hypertrophy and

myocardial fibrosis (164). Fibrosis derived from AS is typically associated with perivascular fibrosis, caused by the excessive blood pressure overload (165). Coincidently, macrophage accumulation was the highest in AS cardiac tissue, and these macrophages mostly accumulated in the fibrotic region surrounding the vessels. Diabetic cardiomyopathy is also associated with extensive perivascular fibrosis and mild interstitial fibrosis. Our data shows that diabetic patients also have an increase in macrophage count. Furthermore, analysis of the infarcted samples revealed a significant increase of CD68-positive cells at the remote zone of the infarcted myocardium. Overall, we observed macrophages in all cardiac tissues examined and a found significant number increase in all pathological tissues.

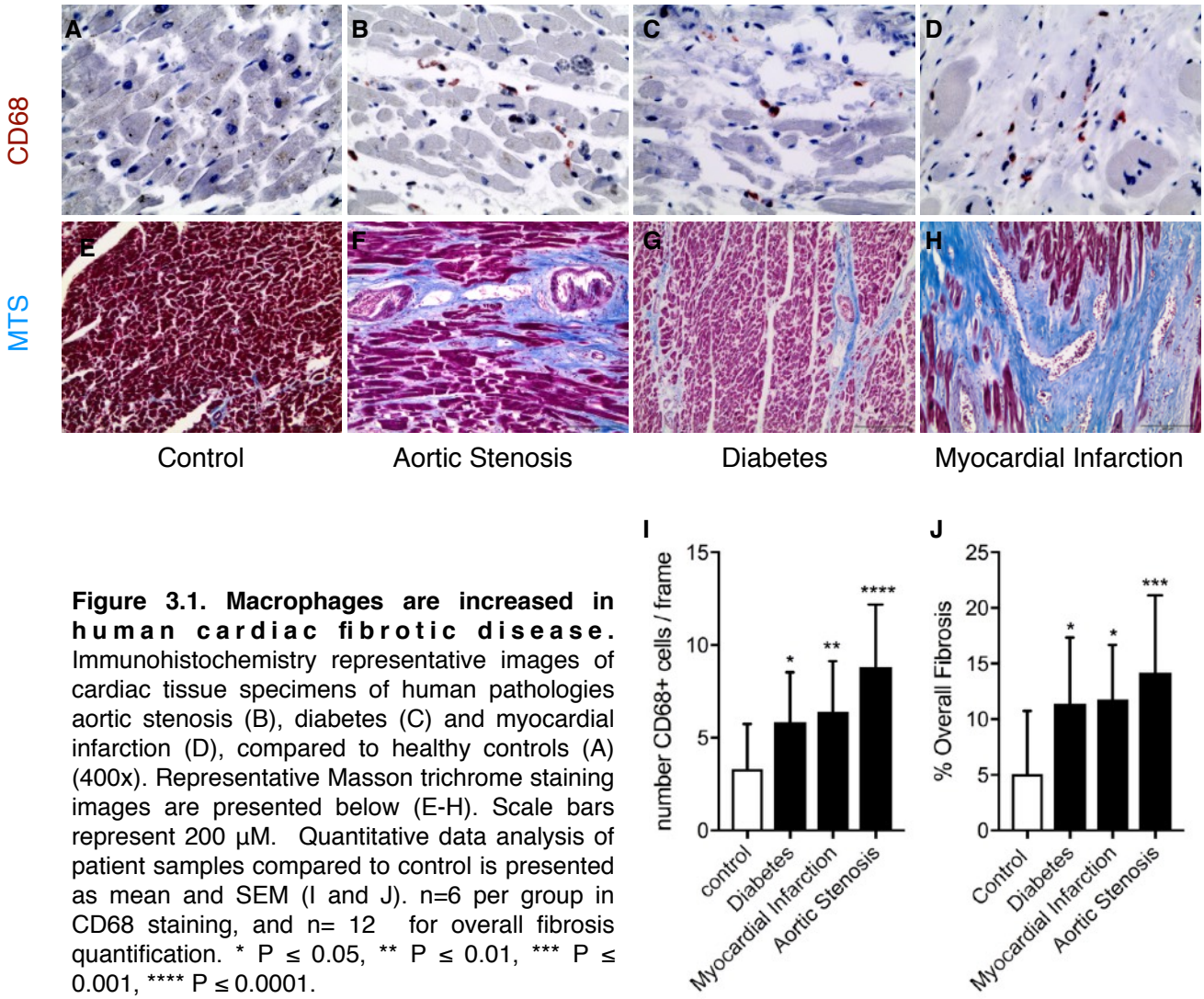

Figure 3.1. Macrophages are increased in human cardiac fibrotic disease. Immunohistochemistry representative images of cardiac tissue specimens of human pathologies aortic stenosis (B), diabetes (C) and myocardial infarction (D), compared to healthy controls (A) (400x). Representative Masson trichrome staining images are presented below (E-H). Scale bars represent 200 μM. Quantitative data analysis of patient samples compared to control is presented as mean and SEM (I and J). n=6 per group in CD68 staining, and n= 12 for overall fibrosis quantification. * $P \leq 0.05$, ** $P \leq 0.01$, *** $P \leq 0.001$, **** $P \leq 0.0001$.

3.1.2. Macrophage numbers are increased in murine models of cardiac fibrosis

Next, we investigated the content of murine macrophages in models of murine experimental cardiac fibrosis. We utilised Angiotensin II (Ang II) and ascending aortic constriction (AAC) models of cardiac fibrosis, which despite a different physiological approach, both succeed to induce robust cardiac fibrosis in mice (Figure 3.2, A-B and Figure 3.3, A-C). Angiotensin II is a pro-fibrotic protein and the central product of the renin-angiotensin system, a signalling pathway known to play a central role in cardiac and renal pathophysiological processes. The production of Ang II by this pathway, is known to cause potent increases in systemic and local blood pressure due to its vasoconstrictive effect (166). Ang II interferes directly with the cardiovascular system and induces

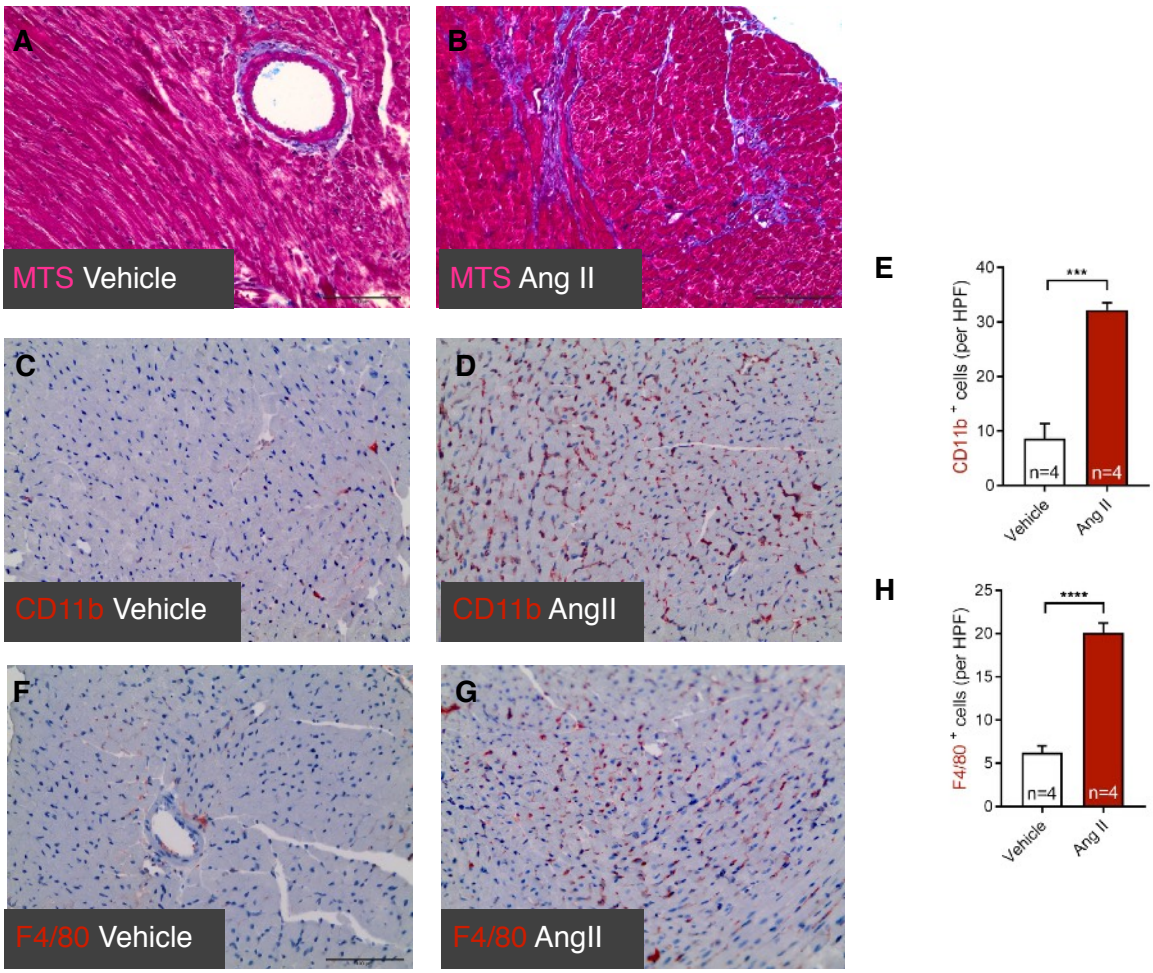

Figure 3.2. Macrophages increase in Angiotensin II murine heart. Immunohistochemistry representative images of paraffin sections of Angiotensin II murine myocardium showing expression of CD11b marker in vehicle control (C) and Angiotensin II treatment (D), and F4/80 macrophage marker in vehicle control (F) and Angiotensin treatment (G). Summarised quantitative findings are showed as means + SEM of 4 animals per group (E and H). *** $P \leq 0.001$, **** $P \leq 0.0001$. Ang = Angiotensin II. Scale bars represent 100µm.

vasoconstriction, cardiac hypertrophy, aortic aneurysms, atherosclerosis and myocardial fibrosis (166-168). Moreover, Ang II has pro-fibrotic effects alone *in vitro*. Pharmacological inhibition of the Angiotensin/Renin system by Ang II receptor blockers has beneficial effects in preventing cardiovascular maladaptive remodelling and CF. Osmotic pumps loaded with Ang II were implanted in mice at a pathophysiological concentration of 2.0 μg/kg/min for 14 days; a time point in which signs of fibrotic deposition were notable (Figure 3.2., B). We found that Ang II-treated myocardium was heavily invaded with macrophages, as indicated by immunohistochemistry staining of specific macrophage markers F4/80 and CD11b (Figure 3.2. C-G). Vehicle (saline) control mice also showed expression of myeloid cells (consistent with other reports showing a substantial amount of macrophages in the steady-state murine heart) (169), albeit to a much lesser extent than Ang II treated mice. F4/80 and CD11b staining patterns were associated with elongated cells located in the interstitial space between cardiomyocytes in fibrotic hearts, while F4/80- and CD11b-positive cells in control mice acquired a more rounded shape. Similarly, we found that AAC operated hearts harboured a significantly enhanced population of F4/80-positive and CD11b-positive cells as compared to sham control hearts (Figure 3.3., D-I). The AAC model is the murine analog of human aortic stenosis, and it is achieved by surgical constriction of the ascending aorta, which leads to pressure overload of the left ventricle and subsequent development of cardiac hypertrophy and myocardial fibrosis. In contrast to other reports showing that macrophage levels are reduced to almost baseline levels 21 days after TAC (170) (Transverse Aortic Constriction, a similar procedure that also induces pressure overload) (171), our findings show that 14 and 28 days post AAC operation, accumulation of macrophages remain significantly increased (Figure 3.3 J, K). This may be due to surgical differences between TAC and AAC models; where TAC involves a constriction of the transverse aorta at the aortic arch, AAC consists of banding of the ascending aorta section, closer to the heart. The AAC model results, in our experience, in a more robust and earlier manifestation of fibrosis, and this may result as well in a longer sustained inflammation compared to the TAC model.

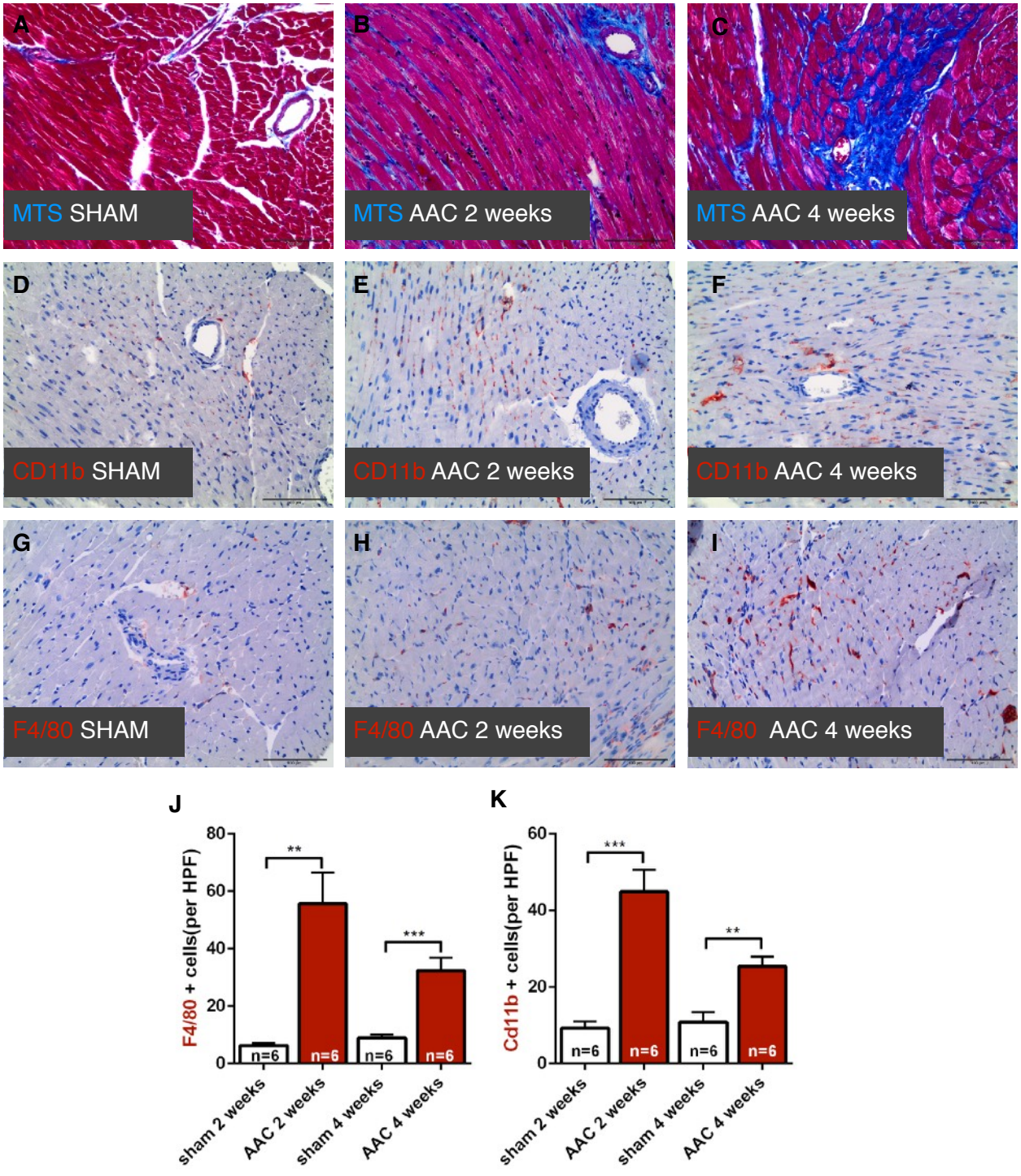

Figure 3.3. Macrophage number increases in AAC murine heart. Immunohistochemistry representative images of paraffin sections of fibrotic AAC mice showing MTS staining of SHAM (A) and AAC operated animals 2 weeks and 4 weeks after operation (B and C, respectively). Below, expression of CD11b marker in control SHAM operated animals(D) and AAC operated 2 and 4 weeks after operation (E and F), and F4/80 macrophage marker in SHAM (G) and AAC operated mice 2 and 4 weeks after operation (H and I, respectively). Summarised quantitative findings are showed as means + SEM of 6 animals per group (J and K). Scale bars represent 100 μm. P values correspond to ** P ≤ 0.01, *** P ≤ 0.001, between sham and AAC groups, calculated using non-parametric t-test analysis. AAC = ascending aortic constriction

3.1.3. EndMT occurs in atherosclerotic ApoE-deficient mice

Atherosclerotic lesions are great examples to explore the object of study in this thesis: they represent a local environment where endothelial damage, high inflammatory and fibrotic mediators and maladaptive macrophage accumulation come together (157). In the atherosclerotic plaque, accumulation of monocytes and macrophages are associated with a focal chronic inflammatory process that leads to necrosis and fibrous cap thinning in advanced atherosclerotic disease (173).

For identification of endothelial cells undergoing EndMT in atherosclerosis, tissue sections from aorta roots of ApoE-deficient mice were analysed using confocal microscopy. The ApoE deficient mouse is a widely used atherosclerotic mouse model that spontaneously develops atherosclerotic lesions, which are accelerated upon a high fat diet (HFD). This is because ApoE functions as a ligand of members of the low-density lipoprotein receptor (LDLR) family that clear chylomicrons and very low–density lipoprotein remnants. ApoE is also synthesised by monocytes and

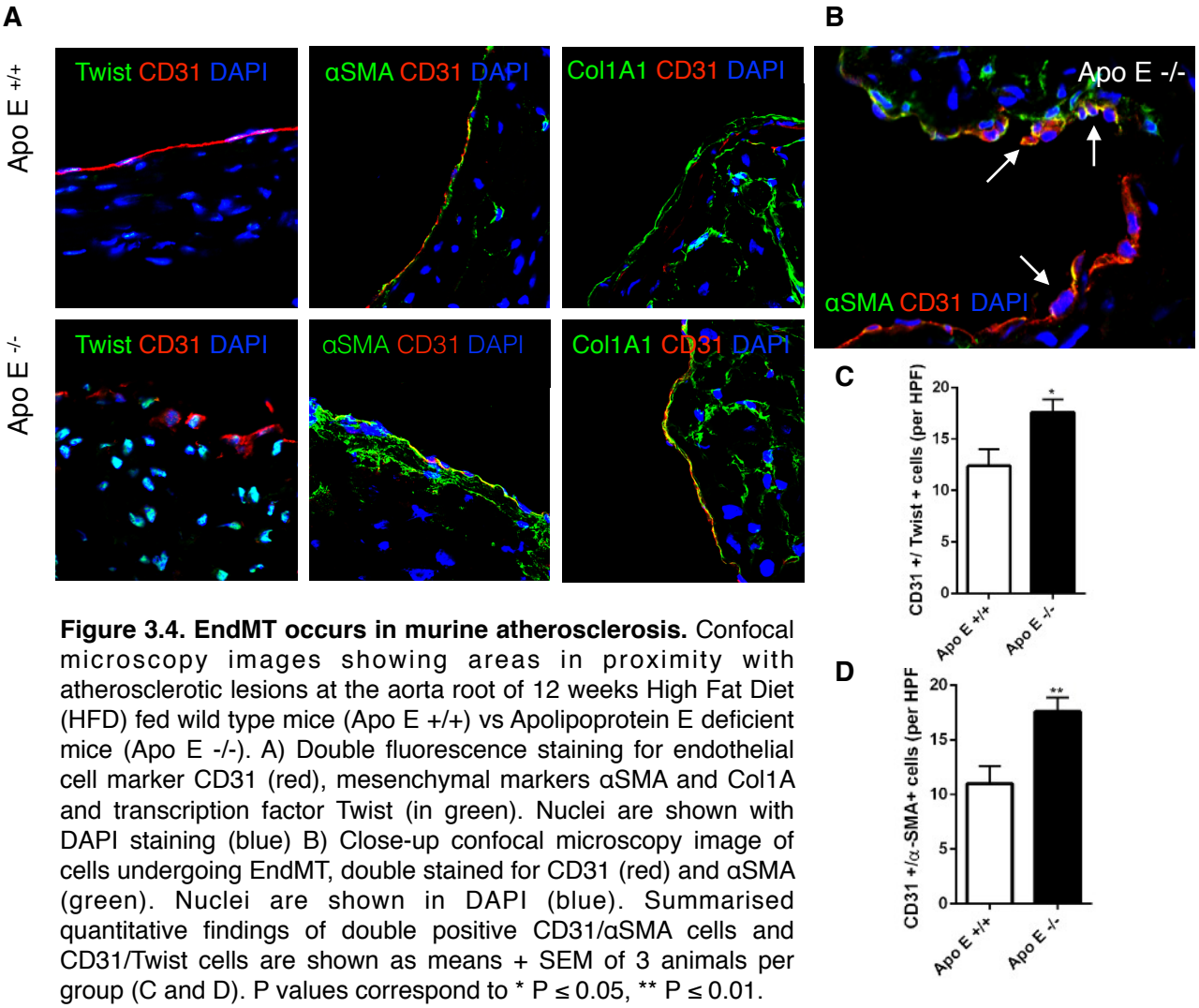

Figure 3.4. EndMT occurs in murine atherosclerosis. Confocal microscopy images showing areas in proximity with atherosclerotic lesions at the aorta root of 12 weeks High Fat Diet (HFD) fed wild type mice (Apo E +/+) vs Apolipoprotein E deficient mice (Apo E -/-). A) Double fluorescence staining for endothelial cell marker CD31 (red), mesenchymal markers αSMA and Col1A and transcription factor Twist (in green). Nuclei are shown with DAPI staining (blue) B) Close-up confocal microscopy image of cells undergoing EndMT, double stained for CD31 (red) and αSMA (green). Nuclei are shown in DAPI (blue). Summarised quantitative findings of double positive CD31/αSMA cells and CD31/Twist cells are shown as means + SEM of 3 animals per group (C and D). P values correspond to * $P \leq 0.05$, ** $P \leq 0.01$.

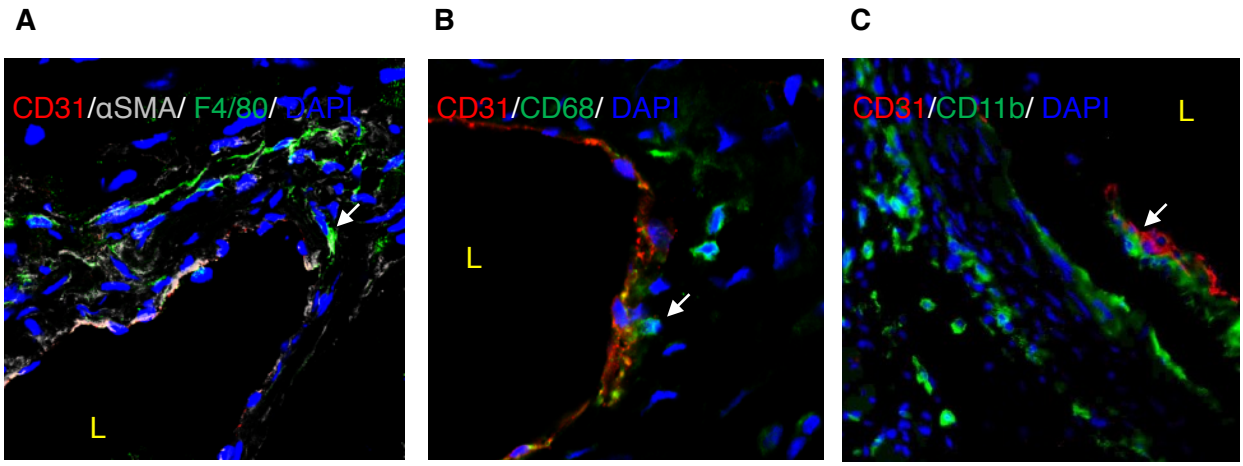

Figure 3.5. Macrophages are located in the vicinity of the endothelium. Accumulating macrophages in atherosclerotic aortas interact with endothelial cells. Representative confocal microscopy images show areas in proximity with atherosclerotic lesions of 12 weeks HFD fed wild type mice (Apo E +/+). A) Triple staining with CD31, a-SMA and macrophage marker F4/80. B) Macrophages are shown stained for CD68 (green). C) CD11b positive cells (green) interact closely with endothelial cells, positive for CD31 (red).Nuclei are shown wit DAPI staining (blue). L= lumen

macrophages in vessels, and is thought to have local effects on cholesterol homeostasis and on inflammatory reactions in atherosclerotic vessels (174).

Because occurrence of EndMT has already been shown elsewhere (71,72) and since endothelial cells in atherosclerosis are exposed to an extensive inflammatory environment fuelled by macrophages, we hypothesised that atherosclerotic macrophages were associated with EndMT. We found cells co-expressing endothelial marker CD31 and mesenchymal markers α-SMA and Collagen I in atherosclerotic plaques of ApoE- HFD- fed mice. We found that the amount of double-positive cells was significantly higher in ApoE-deficient mice compared with wild type HFD fed control group (Figure 3.4.). We also found enhanced expression of EndMT transcription factor Twist in ApoE deficient mice. We found that CD31/Twist double positive cells and CD31/α-SMA double positive cells were increased in ApoE mice compared to wild type (Figure 3.4 C and D). Interestingly, we also found Twist highly expressed in cells negative for CD31 adjacent to the endothelium. Furthermore, we stained macrophages with F4/80, CD68 and CD11b antibodies, and found that macrophages localised in close contact with endothelial cells (Figure 3.5).

3.2. Inflammatory cytokines TNF-α and IL-1ß induce EndMT in MCECs.

In order to develop an effective *in vitro* EndMT system for this study, we chose an immortalised mouse cardiac endothelial cell line (MCECs) as a suitable murine *in vitro* tool, compatible with the following experiments using murine macrophage cell lines. In order to establish experimental canonical EndMT induction in MCECs, we treated MCECs with TGF-ß1 at different concentrations (1 and 10ng/ml) for 1, 2 and 4 days. We found the strongest and most consistent induction of EndMT transcription factors (*Snail*, *Slug* and *Twist*) and mesenchymal marker gene *Acta2* using a concentration of 10ng/ml of human recombinant TGF-ß1 during 2 days of treatment (Figure 3.6., A and B). This was reflected at the protein level with a decrease of the endothelial marker CD31, and an increase of the EndMT transcription factor Snail and the mesenchymal protein alpha-SMA (Figure 3.6., C). TGF-ß1 treatment for 4 days was associated with a morphological change (Figure 3.6, D), in which endothelial cells showed a more elongated and spindle-shaped appearance, typical of migrating mesechymal-like cells.

Next, due to their known potential as EndMT inducers (117,118), we treated MCECs with inflammatory cytokines TNF-α and IL-1ß, to examine whether MCECs were inflammation-responsive and capable of undergoing EndMT in these conditions. Both TNF-α and IL-1ß were able to stimulate expression of *Acta2,* and *Fsp1 (*also known as *S100a4*) expression although considered a modest induction compared to TGF-ß induced-EndMT (Figure 3.7). When comparing both inflammatory cytokines, TNF-α was the strongest inducer.

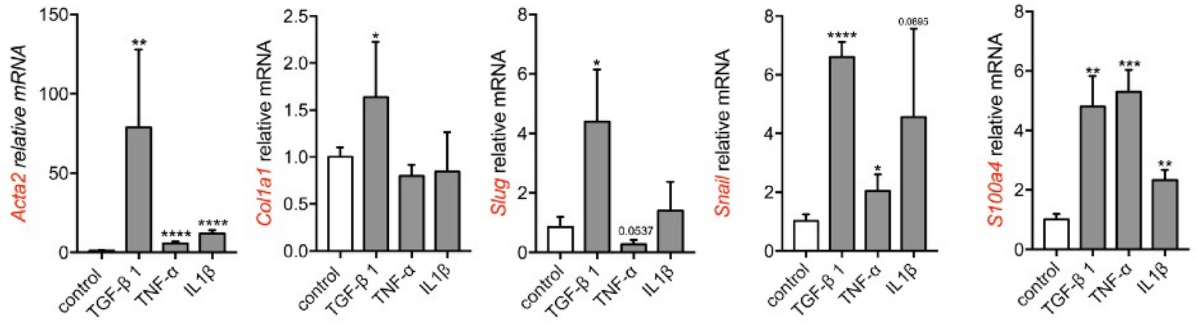

Figure 3.7. Inflammatory cytokines TNF-α and IL-1ß promote mesenchymal phenotype in MCEC. RTq-PCR analysis of EndMT relevant genes upon TGFß-1(10ng/ml), TNF-α.(100ng/ml) and IL-1ß(20ng/ml). Results are shown as means + SEM of triplicate determinants and are representative of two independent experiments (n=2). * P ≤ 0.05, ** P ≤ 0.01, *** P ≤ 0.001, **** P ≤ 0.0001.

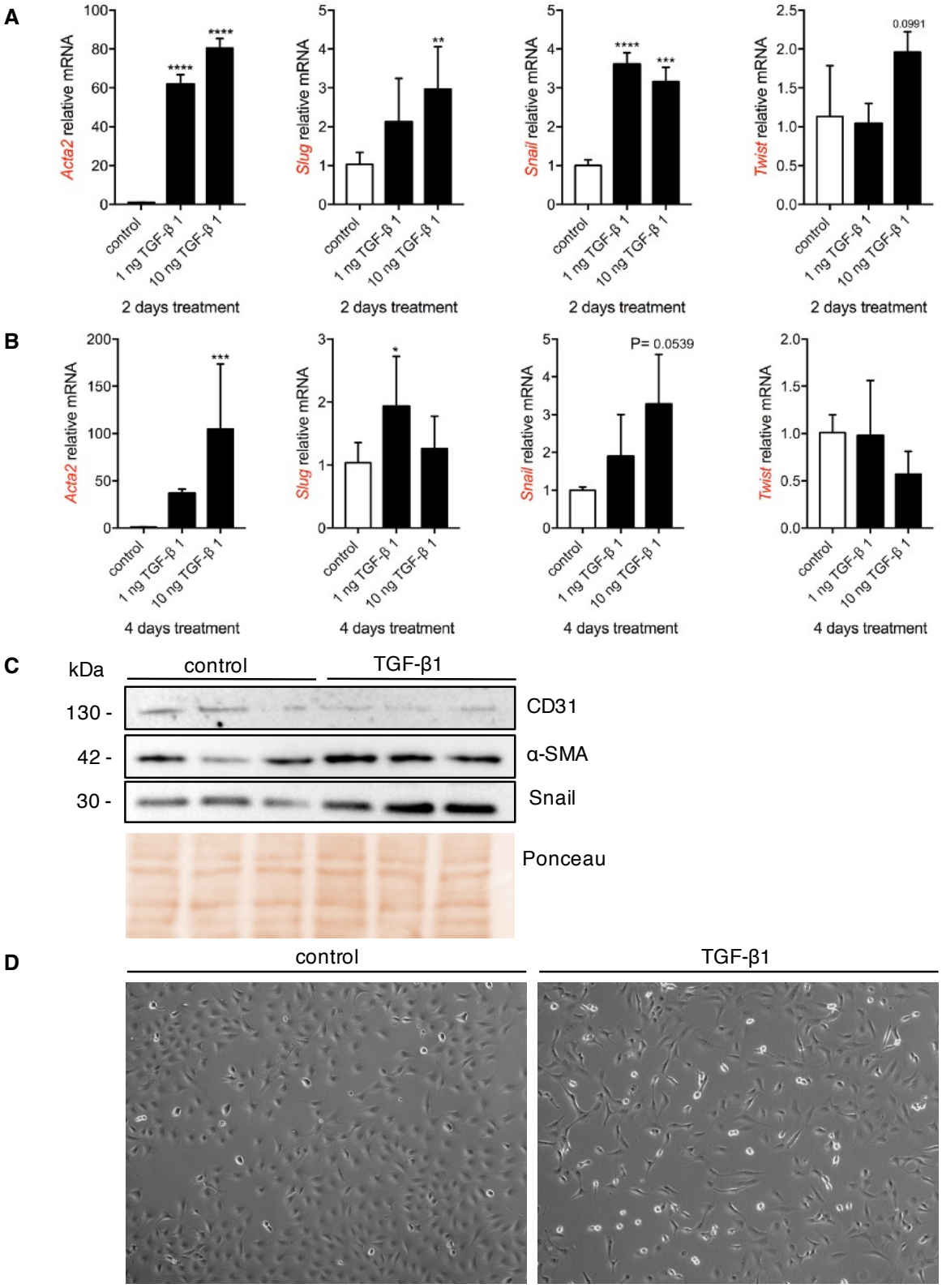

Figure 3.6. Mouse cardiac endothelial cells undergo Endothelial-to-Mesenchymal Transition upon TGF-ß 1 stimulation. A) RTq-PCR analysis of EndMT marker genes of MCECs after 2 days TGF-ß1 treatment. B) qRT-PCR analysis of EndMT marker genes of MCECs after 4 days TGF-ß1 treatment. qRT-PCR results are shown as means + SD of triplicate determinants and are representative of three independent experiments. * P ≤ 0.05, ** P ≤ 0.01, *** P ≤ 0.001, **** P ≤ 0.0001. C) Immunoblot showing protein expression of CD31, αSMA and Snail in MCECs upon 4 days of TGF-ß1 treatment. Loading control is shown in Ponceau total protein membrane staining. This blot is a representative image of three independent experiments. E) Bright field microscopy images showing morphological change of MCECs after 4 days of TGF-ß1 treatment (100x).

3.3. Phenotype profile of bone marrow-derived macrophages in basal and LPS stimulation conditions

Granulocyte-macrophage colony-stimulating factor (GM-CSF) and macrophage colony-stimulating factor (M-CSF) cytokines are known to promote monocyte differentiation into functionally different macrophages (175-177,205). GM-CSF gives rise to GM- bone marrow-derived macrophages (hereafter termed GM-BMDM) that produce pro-inflammatory mediators upon Toll-like-receptor (TLR) stimulation, whereas M-CSF generates M- bone marrow-derived macrophages (M-BMDM) with enhanced anti-inflammatory cytokine IL-10 production in response to pathogenic stimuli. Lipopolysaccharide (LPS) treatment, either alone or in combination with interferon gamma (IFNγ), is considered as the paradigmatic stimulus for acquisition of the classical macrophage polarisation/ activation state. In order to investigate whether macrophages can induce EndMT, we first generated polarised macrophages derived from bone marrow progenitors. Murine bone marrow cells were cultured *in vitro* for 7 days in the presence of GM-CSF or M-CSF cytokines and the adherent cells (GM-BMDM and M-BMDM) were collected. After day seven of macrophage differentiation and polarisation protocol, we confirmed that both populations express common macrophage markers CD11b and F4/80 (Figure 3.8. A and B) by FACS and immunofluorescence staining. Under basal conditions, GM-BMDM and M-BMDM showed limited but significantly different mRNA levels of TNF-α, IL-10 and inflammatory chemokine CCL2. The relative basal levels of CCL2 and Interleukin 12 subunit IL12p40 were enhanced in GM-BMDM compared to M-BMDM ($P < 0.01$) whereas the relative basal mRNA levels of anti-inflammatory IL-10 were enhanced in M-BMDM compared to GM-BMDM (Figure 3.8, C and D). There were no significant differences in the basal mRNA levels of IL-6, TNF-α or IL-23 between the two macrophage populations.

E.Coli derived exogenous LPS treatment was used as the pathogen associated microbial pattern (PAMP) to stimulate macrophage TLR receptors. Upon TLR stimulation, GM-BMDM produced significantly more TNF-α ($P < 0.01$) and IL-6 ($P < 0.01$) compared with M-BMDM (Fig. 3.8. C, pattern bars). Both IL-12p70 and IL-23 are composed of two subunits, a common p40 subunit and either a p35 or a p19 subunit, respectively (176). GM-BMDM secreted IL-23 following LPS stimulation whereas M-BMDM failed to do so over a 24-h period. LPS-stimulated M-BMDM and

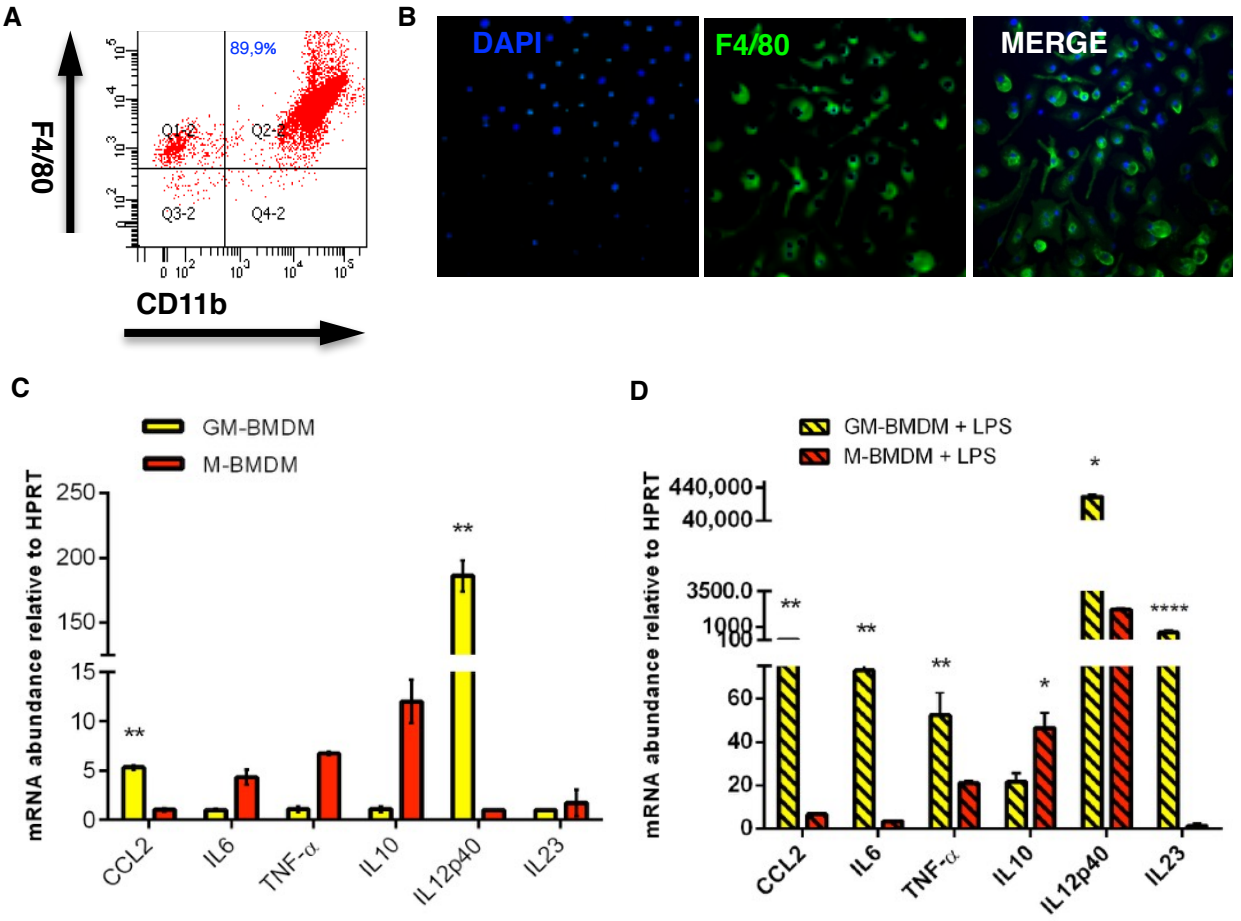

Figure 3.8. Characterisation of GM-BMDM and M-BMDM. BMDM were characterised after 7 + 1 days of differentiation protocol. A) Representative flow cytometry analysis graph of F4/80 and CD11b macrophage marker expression in BMDMs at day 7 of the differentiation protocol. B) Representative immunofluorescence pictures of BMDM expressing F4/80 (95%-99%). C-D) Differential stimulatory activity and basal cytokine mRNA expression of GM-BMDM and M-BMDM. Basal (bold graphs, left) and LPS stimulated (pattern graphs,right) cytokine mRNA expression in GM-BMDM and M-BMDM as measured by qRT-PCR. Levels of CCL2, IL-6,TNF- α, IL-10, IL-12p40 and IL-23p19 mRNA were normalised to an endogenous reference (HPRT) and calibrated to the lowest expression level for each cytokine. The results represent the mean + SEM of values from five independent experiments. n= 5

GM-BMDM robustly produced IL-12p40, although M-BMDM at slightly lower levels than GM-BMDM. In contrast to the above, LPS-stimulated M-BMDM secreted enhanced IL-10 ($P < 0.05$). Taken together, two bone marrow-derived macrophages lineages with differential expression of inflammatory and anti-inflammatory mediators were generated.

3.4. Characterisation of macrophage polarisation in RAW 264.7 cells.

In order to obtain distinct inflammatory phenotypes in RAW 264.7 cell line, a murine immortalised macrophage cell line, an activation protocol was established using the pro-inflammatory cytokine IFNγ, and anti-inflammatory cytokine IL-4, and TLR agonist LPS. RAW 264.7 cells were treated

with either IL-4 (20ng/ml) , IFNγ(100ng/ml), LPS (50ng/ml) or a combination of IFNγ and LPS in a time course of 2, 6, 12 and 24 hours. Pro-inflammatory common markers iNOS (inducible nitric oxide synthase) and MHCII (major histocompatibility class II) protein levels were found increased in IFNγ-RAWs and LPS-RAWs after 24 hours of treatment (Figure 3.9., A), while a modest or no increase was observed in IL-4-treated RAW 264.7 cells. Moreover, the morphology drastically

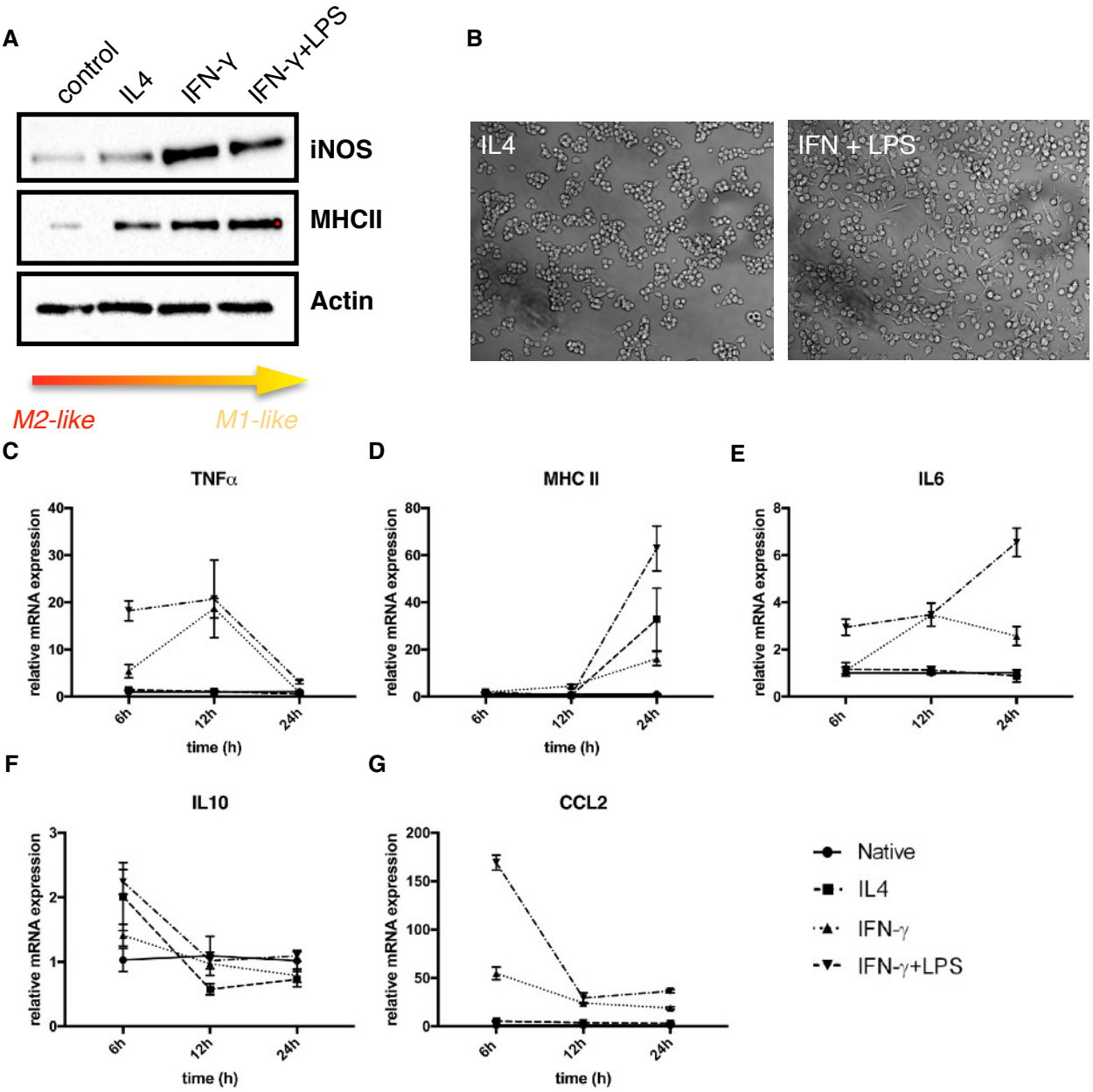

Figure 3.9. Characterisation and polarisation of RAW 264.7 cells. A) Western Blot showing protein expression of activation markers iNOS and MHCII in RAW 264.7 cells after overnight treatment with IL4 (20ng/ml), IFN-γ (100ng/ml) and LPS (50ng/ml). B) Representative bright field microscopy picture showing a differential morphological effect of IL4 and IFN+LPS after 24 hours of treatment. C-G) Stimulatory activity and cytokine mRNA expression of RAW 264.7 cells as measured by qRT-PCR. Levels of TNF- α, MHCII, IL-6, IL-10 and CCL2 mRNA were normalised to an endogenous reference (HPRT) and calibrated to the expression level 6 hours time for each cytokine. Where not visible, error bars are smaller than the symbol. The results represent the mean + SEM values from three independent experiments. n=3.

changed upon treatment, leading to round aggregated cells in IL4-RAWs after 24 hours and stellated filopodia-forming cells in IFN/LPS-RAWs (Figure 3.9., B).

When tested for a time response to distinct activators, native, IL-4-, IFNγ- and IFNγ+LPS RAW 264.7 cells showed a differential expression of MHCII, chemokine CCL2 and cytokines IL-6 and TNF-α (Figure 3.8., C-G). IFNγ- and IFNγ+LPS-RAWs showed the highest induction of TNF-α and CCL2 (Figure 3.8., C,G) after 6h of treatment, and this induction was enhanced in IFNγ+LPS-RAW 264.7 cell line ($P < 0.05$ IFNγ-RAW *versus* LPS stimulated IFNγ-RAW). MHCII and IL-6 expression was increased after 24 hours in IFNγ+LPS-treated RAW 264.7 cells. IL-10 showed a milder increase in IL-4-treated RAWs (not significant) (Figure 3.8 F) at 6 hours of LPS treatment, suggesting that these activators did not promote the IL-10 response in RAWs.

3.5. Macrophage paracrine signalling failed to effectively induce EndMT

Cardiac fibrotic processes are initiated by the activation of inflammatory pathways, which are triggered upon most types of cardiac injury (79). This accounts for an increase of cytokines, chemokines, adhesion factors and proteases during fibrotic injury, which are secreted by myeloid cells that have been recruited to the cardiac injury or resident myeloid and stromal progenitors which are activated at the local site of cardiac injury. Resident cardiac macrophages are localised in direct contact with vascular endothelial cells, at perivascular regions, and contribute to maintain cardiac homeostasis in the steady-state heart (169). We and others have shown that the macrophage number is increased in the pathological heart. This may be due to influx of newly formed monocytes from peripheral hematopoiesis and local proliferation of resident cardiac macrophages (144), and although they are indispensable for wound healing macrophages also contribute to the onset and worsening of pathological conditions in the heart (178,179).

To recapitulate and study intercellular signalling between cardiac macrophages and endothelial cells, we generated mouse GM-BMDM and M-BMDM lines and investigated paracrine communication of GM-BMDM and M-BMDM towards endothelial cells. For this purpose, BMDM cell lines were cultured in basal media to be able to collect GM-BMDM- and M-BMDM derived conditioned medium (CM). MCECs were cultured in media previously conditioned by each BMDM lineage and were analysed thereafter for EndMT marker genes. It was found that CM derived from M-BMDM or GM-BMBM, either LPS-stimulated or non-stimulated, did not succeed to induce

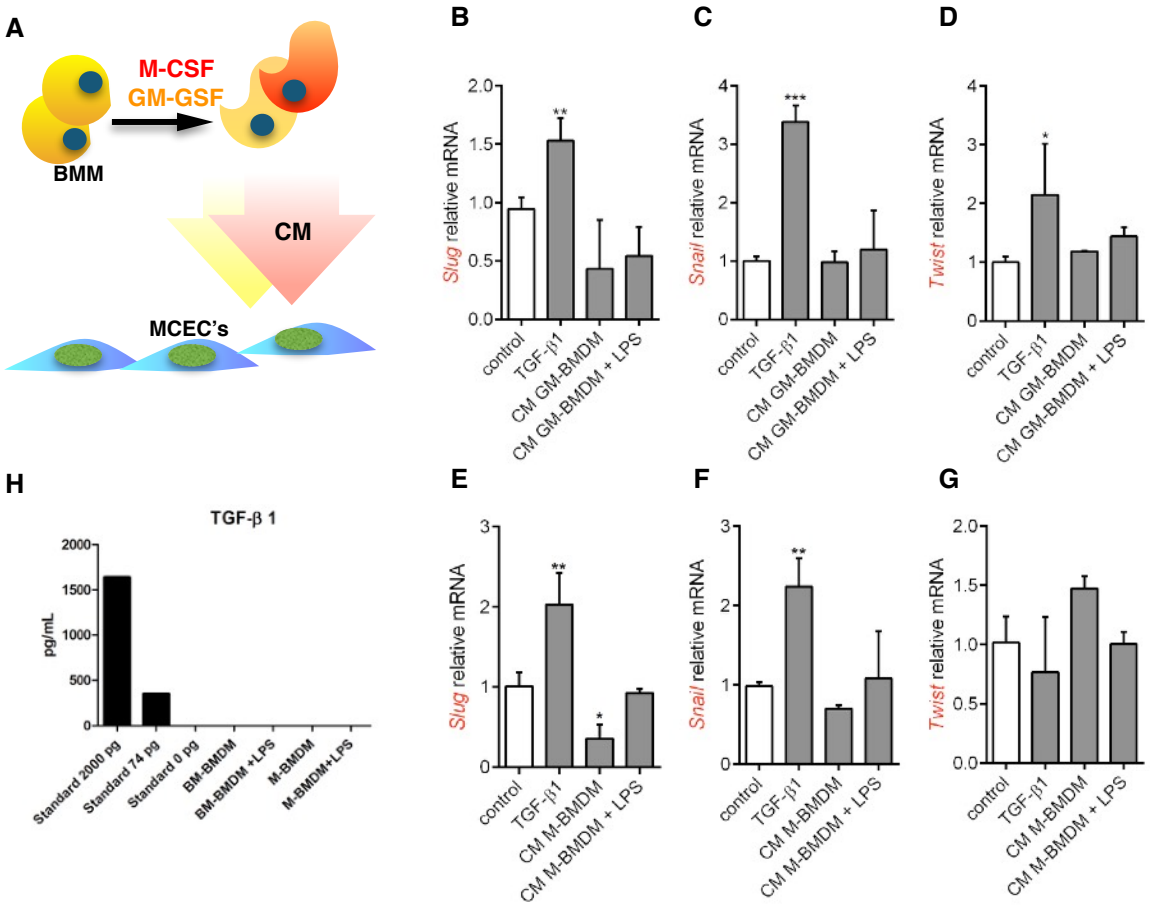

Figure 3.10. BMDMs derived CM has little limited effect on MCECs. A) Schematic drawing of conditioned media (CM) experimental plan. Murine bone marrow derived monocytes are differentiated into GM-BMDM or M-BMDM macrophages with cytokines GM-CSF or M-CSF. After differentiation and LPS stimulation, BMDMs are cultured in basal media, which is conditioned by the macrophages and thereafter applied to MCECs. B-D) qRT-PCR results of EndMT markers gene expression of MCECs grown in CM from GM-BMDMs. E-F) qRT-PCR results of EndMT markers gene expression of MCECs grown in CM from M-BMDMs. Results are shown as means + SEM of triplicate determinants and are representative of eight independent experiments (n=8). * $P \leq 0.05$, ** $P \leq 0.01$, *** $P \leq 0.001$, **** $P \leq 0.0001$ H) TGFß-1 protein levels in culture media from GM-BMDM and GM-BMDMs, as determined by ELISA (n=3).

EndMT alone (Figure 3.10. B-G). Furthermore, supernatants derived from resident peritoneal macrophages also did not promote EndMT when applied to MCECs (Supplementary material, Figure 1). Only CM derived from peritoneal macrophages of thioglycolate solution injected mice was able to induce expression of *Snail*, *Acta2* and *Twist* genes in combination with TGF-ß1 (Supplementary Data, Figure 2). To further evaluate whether TGF-ß1 was present in the BMDMs-derived CM, supernatant protein content of TGF-ß1 was analysed by ELISA and no detectable protein levels of TGF-ß1could be found (Figure 3.10, H).

In light of these results, we asked if bidirectional communication between macrophages and endothelial cells could induce EndMT phenotype in endothelial cells. To address this question, we

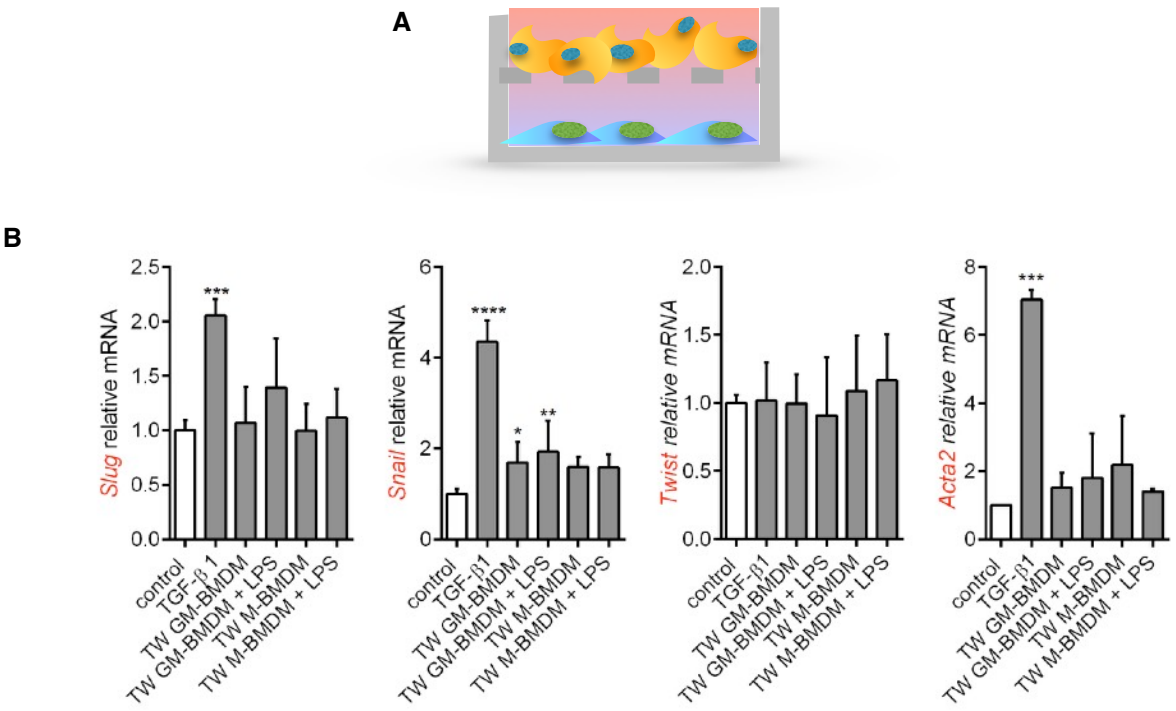

Figure 3.11. Paracrine exchange between BMDMs and MCECs does not induce EndMT. A) Schematic image of paracrine Transwell® system. B) qRT-PCR results of EndMT markers gene expression of MCECs co-cultured with GM-BMDMs and M-BMDMs with and without LPS stimulation. Results are shown as means + SEM of triplicate determinants and are representative of three independent experiments (n=3). * $P \leq 0.05$, ** $P \leq 0.01$, *** $P \leq 0.001$, **** $P \leq 0.0001$

co-cultured the BMDMs and MCECs in a Transwell® system. Using Transwell® inserts with a 0.4 μm pore, there is allowance for the exchange of soluble factors between endothelial cells and macrophages (paracrine communication) without being physically in contact with each other. EndMT gene expression marker analysis after 72 hours of Transwell® co-culture incubation showed no significant change of co-cultured cells compared with their mono-culture controls (Figure 3.11).

.

3.6. Macrophage juxtacrine signalling induces EndMT and is enhanced upon macrophage TLR stimulation.

3.6.1. Efficient contact co-culture tracking and separation

To address the possibility of a contact-dependent induction of EndMT by macrophages, MCECs and BMDMs were co-cultured in the same tissue culture dish, ensuring direct contact between cells. To enable the separation of endothelial cells from macrophages after cell-cell contact

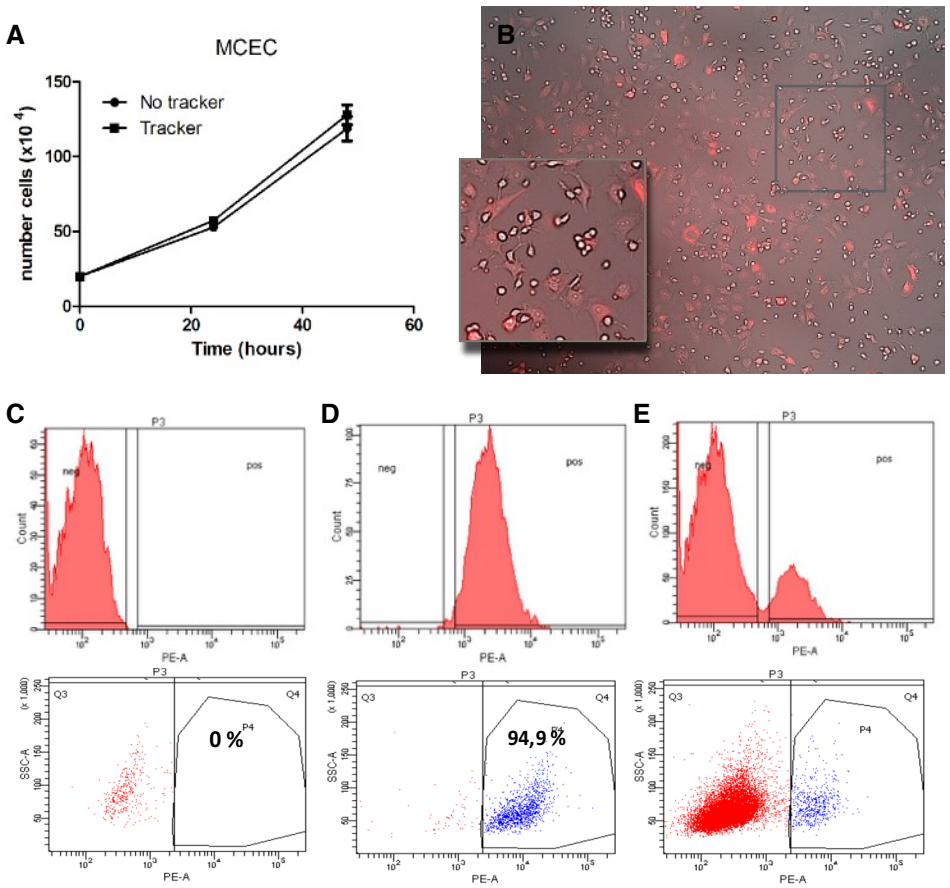

Figure 3.12. Live cell CMTMR fluorescent tracker co-culture and separation. A) Proliferation of MCECs stained with CMTMR tracker. MCECs were seeded into six-well plates at a density of 20,000 cells per well, trypsinized, and counted after 24 and 48 hours. Compared with native MCECs, CMTMR tracker did not increase or decrease MCEC proliferation. Experiments were replicated three times, and data are presented as means. B) Representative bright field image merged with fluorescence microscopy image showing co-culture of RAW 264.7cells (unstained, white) and MCECs (stained, red) magnification is 100x. (C-E) FACS separation of co-cultured cells. Representative FACS data showing negative control of non stained cells (C), positive control of only stained cells (D), and distinguishable populations from co-cultures (E).

interaction for further analysiss, a fluorescence live tracking system was designed. In this system, MCECs were previously stained in culture with a live fluorescent probe, specifically, an orange Cell Tracker CMTMR Dye. CMTMR is taken-up by the cell in culture conditions quickly, and it remains in the cell for at least 48 hours(155). CMTMR did not show any signs of cytotoxicity. Endothelial cells containing the fluorophore did not proliferate at a different doubling rate (Figure 3.12 A) or adopt a different morphology while transporting the tracker (Figure 3.12 B) than native MCECs. Also, we could clearly observe that the tracker staining pattern inside the endothelial cell did not change through cell cycles, and we visualised no signs of transfer of tracker to neighbour unstained cells, as we did not see stained macrophages. Since macrophages are easily distinguishable to the naked eye due to their small size in comparison with endothelial cells, we

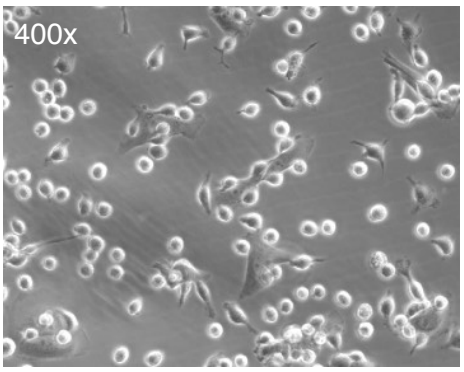

Figure 3.13. Co-cultured peritoneal macrophages. Representative bright field microscopy showing peritoneal macrophages (bright round small cells) attached to MCECs.

could observe that macrophages remained unstained by observing at the fluorescent microscope. This allowed for an efficient separation by FACS sorting (Figure 3.12. C-E). The efficient cell separation using Cell CMTMR Tracker live-staining has been confirmed in other studies (155,180).

3.6.2. MCECs analysis after co-culture with macrophages

3.6.2.1. Co-culture of MCECs with peritoneal resident macrophages

Peritoneal macrophages (PM) were harvested from the peritoneum of healthy wild type mice and cultured following standard procedures. The idea behind using PM was to use a primary cell line that could resemble steady-state resident macrophages. We found that PM were strongly attracted to endothelial cells and after overnight incubation, the majority of the macrophages were attached to endothelial cells (Figure 3.13).

After co-culture and FACS sorting, MCECs were analysed for EndMT markers using qRT-PCR, which showed a significant 5-fold induction of EndMT transcription factor *Snail* and a 60-fold

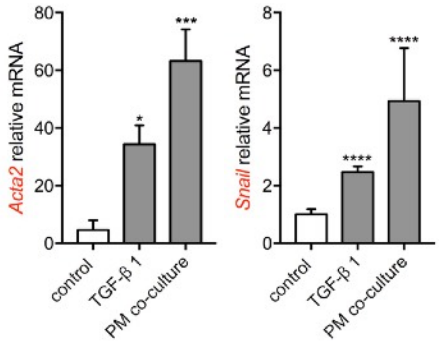

Figure 3.14. Juxtacrine communication between peritoneal macrophages and MCECs induces EndMT. qRT-PCR analysis of MCECs after co-culture with peritoneal macrophages (PM). Results are shown as means + SEM and are representative of nine independent experiments (n=9). * $P \leq 0.05$, *** $P \leq 0.001$, **** $P \leq 0.0001$.

increase of *Acta2* mRNA expression. Macrophage-induced EndMT was enhanced in comparison with mono-cultured MCECs and also in comparison with TGF-ß1 treated MCECs (Figure 3.14).

3.6.2.2. Co-culture of MCECs with polarised macrophage cell lines

To also examine the effect of co-culture of MCECs with BMDMs, GM-BMDM and M-BMDM cell lines were co-cultured with MCECs. BMDMs were either LPS-stimulated or non-stimulated before co-culturing. Co-cultured MCECs were compared to MCECs grown in mono-culture. It was found that MCECs grown in contact with BMDMs had an overall enhanced mesenchymal phenotype compared to mono-cultured MCEC controls (Figure 3.15). LPS-treated cell lines, both GM-BMDMs and M-BMDMs, had an stronger effect than non-stimulated BMDMs. *Acta2* and *Snail* mRNA expression was robustly up-regulated in LPS-GM-BMDM and LPS-M-GMDM cell lines, being slightly higher in GM-BMDMs. *Slug* was also up-regulated in native GM-BMDM and LPS-GMDM macrophages co-cultures. Interestingly, in MCECs co-cultured with LPS-stimulated M-BMDMs we observed a strong induction of *Twist*, an EndMT transcription factor that does not get up-regulated in TGF-ß1-treated MCECs. Overall, this data suggests that TLR-activation in macrophages via LPS-stimulation enables them to induce EndMT, and that M-BMDM and GM-BMDM do not seem to act distinctly regarding EndMT induction.

Next, we investigated the effect of co-cultures using RAW 264.7 on MCECs. Native, IL-4-, and LPS-stimulated IFNγ-RAW 264.7 cells were utilised for co-culture and found that LPS-stimulated IFN-γ RAW 264.7 cells consistently induced EndMT (as shown in Figure 3.16) by significantly up-

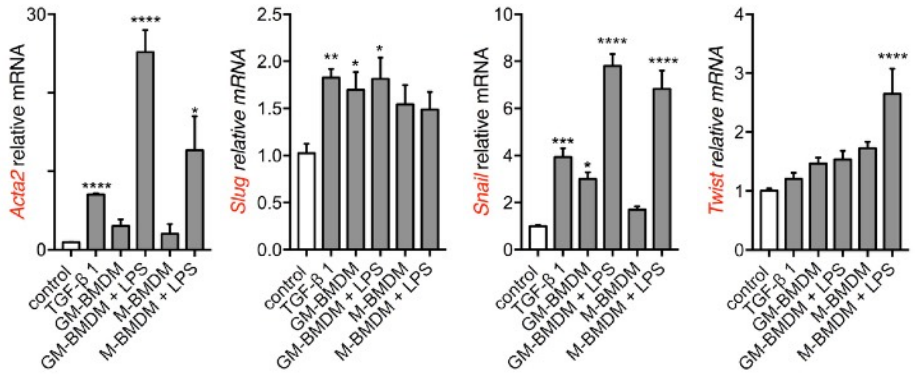

Figure 3.15. Juxtacrine communication between LPS stimulated BMDMs and MCECs induce EndMT. qRT-PCR analysis of MCECs after co-culture with BMDM cell lines. Results are shown as means + SEM of triplicate determinants and are representative of three independent experiments (n=3). * P ≤ 0.05, ** P ≤ 0.01,*** P ≤ 0.001, **** P ≤ 0.0001.

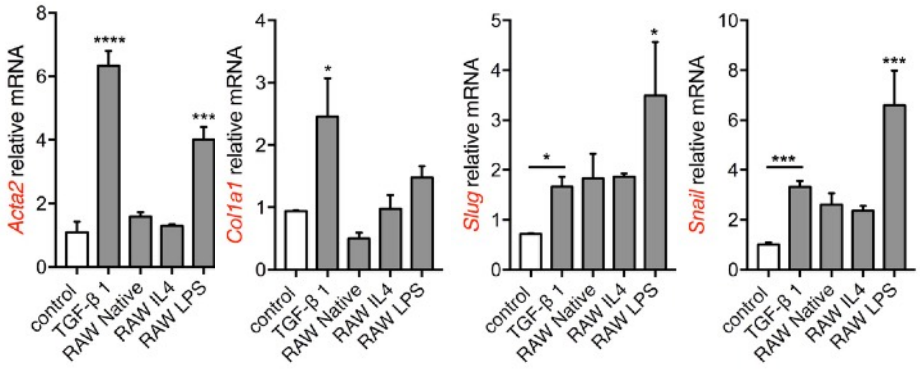

Figure 3.16. Juxtacrine communication between LPS stimulated IFNγ-RAW 264.7 and MCECs induce EndMT. qRTq-PCR analysis of MCECs after co-culture with RAW 264.7 cell lines. Results are shown as means + SEM of triplicate determinants and are representative of three independent experiments (n=3). * P ≤ 0.05, *** P ≤ 0.001.

regulating *Slug*, *S*nail, and *Acta2* mRNA expression. *Col1a1* mRNA expression was enhanced almost significantly (P = 0.056008) in LPS-stimulated IFNγ-RAWs, whereas no changes in *Twist* (data not shown) were observed.

To rule out the possibility that LPS itself was the inducer of EndMT despite extensive washing of macrophages after LPS-stimulation and before co-cultures with MCECs, we treated MCECs mono-cultures with macrophage inflammatory inducers IFNγ and LPS, and analysed the cells for EndMT markers gene expression after 48h incubation. We found no statistically significant differences in EndMT markers mRNA expression in MCECs treated with IFNγ, LPS, or a combination of both. In contrast, we found that combination of IFNγ- and LPS-stimulation significantly reduced *Snail* and *Col1a1* mRNA expression (Figure 3.17).

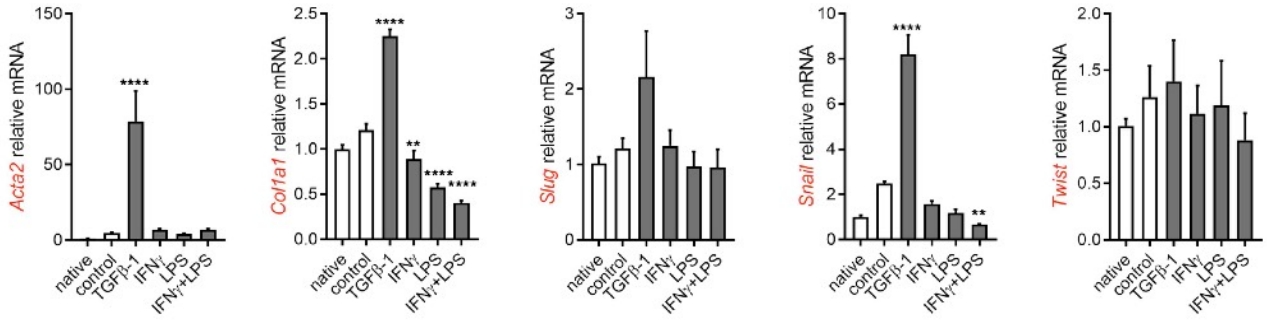

Figure 3.17. Exogenous LPS does not induce EndMT in MCECs. qRT-PCR analysis of MCECs after treatment with IFNγ, LPS, and IFNγ and LPS combined. Results are shown as means + SEM of triplicate determinants and are representative of three independent experiments (n=3). ** P ≤ 0.01, **** P ≤ 0.0001.

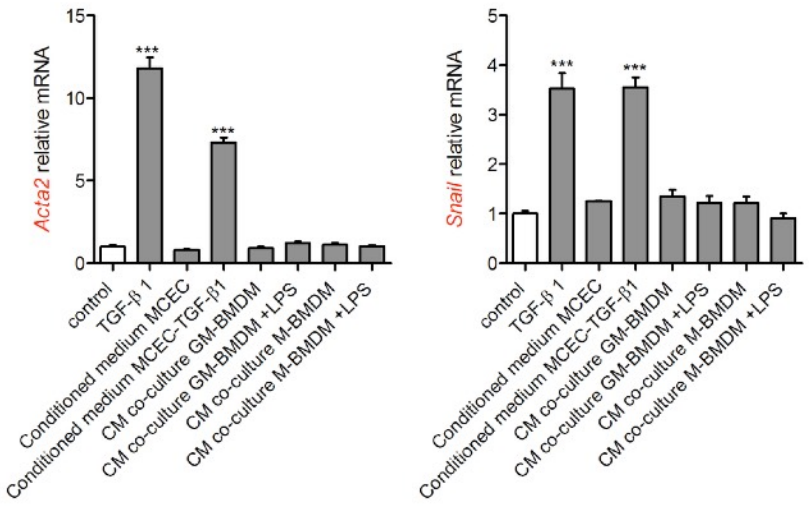

Figure 3.18. Conditioned medium derived from co-cultures does not induce EndMT. RTq-PCR analysis of MCEC treated with conditioned medium (CM) derived from native MCEC, from TGF-ß 1 treated MCEC, and from co-cultures of MCECs and BMDMs cell lines. Results are shown as means + SEM of triplicate determinants and are representative of three independent experiments (n=3). *** $P \leq 0.001$

In light of these results, we hypothesised that even though cell-cell contact seemed a necessary stimulus for macrophages to induce EndMT, cell-cell contact might not be the underlying mechanism that directly induces EndMT, but cell contact could rather be an initial step necessary for the effector cell (macrophage or endothelial cell) to release soluble signals which in turn induce EndMT. To investigate whether cell-contact between macrophages and endothelial cells could be a process that results in extracellular production of EndMT-inducing factors, we collected the medium conditioned by co-cultures of BMDMs and MCECs (co-culture-CM), and applied them to MCECs. We found that endothelial cells treated with TGF-ß1 underwent EndMT, and conditioned medium from TGF-ß1-treated cells also induced EndMT (probably reflecting the autocrine feedback mechanism effect of TGF-ß reported in endothelial cells and fibroblasts, or due to an unexpected long half time of exogenous recombinant TGF-ß). However, we found no effect on MCECs treated with CM derived from co-cultures of BMDMs and MCECs(Figure 3.18), suggesting that the cell-cell contact itself is necessary for EndMT to occur.

3.6.2.3. Co-culture of MCECs with non-macrophage cells

Next, we wanted to investigate whether the observed effect of macrophage induced-EndMT was a macrophage-specific effect or instead, an effect triggered by unspecific cell-contact, regardless of the cell source. We wanted to rule out that interaction with a high number of cells could induce stress in MCECs which could induce EndMT. In macrophage-MCEC co-cultures, the system was

designed so that an average of five to six macrophages were in contact with a single MCEC. To explore the possibility that unspecific cell contact interaction could induce EndMT, we chose three non-related cell types and performed co-cultures with MCECs following the same protocol used for the macrophage cell lines. We used HeLa cancer cells, MCT tubular epithelial cells, and C2C12 skeletal muscle cells. We examined different cellular ratios (5:1 and 25:1 of MCT and C2C12 to MCEC, and 1:1, 5:1, 10:1, 25:1 of HeLa cells to MCEC).

The results showed no significant up-regulation of EndMT marker genes upon co-culture of MCECs with cancer and tubular epithelial cells (Figure 19, A-F). However, we found interesting results regarding co-culture with the C2C12 cell line. C2C12 cells are undifferentiated murine skeletal muscle cells, e.g. striated muscle myoblasts which share similarity to the striated cardiac muscle cells. In fact, studies showed that cardiac-specific proteins like Troponin T can be

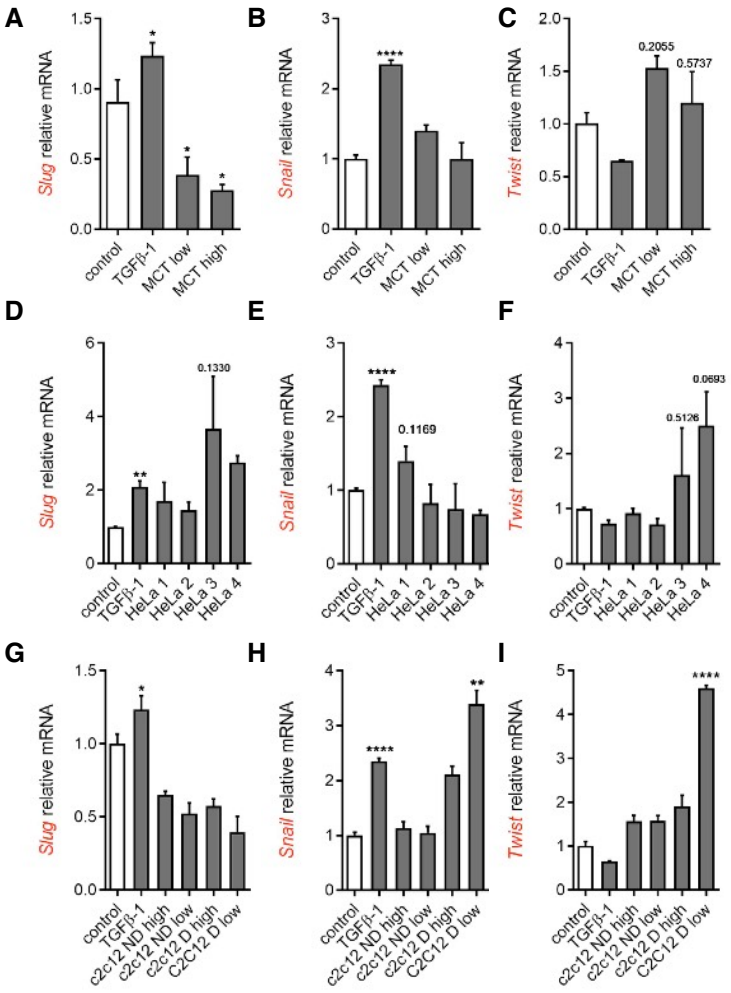

Figure 3.19. Juxtacrine communication between non macrophage cell lines and MCECs. qRT-PCR analysis of MCECs after co-culture with MCT, HeLa, and C2C12 cell lines. Results are shown as means + SEM of triplicate determinants and are representative of three independent experiments (n=3). * $P \leq 0.05$, **** $P \leq 0.001$.

expressed in C2C12 cells and can be incorporated into their myofibrils (181). C2C12 myoblasts are flat, fusiform or star-shaped mononucleated cells. They express sarcomeric and filamentous actin, mainly localised at the cell periphery and focal contacts; and they also appear positive for skeletal myosin(182). Myoblasts progressively fuse to form multi-nucleate syncytia, the myotubes, which further differentiate to acquire the final morpho-functional features of the muscle cells (myocytes) (181,183). There are several C2C12 differentiation protocols available: addition of 2% horse serum to the culture medium, starvation protocols, or addition of insulin supplements (151). Besides, subculturing C2C12s to a confluence higher than 70% is also reported to initiate spontaneous differentiation(151). In our study, we used two distinct protocols to culture C2C12: one low-confluence subculture protocol, and a second protocol in which C2C12s were grown until 90-100% confluence, to induce spontaneous differentiation. Thereafter, C2C12s were prepared for co-cultures with MCECs. Co-cultures with undifferentiated, low C2C12:MCEC ratio reported no influence on EndMT marker genes in MCECs (Figure 3.19, G-I, *"C2C12 ND low"*). In contrast, we observed a significant up-regulation of *Snail* and *Twist* mRNA expression in differentiated C2C12 with a low C2C12:MCEC ratio (Figure 3.19, G-I *"C2C12 D low"*). This data suggests that under certain conditions cardiomyocytes or muscle cells may be involved in inducing EndMT.

3.6.2.2. Co-culture of native RAW 264.7 and mouse cardiac fibroblasts

Macrophages are known to have pleiotropic functions in the healing heart. They are known to induce distinct effects in other cells such as angiogenesis in endothelial cells and myofibroblast activation in fibroblasts. Based on reports that evince macrophage link to fibroblast activation, we used our established co-culture system with mouse cardiac fibroblasts (MCF) and native RAW 264.7 cells. Results showed that co-cultures of MCFs with RAW264.7 cells promote myofibroblast activation by inducing Collagen I and αSMA mRNA expression in MCFs (Figure 3.20, A-B). Furthermore, co-cultures between MCFs and native RAW 276.7 cells dramatically changed fibroblast morphology to a stellate morphology with numerous cell extensions (Figure 3.20, C).

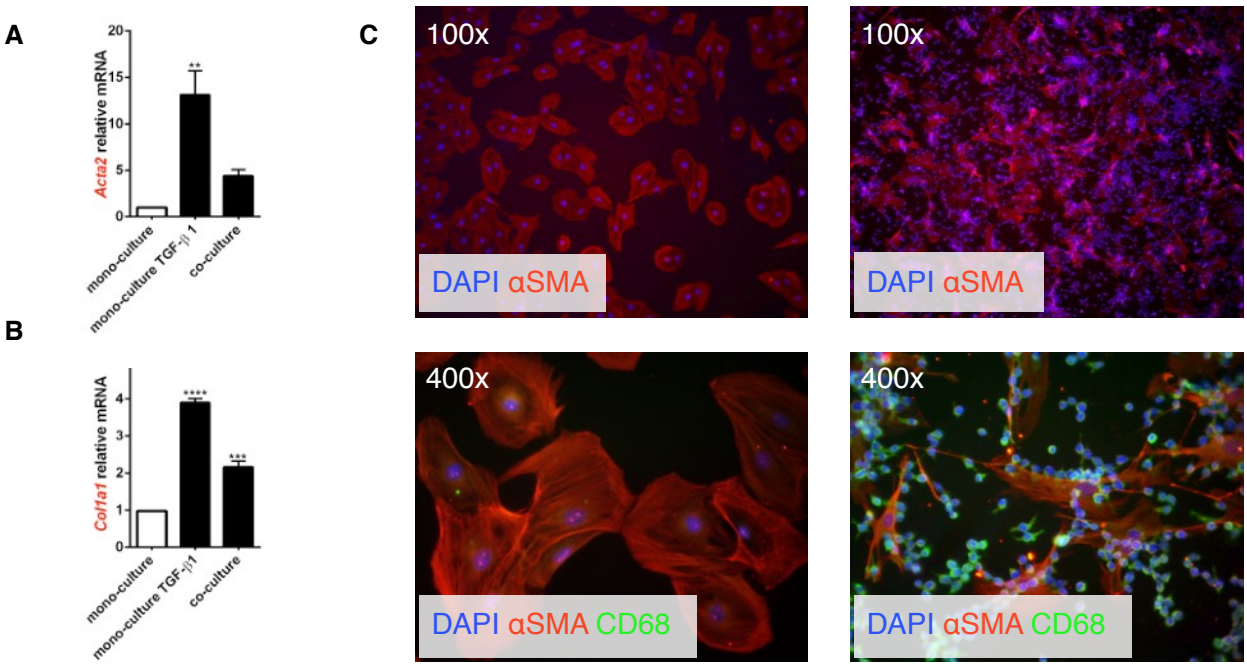

Figure 3.20. Co-cultures between RAW 264.7 macrophages and Mouse Cardiac Fibroblasts. A)qRT-PCR analysis of *Acta2* expression in MCFs after co-culture with native RAW 264.7 macrophages. Results are shown as means + SEM of triplicate determinants and are representative of three independent experiments (n=3). ** P ≤ 0.01. B) qRT-PCR analysis of *Col1a1* expression in MCFs after co-culture with native RAW 264.7. Results are shown as means + SEM of triplicate determinants and represent three independent experiments (n=3).*** P ≤ 0.001, **** P ≤ 0.0001 C) Representative immunofluorescence pictures showing MCF expressing αSMA (red) in mono-culture (left) and co-culture conditions(right). RAW264.7 macrophages are positive for CD68 (green).

3.7. LPS-stimulated IFNγ-RAW 264.7 cells induce Notch signalling in MCECs.

Next, we investigated the underlying mechanism behind juxtacrine macrophage-induced EndMT further. Literature on juxtacrine signalling reveals Notch pathway as the paradigmatic intercellular signalling mechanism between neighbouring cells. The Notch pathway is activated upon interactions between a ligand on the cellular surface of a signal-sending cell, whereas the receptor is located on the membrane's cell surface of an adjacent signal-receiving cell (94-96). Additionally, Notch signalling is an unequivocal regulator of developmental cardiac EndMT and has also been implicated in adult fibrotic EndMT (93,100,101). Based on these facts, we hypothesised that the Notch signalling pathway could be involved in the juxtacrine interplay between macrophages and MCECs in our co-culture system. First, whole protein lysates from co-cultured RAWs-MCECs were analysed and revealed a strong induction of total Notch1 and its activated form, Notch intracellular domain (NICD), only in samples derived from LPS stimulated IFNγ-RAW-MCECs co-

cultures(Figure 3. 21, A). This is consistent with earlier results indicating that this phenotype is the strongest inducer of EndMT. We also found that MCECs expressed NICD only in co-cultured conditions (Figure 3.21, B). We did not observe a significant change in the mRNA expression of any Notch receptor (Notch1, Notch2 and Notch4) in MCECs (Figure 3.21, C-E). The Notch pathway activation relies on protease ectodomain cleavage (shedding) of Notch1 by disintegrin and metalloproteinase (ADAM) proteases, a process that is initiated upon ligand binding(96). Such cleavage releases the activated NICD form, which does not involve an increase in total Notch1 expression but the nuclear transport of NICD to the nucleus, where it activates target genes. Therefore this may explain why RNA levels of endothelial Notch are unchanged in MCECs while localisation of NICD is changed. Notch target genes *Hes1* and *Hey1* were found induced in MCECs upon co-culture with LPS-stimulated RAW 264.7 macrophages (Figure 3.21, F-H),

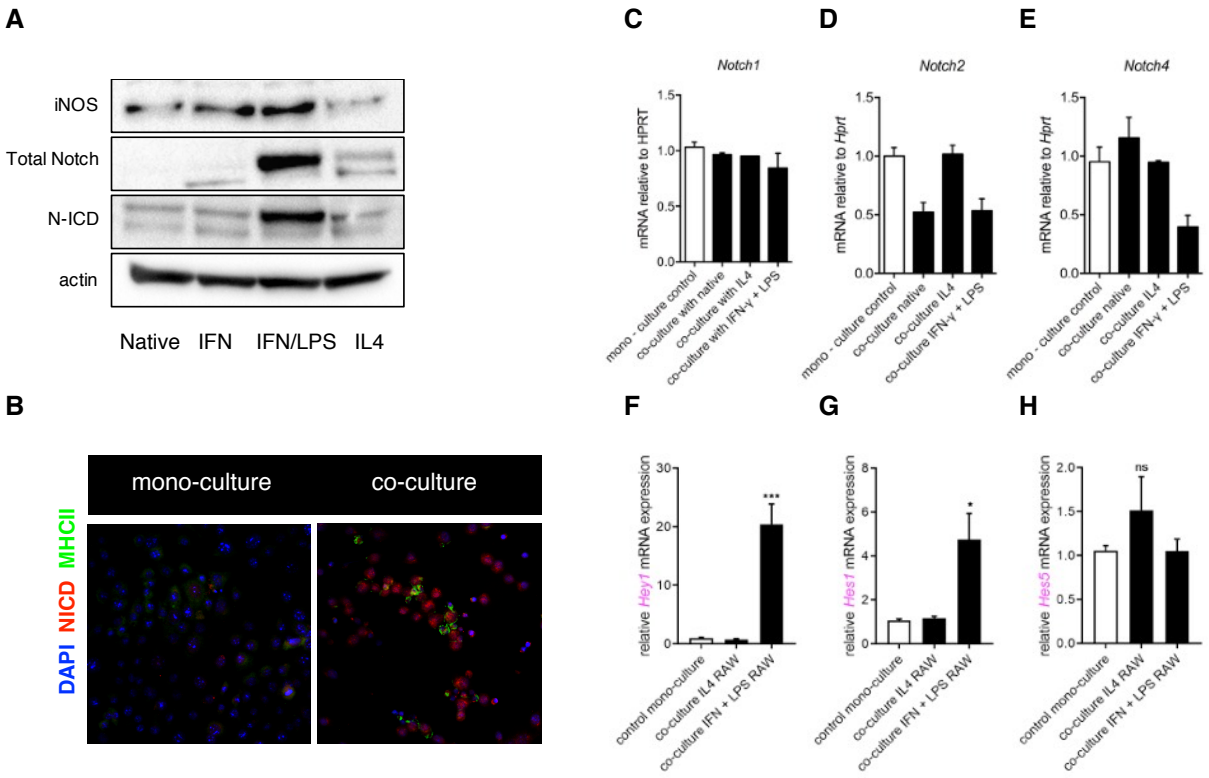

Figure 3.21. LPS-stimulated IFNγ-RAW 264.7 cells induce Notch signalling in MCECs. A) Western Blot showing protein expression of protein lysates harvested from co-cultures of IL4-, IFNγ- and IFNγ+LPS-RAW 264.7 cells and MCECs, showing polarisation marker iNOS and Notch signalling proteins Notch-1 and NICD. B) Fluorescence microscopy picture showing expression of NICD and MHCII markers in mono-culture of MCECs and co-culture of MCECs with IFNγ/LPS stimulated RAWs. C-E) qRT-PCR analysis of expression of *Notch*-1, -2 and -4 on MCECs (monoculture) and MCEC (RAW co-cultures). The results represent the mean + SEM values from two independent experiments. n=2. F-H) qRT-PCR analysis of expression of *Hey1 Hes1* and *Hes5* on MCECs (monocultured) and MCEC with IL4 and IFN+LPS-RAW cells (co-cultured). The results represent the mean + SEM values from three independent experiments. n=3. * $P \leq 0.05$, ** $P \leq 0.01$, *** $P \leq 0.001$.

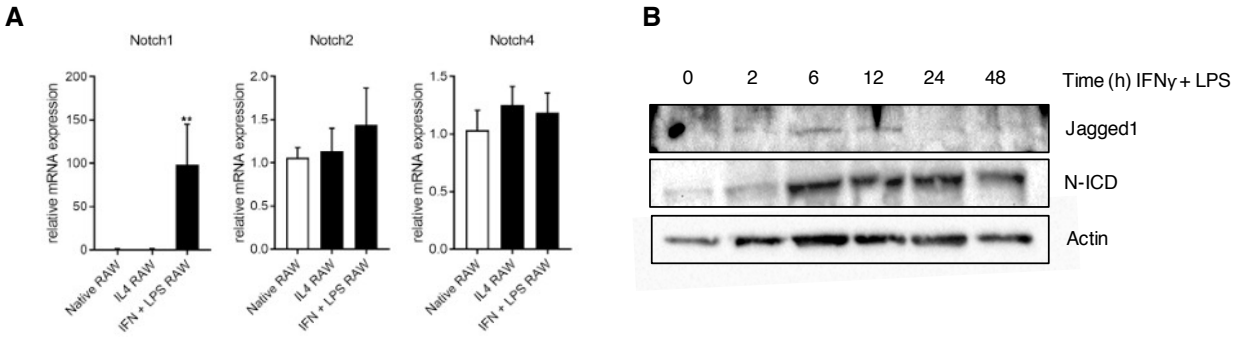

Figure 3.22. **Notch is activated upon TLR simulation in IFNγ-RAW 264.7 macrophages.** A) qRT-PCR analysis of expression of Notch-1, -2 and -4 on RAW264.7 mono-cultures upon cytokine IL4 and IFN/LPS overnight stimulation. The results represent the mean + SEM values from three independent experiments. n=3.** P ≤ 0.01. B) Representative immunoblots of IFN-RAW mono-cultures Notch expression upon time-course stimulation with LPS showing expression of Jagged1 and NICD. Loading control is shown with Actin expression.

indicating activation of Notch pathway. However, the expression of *Hes5* , another Notch signalling pathway target gene, was not induced.

We next investigated whether the increase of total Notch observed in total lysates could be due to induction in RAW 264.7 cells. Analysis of RAW264.7 cells revealed an increase of *Notch1*, and no increase in *Notch2* and *Notch4* mRNA expression, in RAW264.7 cells that were stimulated with IFNγ and LPS(Figure 3.22 A). In addition, we found that LPS-stimulated IFNγ-RAW expressed the mammal Notch ligand Jagged1, after 6 hours of LPS-stimulation (Figure 3.22 B).

Taken together this data suggest that Notch1 is shed and therefore is activated in MCECs upon contact with LPS-stimulated RAW 264.7 macrophages, resulting in upregulation of Notch targets genes *Hey1* and *Hes1*. This induction may be triggered by induced expression of Jagged 1 in LPS stimulated IFNγ-RAW cells, therefore functioning as the Notch signal-sending cells.

3.8. Wnt canonical signalling is affected in LPS-co-cultures.

Wnt signalling modulates intercellular communication between neighbouring cells, playing an important role in cell fate decisions. Similar to other intercellular signalling pathways, the Wnt ligand is synthesised and secreted from one cell and binds to a co-receptor complex on a neighbouring cell. β-Catenin is the central protein in the canonical activation of the Wnt pathway. When ß-catenin is located at the cell membrane, it interacts with E-cadherin and α-catenin, stabilising the intracellular part of adherent junctions and serving as a coupling connection to the cytoskeleton. When Wnt is absent, β-catenin is phosphorylated on the serine–threonine residue of the amino-terminal domain by glycogen synthase kinase 3 beta (GSK3β) and casein kinase (CKI),

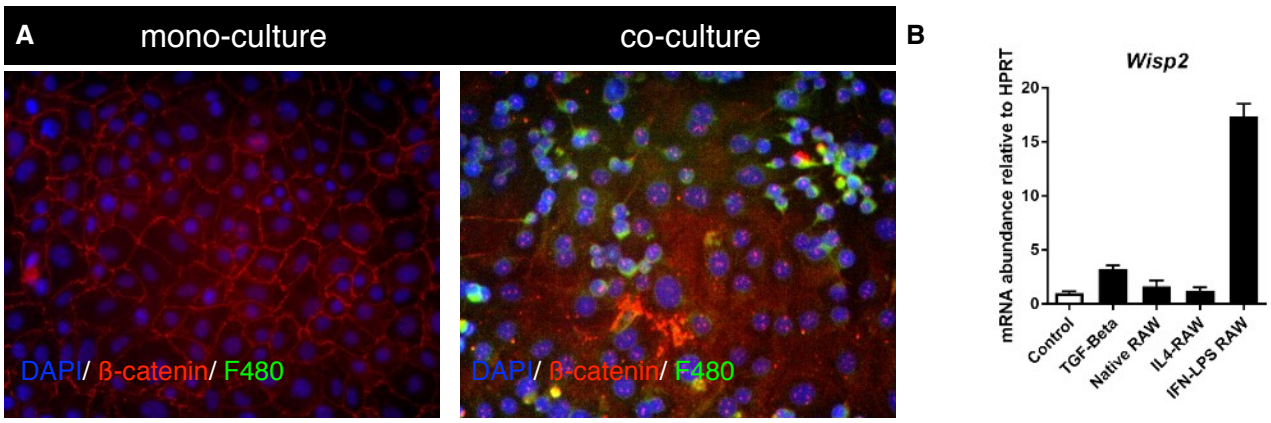

Figure 3.23. ß- catenin exhibits nuclear localisation in MCECs under co-culture conditions with LPS stimulated IFNγ-RAW 264.7 macrophages. A) Representative immunostaining pictures of ß-catenin expression in MCECs. Left panel, mono-cultured MCECs express ß-catenin (red) at the membrane regions. Right panel, MCECs co-cultured with LPS stimulated IFN-RAW macrophages expressing F4/80 (green) showing ß-catenin (red) transported to the nuclei (blue). B) Wisp2, a downstream target of ß-Catenin pathway, is induced in LPS stimulated IFNγ-RAW cells. qRT-PCR data from a three technical replicates from one experiment (n=1).

forming a complex with APC and Axin. This complex is recognised by ß-transducing repeat containing protein and the E3 ubiquitin ligase, which induce proteasome degradation of β-catenin. When the Wnt pathway is activated upon Wnt ligand binding to Frizzled co-receptors, Wnt promotes a conformational change in Frizzled that results in the exposure of a binding cytoplasmic domain that competes for Axin. Degradation machinery led by Axin becomes obsolete and allows ß-catenin to accumulate in the nucleus, where it promotes transcription of target genes (104).

The canonical Wnt pathway has been implicated in EMT in cancer and kidney fibrosis, and furthermore in adult and developmental EndMT. Wnt is an antagonist for VEGF during cardiac valve formation and is increased in endothelial cells undergoing EndMT. After myocardial infarction, canonical Wnt-positive cells accumulate in the infarcted area, and evidence from lineage tracking studies has revealed that mesenchymal Wnt-positive cells in this region are derived from endothelial cells(107,108).

We were therefore interested in the role of canonical Wnt signalling during macrophage induced-EndMT. Interestingly, we found that localisation of ß-catenin changed from the membrane to the nucleus upon co-culture of MCECs with native RAW264.7 macrophages,(Figure 3.23, A), what corresponded to an increase in mRNA expression of the transcription factor Wisp2 (Wnt1-inducible signalling pathway protein 2) (Figure 3.23, B).

3.9. MCECs and MCECs undergoing EndMT change RAW 264.7 phenotype.

Macrophages are highly sensitive cells that are continuously surveying their surroundings in search for pathogens or damage signals, sensing changes in homeostasis (135). In the heart, macrophages have been detected to be in direct contact with cardiomyocytes and endothelial cells(169). It is safe to assume that when a macrophages's neighbouring cells change their morphology, the macrophage will detect that stimulus and respond to it, in order to achieve homeostasis. For example, protective alternative phenotype CX3CR1^{high}, Ly-6C^{low} patrolling monocytes are reported to be increased in the dysfunctional endothelium of atherosclerotic plaques, where they attempt to protect the endothelial layer (184). We hypothesised that macrophages that were in direct contact with MCECs could also respond differently when encountering endothelial cells undergoing EndMT, in comparison to encountering native endothelial cells. Therefore, we questioned whether macrophage inflammatory patterns changed under co-culture with MCECs or MCECs undergoing EndMT. To investigate this, we performed co-cultures between polarised RAW.264.7 cells and MCECs that had been cultured before in either normal growth conditions or in TGFß-1-treated conditions, and thereafter macrophage phenotype was analysed. We examined pro-inflammatory markers TNF-α, CCL2, and MHCII in native, IL-4- and IFNγ/LPS-treated RAW 264.7 cells. Results showed a significant impact on endothelial cells in macrophages. This was reflected by a robust induction of CCL2 expression in all RAW cell lines tested upon contact co-culture with native endothelial cells (Figure 3.24). Interestingly, this induction was significantly reduced when macrophages were co-cultured with EndMT-MCECs. Nevertheless, macrophage CCL2 expression was still enhanced in all co-cultures in comparison with mono-cultured macrophages. TNF-α expression did not change upon co-culture conditions in native and IL-4- RAWs. By contrast, TNF-α of pro-inflammatory IFN-LPS RAW macrophages was repressed upon co-culture with MCECs undergoing EndMT. Co-culture did not have a strong effect on MHCII mRNA expression in native and IL-4-RAWs, with a mild but significant decrease in native

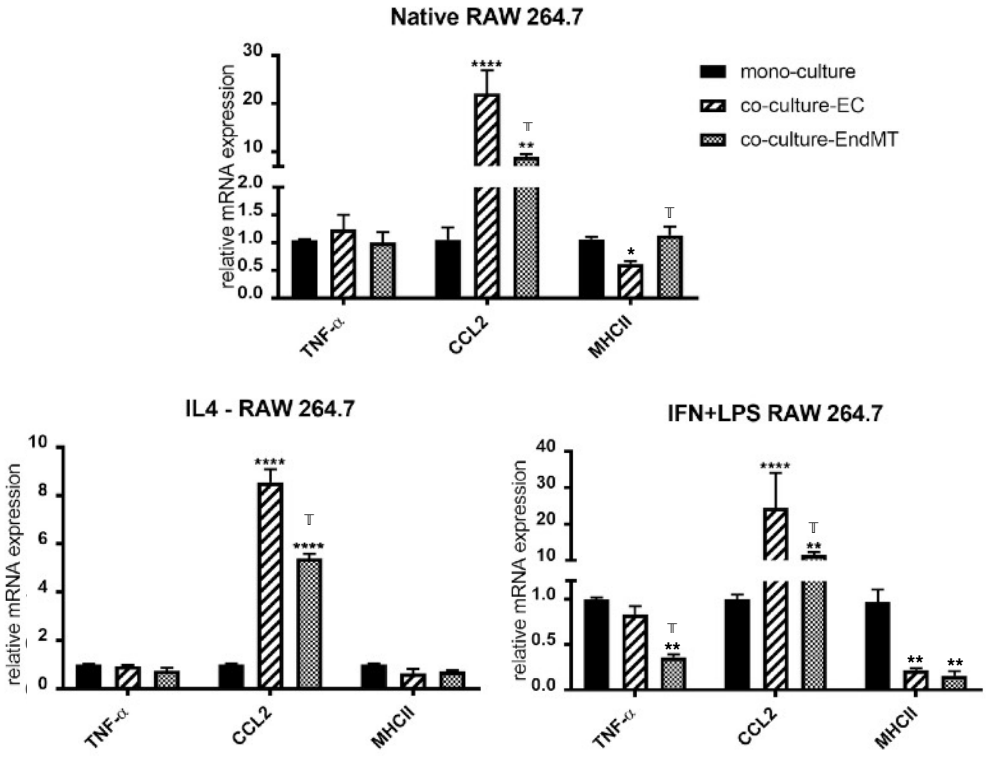

Figure 3.24. Polarisation marker mRNA expression of RAW 264.7 macrophages under MCEC juxtacrine co-culture conditions. Differential cytokine mRNA expression and activation pattern of RAW 264.7 when mono-cultured, co-cultured with native MCECs and co-cultured with EndMT-MCECs as measured by qRT-PCR. Levels TNF-α, CCL2 and MHCII were normalised to an endogenous reference (B2M) and calibrated to mono-culture conditions for each marker. The results represent the mean + SEM of values from two independent experiments. * $P \leq 0.05$, ** $P \leq 0.01$, **** $P \leq 0.0001$ in co-cultures *vs* mono-culture control. 𝕋 * $P \leq 0.05$ in EndMT co-culture *vs* native MCECs co-culture.

RAWs-native MCECs co-cultures. Instead, in pro-inflammatory IFNγ/LPS stimulated RAWs, MHCII expression was strongly repressed, in co-cultures with either native or EndMT-MCECs. This data suggests that pro-inflammatory macrophages are taken back to a less inflammatory, resting-like state upon contact with endothelial cells, an effect that is enhanced upon co-culture with EndMT-MCECs.

Next, we investigated whether the effects of endothelial cells on pro-inflammatory macrophages in co-cultures could be recapitulated in a paracrine system. Therefore, we collected conditioned medium from endothelial cells cultured in normal conditions or according to the EndMT protocol. We put special attention that TGF-ß1-treated cells were extensively washed and passaged to a new dish to avoid contamination of exogenous recombinant TGF-ß1. After culturing IFN/LPS-RAW in Native-CM or EndMT-CM, we analysed mRNA expression of pro-inflammatory markers and found consistently that TNF-α and MHCII were significantly repressed upon treatment with EndMT-

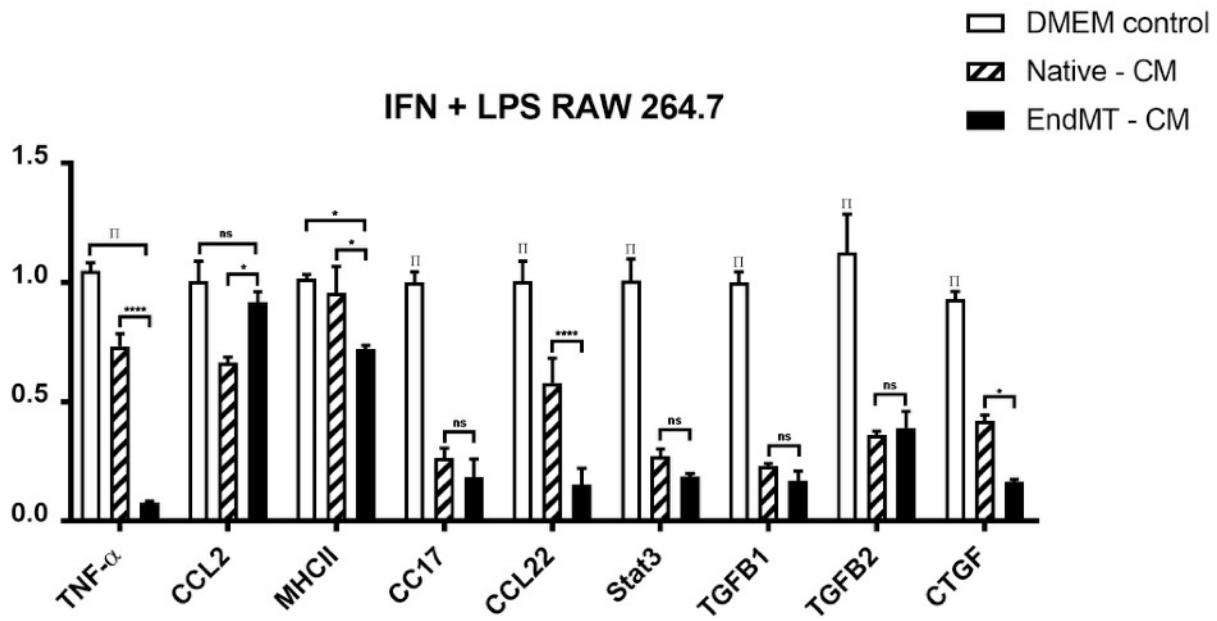

Figure 3.25. Endothelial derived CM changes RAW 264.7 phenotype. Differential cytokine mRNA expression and activation pattern of RAW 264.7 upon treatment with MCEC derived CM, as measured by RTq-PCR. Levels of TNF-α, Ccl2 and MHCII (pro-inflammatory), Ccl17, Ccl22, Stat3, Tgfß1, Tgfß2 and CTGF (pro-fibrotic9), were measured and normalised to an endogenous reference (HPRT) and calibrated to control cells. The results represent the mean SEM of values from two independent experiments. * $P \leq 0.05$ and **** $P \leq 0.0001$ represent statically significance between Native and EndMT derived CM. $\mathbb{T}$ $P \leq 0.0001$, represent statically significance between DMEM control and EndMT derived CM treated cells. ns= no significant.

CM in comparison with native CM and basal DMEM culture control (Figure 3.25). Paradoxically, we found that Ccl2 mRNA expression was downregulated under treatment with Native-CM in comparison with control DMEM and to EndMT-CM, which appeared to have no effect on CCL2.

We further wanted to explore whether downregulation of pro-inflammatory markers observed in CM experiments corresponded with an upregulation of pro-fibrotic macrophage phenotype associated markers. We analysed markers associated with macrophages and monocytes in pro-fibrotic environments, as we hypothesised that MCECs undergoing EndMT are detrimental pro-fibrotic signal-sending cells. Endothelial cells under pro-fibrotic stimuli (such as TGF-ß1), contribute to the release of TGF-ß1 by an autocrine feedback mechanism. In addition, we hypothesised that cells undergoing EndMT may behave as a fibroblast-like cell and therefore contribute to the fibrotic microenvironment. Analysis of chemokines Ccl17 and Ccl22, alternative-activated transcription factor promoter Stat3, and pro-fibrotic factors TGFß-1, TGFß-2 and CTGF revealed a significant downregulation upon treatment with CM derived from native MCECs. This negative effect was

significantly stronger in Ccl22 and Ctgf mRNA expression levels of EndMT-CM treated macrophages.

Discussion

EndMT is a process that is active in embryonic cardiac development and under stress pathogenic conditions in adulthood. Biochemical inducers of EndMT have been described by many, pointing at damage-inducing signals such as TGF-ß 1 and 2, hypoxia, and others. Still, specific cellular effectors that induce EndMT in the context of disease remain elusive. Macrophages are immune cells present at pathogenic sites modulating the interstitial environment and are known to contribute to homeostasis and disease.

The aim of this project was to investigate the crosstalk between macrophages and EndMT in the context of cardiac fibrotic disease. To this end, macrophages were detected in human and mouse models of cardiac fibrosis from diverse disease backgrounds and found to be significantly increased with respect to healthy controls, correlating with fibrosis. To evaluate the effect of macrophages alone on endothelial cells, cell culture tools were established to distinguish paracrine from juxtacrine intercellular signalling. An efficient live cell tracking separation method for co-culture of endothelial cells and macrophages under cell contact conditions was established, and served to find that macrophages robustly induced EndMT solely under juxtacrine but not under paracrine conditions. Interestingly, pro-inflammatory, TLR stimulated macrophage phenotype induced EndMT even more than generated anti-inflammatory and steady-state macrophages. We further observed that Wnt and Notch intercellular signalling pathways were activated in endothelial cells under co-culture conditions. Finally, we found that a negative feed back loop exists in that sense that macrophage inflammatory properties were impaired under contact with endothelial cells undergoing EndMT.

4.1. Cellular interplay in Cardiac Fibrosis

4.1.1.Myocardial Infarction

In humans, MI occurs as a consequence of a thrombotic occlusion, which occurs as a complication of atherosclerotic plaque rupture in patients with other underlying diseases. Metabolic conditions such as diabetes and obesity accelerate the atherosclerotic process. Immediately after myocardial acute ischemic failure, a sequential cascade of cellular events takes place to repair the damage: In

short, an effective healing process after myocardial infarction is initiated by i) an inflammatory phase, with the purpose to clear the wound from dead cells, seconded by ii) a proliferative phase with an inhibition of the inflammatory response and induction of ECM secreting myofibroblasts and new vasculature formation, and finalised by iii) an inhibitory phase, where fibroblasts and nude vessels leave a life-saving scar (4, 79, 114).

Such a timely regulated process requires a complex intercellular coordination that involves several events. Firstly, cardiomyocytes near blood-depleted vasculature become ischemic, and die rapidly by necrosis. Necrotic myocytes release their intracellular content to the extracellular space, a process that initiates an inflammatory response when cell membrane receptors detect intracellular ligands and fragmented matrix as “danger signals” (DAMPs), which activate the innate immune system. Thereafter, complement cascade, TLR-mediated pathways and ROS activate the expression of adhesion molecules in endothelial cells and the production of pro-inflammatory cytokines and chemokines in fibroblasts, leukocytes and vascular cells through NF-κB related pathways.

By this point, pro-inflammatory cytokines TNF-α, IL-1ß and IL-6 are released. IL-1ß is known to stimulate leukocyte recruitment and mediates synthesis of chemotactic mediators. TNF-α stimulates expression of pro-inflammatory cytokines, chemokines and adhesion molecules in leukocytes and endothelial cells and regulates extracellular matrix metabolism in fibroblasts, while its actions on cardiomyocytes are apoptotic and contraction inhibiting. Pleiotropic effects of TNF-α may be due to binding to TNFR1 and TNFR2 receptors with differential biologic consequences.
Release of such damage signals stimulate the infiltration of circulating cells. In mice, the first population to infiltrate the infarcted myocardium are leukocytes, in charge of debris removal by phagocytosis. Monocytes recruitment appears next and rapidly outnumber leucocytes. There is evidence of a phenotypical shift in monocyte populations detected in the infarcted heart as inflammation resolves. Immediately after MI, a population of Ly-6C^{high} monocytes invades the myocardium. Ly-6C^{high} monocytes are known to exhibit pro-inflammatory features, producing high levels of pro-inflammatory cytokines and proteases. A less inflammatory milieu follows, Ly-6C^{low} monocytes, which are known to express VEGF and TGF-ß, partially substitute the initial pro-inflammatory monocyte population (Figure 4.1). Accordingly, human clinical data describe a similar

scenario with high accumulation of pro-inflammatory $CD16^{-}$ $CD14^{+}$ monocytes post MI and the emergence of less inflammatory $CD16^{high}$ $CD14^{low}$ after. Once at the organ tissue, monocytes differentiate to macrophages, acquiring tissue-specific characteristics (169). Macrophages are thought to orchestrate resolution of inflammation and modulate transition to a reparatory phase by mechanisms like production of extracellular TGF-ß 1, a cytokine that because of its pleiotropic identity induces apoptosis of leukocytes and stimulates proliferation of fibroblasts and myofibroblast activation. When apoptotic, neutrophils are engulfed by macrophages, a process that releases TGF-ß, which is therefore essential for inflammation resolution. This is in contrast to necrotic digestion, which occurs during earlier phases and conversely enhances inflammation.

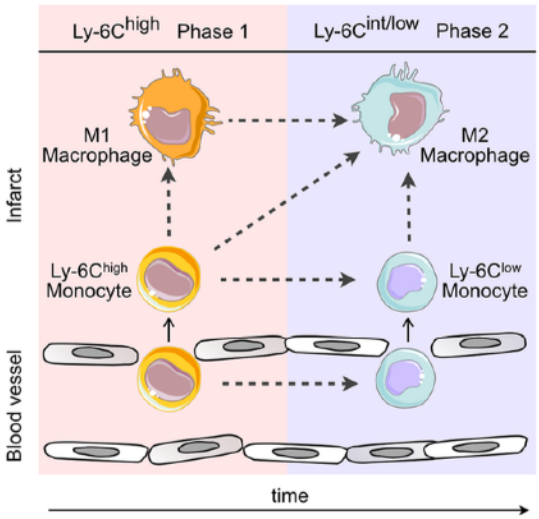

Figure 4.1. Potential lineage relationships of monocytes and macrophages after myocardial infarction. Adapted from Nahrendorf and Swirski *et al* 2013.

Evidence regarding the time frame when EndMT is triggered during MI resolution demonstrates that mesenchymal cells with endothelial origin are detectable at day 7 after LAD coronary artery occlusion. Induction of Wnt signalling and chronic inflammation exhibited in patients with thrombosis which together with the hypoxic environment at the site of the infarct indicates a precondition known to induce EndMT (57). This therefore may lead to early induction of EndMT. Our data regarding the EndMT-inducing effect of TNF-α and IL-1ß in MCECs suggests that during the inflammatory phase after MI a number of endothelial cells undergo EndMT induced by the direct effect of TNF-α and IL-1ß signals. In addition, TGF-ß 1 signalling is initiated at the interphase between inflammatory and proliferative phases. It therefore seems plausible that TGF-ß 1, under such scenario, also triggers EndMT.

In the last years a few studies have been able to shed some light on cardiac macrophage ontogeny providing evidence that distinct lineages that accumulate in the healthy heart have both embryonic and hematopoietic origin. Under stress, sources of macrophages are also very likely to arise from

resident proliferation, bone marrow and even liver derived progenitors (186). Importantly, these populations have been shown to have differential functionality (126). Considering this, in this study, we sought to gain insight in the macrophage phenotype able to induce EndMT. We found that EndMT was better induced, although not exclusively, by macrophages with a pro-inflammatory phenotype and stimulated with TLR-agonist, *E.Coli* derived LPS. Although Toll like receptors are specialised in their recognition of special patterns typically associated with pathogens, they also recognise endogenous signals derived from damaged tissues, such as heat shock proteins or fibronectin fragments. For example, LPS induces signalling by activating TLR-4 through TLR-2 receptor (186). TLR4 is expressed in the heart and is induced in murine infarcted myocardium and in samples obtained from cardiomyopathic hearts (187). Interestingly, while TLR4 knock out mice have decreased infarct size, suppressed inflammation, (188) and attenuated adverse remodelling post infarction (189), TLR2 deficient mice exhibit similar infarct size and inflammatory leukocyte infiltration compared to wild type controls, but display decreased fibrosis in the non-infarcted area and attenuated post- infarction ventricular remodelling (190). Taken together, this data suggest that in the context of post MI healing process, TLR activated macrophages recruited or resident at the infarct could, via TLR2 or TLR4 activation, induce EndMT.

Even though the physiological role, beneficial or detrimental, of EndMT after MI is not yet clear, findings in related pathomechanisms are insightful to speculate on its putative role. EndMT has been associated with vasculogenesis in embryonic development (54). EndMT signalling after MI could serve as a source of mural cells to offer support for newly formed vessels to progress to promote healing. Furthermore, EndMT could contribute, as a source of ECM producing mesenchymal cells, to help scar formation. Nevertheless, fibroblasts derived from EndMT have not been yet fully characterised. The insightful study by Evrard and Lecce (72) revealed that EndMT derived fibroblast-like cells behave as deleterious “incompetent” fibroblasts, exhibiting impaired MMP metabolism with respect to control fibroblasts. Thus, similarly to atherosclerotic plaque in which EndMT contributes to instability, EndMT may contribute not to facilitating scar formation, but contrarily to destabilisation of its formation.

4.1.2. Progressive and chronic cardiac fibrotic conditions

While inflammatory and fibrotic responses after MI are well established, evidence demonstrated that inflammation and fibrogenic pathways are also triggered in chronic cardiac disease (114). Sublethal insults such as pressure overload, volume overload and short recurrent ischemic events that result in microscopic or no cardiomyocyte loss, lead to transient, low-key levels of inflammation. Pathophysiological mechanisms of chronic cardiovascular diseases leading to interstitial and perivascular fibrosis are heterogeneous and caused by several factors such as age, metabolic and genetic conditions (11-13). In these cases, the cellular effectors involved in progression of fibrosis (direct mediators such as fibroblasts, or indirect mediators such as: macrophages, mast cells, lymphocytes, cardiomyocytes and vascular cells) are similar however it is it is their relative contribution that dictates the underlying cause of fibrosis.

4.1.1.1. Aortic Stenosis

In patients with aortic stenosis (AS), the adaptation to normalise systolic wall stress triggered by high intracavitary pressure results in left ventricular hypertrophy, cardiac disfunction and myocardial fibrosis (165). In fact, higher values of myocardial fibrosis in these patients have been associated with worse prognoses (165). Our data shows accumulation of macrophages in the myocardium of patients with AS and a positive correlation with the amount of cardiac fibrosis. Furthermore, this is also reflected in the murine aortic stenosis model of ascending aorta constriction (AAC) and also in Angiotensin II (Ang II). Recruitment of macrophages in AS in humans and in murine models of Ang II and aortic banding indicates a role of the immune system even in absence of acute inflammatory response. These findings, suggesting that macrophages induce EndMT through a close contact mechanism, are in line with the fact that in myocardial fibrosis progression there is no acute inflammation. Since mild transient inflammatory induction may occur in chronic disease (114), macrophages which, according to our data, present in substantial numbers in the steady-state myocardium, and which are reported to be located in close contact with vascular cells (169), may be able to induce EndMT by juxtacrine contact mechanism. Thus, acute inflammation may to be needed *in vivo* for macrophages to induce EndMT. Our data shows that even steady-state macrophages, when in contact with endothelial cells are capable of inducing EndMT. Peritoneal macrophages exhibited a strong capacity to induce EndMT under contact conditions (Figure 3.14) while their EndMT induction through CM was limited. This data

suggests that in situations where inflammation is reduced, the impact of macrophages in tissue can still promote mesenchymal fibrotic phenotype in endothelial cells.

At the aortic valve, accumulation of macrophages is associated with valve calcification, a common feature of valve stenosis clinical complication (165). In the valve, valve interstitial cells (VICs) differentiate to myofibroblast-like cells and to osteoblast-like cells, a process linked with age, atherosclerosis and inflammation. Osteoblast accumulation has been directly associated with EndMT, as valve aortic endothelial cells (VECs) have been demonstrated to delaminate and express pluripotent and osteogenic-like markers (165,191). Moreover, LPS stimulated macrophages have been shown to induce calcification in VICs (192). Taken together this suggests that while located within the myocardium and in perivascular regions macrophages may be involved in promoting fibrosis through EndMT. In addition, , macrophages at the valve may be involved in stimulating EndMT in VECs, contributing to thickening and stiffening of the valves via a valve osteogenic EndMT process.

4.1.1.2. Diabetic Cardiomyopathy

Diabetes is an independent risk factor for cardiovascular diseases and it contributes to cardiomyopathy and fibrosis (206). Reports show that inflammation is induced in rodent models of diabetes, which has also been corroborated in diabetic patients (186). Inflammation has a deleterious impact in the cardiac endothelium and plays an important role at the onset and progression of diabetes and obesity (13). Pro-inflammatory macrophages promote insulin resistance and adipose inflammation. The release of inflammatory cytokines and fatty acids by adipocytes induces activation of macrophages and a generalised chronic low grade inflammation in tissues. Pro-inflammatory, LPS-stimulated macrophages are known to produce resistin, which promotes insulin resistance and adipose inflammation.

Macrophages have been directly linked to diabetic cardiomyopathy in studies showing that an anti-inflammatory macrophage conversion via BMP-7 signalling ameliorates adverse cardiac remodelling (193). Studies have shown that high glucose levels are able to directly induce the expression of inflammatory cytokines TNF and IL-6 in fibroblasts, cardiomyocytes and macrophages. Moreover, high glucose levels also have been shown to promote EndMT in human aortic endothelial cells (59). Our study demonstrates that macrophages accumulate in the

myocardium of patients with diabetes and suggests that macrophages may be associated with a pathological role in promoting fibrosis via EndMT in these patients**.**

4. 1.1. 3 Atherosclerosis

Macrophages and endothelium are key cellular mediators of atherosclerotic process. Accumulation of atherogenic low-density lipoprotein (LDL) and remnant proteins, together with the atherogenic susceptibility of focal flow-disturbed arterial regions, and usually in parallel to other systemic conditions such as age, diabetes and obesity (diabetes is known to accelerate atherosclerosis (194), induce activation of endothelium and subsequent endothelial dysfunction and progressive recruitment of monocytes within the inflamed region. This study was interested in this model due to the known established contribution of macrophage accumulation to the pathological process, and found that accumulation of macrophages in ApoE deficient mice is associated with increased EndMT and induction of Twist in atherosclerotic lesions (Figure 3.4) as compared to their wild type counterparts. In this model, wild type mice also acquire certain atherosclerotic condition after being fed with a high fat containing “western” diet, which includes high fat nutrients, promoting atherosclerosis. In a recent atherosclerosis study reported by Evrard and Lecce *et al*, EndMT was a recurrent mechanism in atherosclerotic plaques that promotes fibroblast homeostasis disruption by accumulation of mesenchymal-like cells with an endothelial origin that exhibit aberrant ECM regulation properties. In their study, macrophages direct contribution is not investigated nor quantified, although it was indicated that some macrophages were found in plaques express TGF-ß.

4.2. Underlying mechanisms of macrophage-induced EndMT

4.2.1. Paracrine signalling

In this study it was demonstrated that macrophages alone are capable of directly inducing EndMT in MCECs. In light of the *in vivo* data in human and mouse correlating increase of macrophage number with fibrosis, *in vitro* studies allowed us to elucidate whether macrophages have direct EndMT inducing capabilities and under which conditions this may occur. An interesting and yet surprising finding was that macrophages were unable to induce EndMT in a paracrine manner.

Inflammatory cytokines are known to be expressed in the fibrotic myocardium of mice models of Ang II and aortic banding models (79,120). In this study we have shown that inflammatory cytokines TNF-α and IL-1ß induce EndMT, however experiments with conditioned medium from macrophages failed to induce EndMT in a paracrine dependent manner. It is evident that macrophage cytokine signalling is a paracrine intercellular signalling. However, contrary to our expectations, we did not observe EndMT induction in MCECs treated with macrophage-derived CM. The are several possible explanations for this perplexing result. First, EndMT is a process highly regulated in endothelial cells, that only occurs under discrete situations when several damage-related signals are applied. In both embryonic development and in the context of fibrosis, hypoxia and TGF-ß signalling are known to co-stimulate EndMT processes. It is possible that the inflammatory concentration of macrophage-derived CM was not a strong enough stimuli to induce EndMT alone, and that perhaps stronger and additional signalling is needed to activate EndMT program in MCEC cells.

Moreover, cytokine IL-1ß, known to be induced upon TLR stimulation in macrophages and also known to induce EndMT, requires several stimuli to induce its activation. IL-1ß is transcribed upon TLR stimulation, however, it is transcribed into its precursor form pro-(IL-1ß) (195). In order to be catalysed into its biologically active and secreted form, pro-(IL-1ß) needs the further activation of the inflammasome, a complex that needs an additional stimulation to be formed (196). Interestingly, we observed stimulation of EndMT in experiments where conditioned medium was isolated from thioglycollate elicit peritoneal macrophages. However, these experiments could not be continued due to animal-handling challenges, as the use of thioglycollate is no longer supported by the agency of animal care (LAVES Niedersachsen). Thioglycollate elicit macrophages (thio-PMs) are newly recruited macrophages to the murine abdominal cavity as a response of a highly acute inflammatory reaction caused by the intraperitoneal injection of Thioglycollate medium, a highly nutritious bacterial broth solution that promotes bacterial growth. Newly recruited thio-PMs are typically highly inflammatory, therefore it is possible that the “primary cell line” nature of thio-PMs, together with their high pro-inflammatory profile permitted access to harvesting of highly inflammatory CM that was able to induce EndMT in combination with TGF-ß 1. However, this highly inflammatory conditions do not reflect the purpose of this study. Therefore it is proposed that the thioglycollate model may be a model more suitable for pathophysiological infectious or acute

cases such as endocarditis or sepsis conditions, rather than mimicking a study of chronic inflammation in the context of cardiac fibrosis.

Nevertheless, in an attempt to rule out the possibility that the soluble cytokines and factors contained in CMs could undergo protein degradation rapidly, and therefore be unable to induce EndMT when applied to MCECs, Transwell® inserts were utilised. In such experiments, macrophages and MCECs shared the same culture medium, allowing for bidirectional signalling between the two cell types (Figure 3.11). Direct cell-cell contact, however, is not possible in this system. Here, the possibility that proteins were degraded was null, and yet we still saw no effect in EndMT gene expression.

Experiments of MCEC-derived CM on macrophages need to be considered for a careful interpretation of results. In light of the findings studying macrophage activation behaviour under co-culture with MCECs, we found macrophage activation markers downregulated upon CM of native MCEC cells. It is possible that in Transwell® experiments macrophage activation was being hampered by endothelial signalling and thus disabling them from activating EndMT. Since macrophages may be inactivated by MCEC-derived CM, it is possible that they were also ongoing inactivation under Transwell® co-culture. These findings may seem paradoxical, however, may as well be interpreted that as macrophages induce EndMT juxtacrinally, MCECs try to avoid undergoing EndMT by blocking the macrophage effect in a paracrine manner in what appears to be a negative feedback loop. As previously stated, EndMT is a highly regulated phenomena as such for EndMT to occur a highly pro-fibrotic, pro-inflammatory environment, or close contact is necessary in order to unbalance endothelial identity. The role of macrophage inactivation by endothelial cells is furthered discussed in the proceeding section.

4.2.2. Juxtacrine signalling

In this study we unequivocally, in this study we demonstrated that macrophages induce EndMT in MCECs via a juxtacrine mechanism. This was shown by co-culturing macrophages and live-fluorescent endothelial cells in cell-cell contact conditions and separating different cell populations by FACS sorting (Figure 3. 12). After separation, MCECs were analysed for EndMT and mesenchymal markers. *Snail*, *Slug* and *Acta2* (gene coding for α-SMA) were consistently up-

regulated in MCECs co-cultured with LPS-stimulated GM-BMDMs and LPS stimulated IFN-RAW 264.7 macrophages. PMs recovered from healthy mice also showed strong induction of genes *Snail* and *Acta2* under this mechanism.

Further investigation in the signalling mechanism under macrophage-endothelial juxtacrine communication led to interesting findings in the Notch signalling pathway, a classical and well-known example of juxtacrine signaling relevant for EndMT. A strong increase of total Notch 1 and activated Notch (NICD) at the protein level in whole co-cultures of IFNγ- and LPS-stimulated RAW264.7-MCECs, but not in basal or IL4-RAW264.7 cells was identified (Figure 3.21., A). Notch signalling pathway activation in MCECs was detected by immunostaining of NICD and confirmed Notch signalling activation in co-cultured MCECs by analysing consequent expression of Notch target genes *Hes1* and *Hey1* (Figure 3.21., B-H). This activation was also specific of LPS-treated RAW 264-7 co-cultured MCECs. mRNA transcripts of Notch 1, 2 and 4 were further analysed and it was found that while endothelial Notch 1 remain unchanged in endothelial mono-cultures and co-cultures, in INF-LPS RAW cells Notch 1 was increased (Figure 3.21., C-D and Figure 3.22 A). Literature shows that Notch signalling has a specific role in macrophages by driving polarisation towards a pro-inflammatory phenotype (197,198). This is probably reflected in the Notch induction observed in co-cultures using IFNγ-RAW 264.7 cells stimulated with LPS, consistent with findings by other groups using LPS stimulated RAW 264.7 cells (197). This data suggests that even though Notch1 is activated in macrophages, Notch activation in endothelial cells, as reflected by NICD intracellular staining and up-regulation of *Hes1* and *Hey1* (100), has a different function than macrophage-Notch, and may play a role in inducing EndMT. Notch signalling is known to drive EndMT in development and is known to promote EndMT *in vitro* (93,98). We speculate that activated macrophages may function as the signal sending cells via a juxtacrine signalling process to induce EndMT in endothelial cells. This may be driven by increased expression of Jagged 1 ligand at the macrophage membrane (Figure 3.22), increasing Jagged1 binding to endothelial Notch and favouring endothelial Notch shedding and activation of endothelial Notch intracellular signalling.

In addition, it was found that canonical Wnt signalling was activated in co-cultures of RAW 264.7 cells and MCECs by visualising ß-catenin located at the nuclei in MCECs upon co-culture (Figure

3.23). Further work has to be done to investigate the putative link between ß-catenin internal localisation in endothelial cell contact co-culture with macrophages. It has been suggested that canonical Wnt activation and ß-catenin internal localisation can be achieved via an independent Wnt process, by changes in cadherin organisation at the cell membrane (207). Wnt pathway has been shown to be active in neural crest cells undergoing EMT, despite not expressing significant amounts of Wnt ligand (208). Moreover, during gastrulation, epiblasts delaminate and migrate to form the mesoderm in another form of EMT, in a process dependent of Wnt/ß-catenin pathway but independent of Wnt ligand expression (209,210). The role of ß-catenin nuclear localisation independent of Wnt ligand is thus an interesting hypothesis to follow up in the investigation of macrophage-induced canonical Wnt.

Furthermore, there is evidence of cooperative and antagonistic crosstalk between Notch and Wnt signalling (211,212), highlighting the importance of cellular context to drive cell fate decisions.

4.3. Macrophage polarisation in the context of EndMT

Macrophages are cells highly dynamic and vulnerable to microenvironment changes in their surroundings. Failure of macrophages to be properly activated in response to their environment contributes to a broad spectrum of pathologies (213-215). We sought to gain insight in macrophage biology in the context of EndMT by analysing macrophage phenotype after a period of exposure to endothelial and EndMT signals. The markers chosen to address macrophage activation status were representative of a spectrum of polarisation: TNF-α, MHCII and CCL2 are known pro-inflammatory markers, while chemokines Ccl17 and Ccl22 are known markers for wound-healing macrophages (216), transcription factor Stat3, is a known marker for alternative activated macrophages involved in phagocytosis and repair, and its activation is required for effective inhibition of TNF-α (217). Tgfb1, Tgfb2 and Ctgf are genes associated with pro-fibrotic macrophages (217). Strikingly it was found that macrophage expression of pro-inflammatory markers, as well as pro-fibrotic markers, was reduced upon treatment with CM derived from native MCECs. This inhibition was significantly intensified, in macrophages treated with CM derived from EndMT-MCECs, especially with respect to the expression of TNF-α, MHCII , Ccl17, Ccl22, Stat3, Tgfß1 and Ctgf markers.

Endothelial cells are known to display differential effects on monocytes and macrophages depending on their status: Upon injury, activated endothelium is known to undergo activation and up-regulate selectins, CCL chemokines, complement and inflammatory mediators (218). Moreover, necrotic endothelial cells have been reported to promote recruitment of $Ly6C^{low}$ anti-inflammatory monocytes, which then orchestrate the killing of the necrotic endothelial cell via leukocyte action (219). Additionally, necrosis promotes inflammatory microenvironment that further recruits inflammatory cells (4). Whether necrotic cells are able to shift macrophages phenotype has not been investigated. By contrast, apoptotic endothelial cells are known to have an anti-inflammatory effect in macrophages, not only by the release of TGF-ß1 upon phagocytosis, but also through modifying the microenvironment by secretion of particles, in a mechanism that shifts macrophages to a less inflammatory phenotype (220). Endothelial cells undergoing EndMT are not yet defined as neither necrotic nor apoptotic cells. Our data indicates that EndMT cells dramatically reduce macrophage activation via a paracrine mechanism, shown by the negative regulation of inflammatory and pro-fibrotic gene expression markers (Figure 3.24).

However, the collected data indicates a differential effect in paracrine versus juxtacrine signalling in between RAW 264.7 cells and MCECs. In RAW 264.7 cells, the inhibition of pro-inflammatory markers observed in CM experiments is associated with a similar inhibition of pro-inflammatory markers observed in RAW cells under contact-co-culture experiments, with the exception of CCL2 chemokine. CCL2 chemokine was found up-regulated in macrophages upon contact co-culture with native MCECs and with MCECs undergoing EndMT. CCL2 chemokine is one of the most studied CC chemokines and is known foremost because of its monocyte chemoattractant effect (221). CCL2 binds to CCR2 receptors of myeloid cells, inducing chemotaxis and it is known to be essential for recruitment of monocytes and for bone marrow monocyte haematopoiesis (222). Furthermore, CCL2 also exhibits specific effects on stromal cells: it has been associated with promoting angiogenesis and arteriogenesis in endothelial cells (223), and modulating fibroblast phenotype and activity by increasing collagen expression and by regulating MMP synthesis (224). Interestingly, in CCL2 deficient mice, infarcts have delayed and decreased monocyte infiltration and decreased myofibroblast accumulation, while angiogenesis appeared unaffected, highlighting that the effect of CCL2 in endothelial cells remains elusive (225). Whether CCL2 has the capacity

to induce EndMT is a matter worth of further investigation, given the already known effects in endothelial cells and fibroblasts.

In addition, CCL2 has been recently linked with its polarisation modulating effect in GM and M-BMDMs (203,204). In the study, it was found that CCL2 and its receptor CCR2 determine the extent of macrophage polarisation, showing that CCL2 enhances IL-10 production and CCL2 blockage enhances pro-inflammatory polarisation, while impairing expression of M2-like associated markers. These findings are consistent with our data that CCL2 expression in macrophages is induced by MCEC while repressing TNF-α and MHCII (Figure 3.23). Further work focusing in accurate detection of protein secretion of inflammatory or anti-inflammatory proteins by macrophages upon contact with endothelial cells has to be done in order to better understand the significance of macrophage biology in the context of EndMT.

4.4 Conclusion and future perspectives

In conclusion, the findings of this study show that macrophages indeed have a role in inducing EndMT. It was shown that *in vitro* bone marrow-derived, peritoneal-derived and immortalised RAW 264.7 macrophages all directly induce EndMT via cell-to-cell contact. It was shown that via a juxtacrine contact pro-inflammatory LPS-stimulated macrophages are stronger inducers of EndMT than non-inflammatory control macrophages. This induction was associated with induction of juxtacrine intercellular signalling Notch pathway. However, critical experiments need to be performed in order to demonstrate causality between macrophage induced-EndMT and macrophage-induced Notch signalling pathway. Mechanistic studies involving blocking and silencing of Notch pathway in endothelial cells are promising strategies to evaluate the direct contribution of Notch signalling to macrophage induced-EndMT.

Additionally, in this study it was shown that EndMT cells hindered macrophage activation via a paracrine and juxtacrine manner. Macrophage's immense dynamism to respond to their environment is therefore reflected in our experiments using endothelial and EndMT supernatants on RAW 264.7 cells. Indeed, endothelial cells undergoing EndMT and their environment had an impact on macrophage polarisation phenotype. However, the direction and putative function of macrophage change of phenotype is not clear, as some fibrotic and alternative activated markers

were inhibited. Future work in this direction should put emphasis on clarifying the phenotype that macrophages acquire when encountering an EndMT cell. Macrophages adopt different responses when encountering apoptotic versus necrotic endothelial cells, and EndMT is associated with high levels of apoptosis. It is thus likely that EndMT contributes to a distinct phenotype via apoptotic endothelial cells. mRNA array profiling or RNA sequence arrays are suitable strategies to delineate differential macrophage RNA expression on the impact of EndMT.

This study supports the growing notion that macrophages are highly plastic cells involved in a smorgasbord of activities in the healthy and injured organism. In the fibrotic heart, macrophages are involved in modulating inflammation, promoting fibrosis and regulating the resolution of the fibrotic process (137,140). The addition of modulating EndMT to this spectrum of activities is of timely relevance, however further subsequent investigation is now mandatory to elucidate accurate specific cardiac macrophage phenotypes in the healing and fibrotic heart and their contribution to differential functions. Cardiac macrophage heterogeneity is a growing field which is particularly interesting in this context because of the potential clinical perspectives. Considering the extreme difficulties with which investigators were confronted when targeting specific cytokines in failed clinical trials (114,158,159) it seems more plausible to target specific macrophage populations as a therapeutic strategy to modulate inflammatory and pro-fibrotic responses. For these reasons, the next steps into elucidating macrophage-induced EndMT must be in the direction of analysing specific macrophage phenotypes and the *in vivo* signalling mechanisms responsible for EndMT induction.

Supplementary Material

1. Conditioned Medium derived from resident macrophages does not induce EndMT

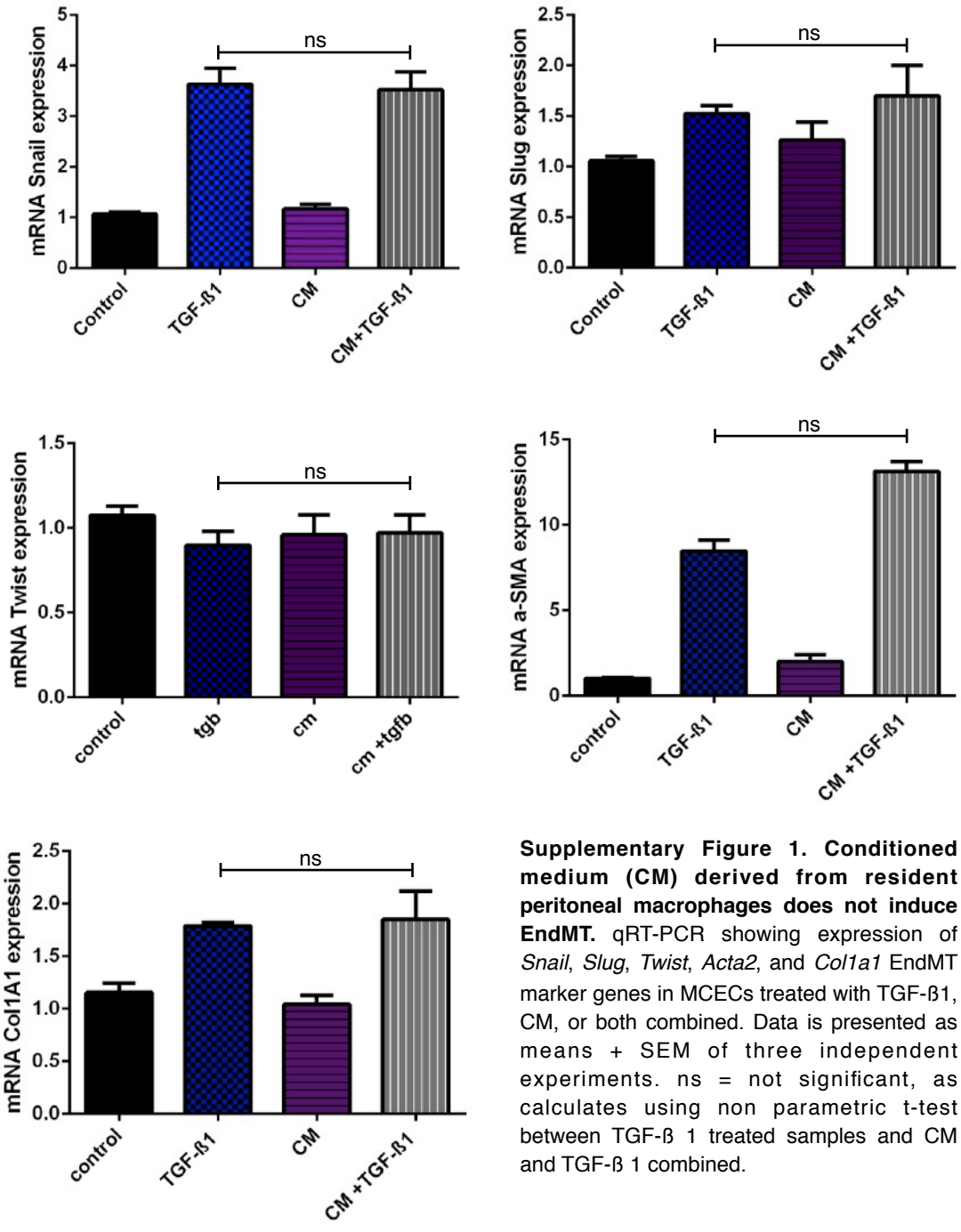

Supplementary Figure 1. Conditioned medium (CM) derived from resident peritoneal macrophages does not induce EndMT. qRT-PCR showing expression of *Snail*, *Slug*, *Twist*, *Acta2*, and *Col1a1* EndMT marker genes in MCECs treated with TGF-ß1, CM, or both combined. Data is presented as means + SEM of three independent experiments. ns = not significant, as calculates using non parametric t-test between TGF-ß 1 treated samples and CM and TGF-ß 1 combined.

2. CM derived from Thioglycollate-elicited , but not resident peritoneal macrophages, induced EndMT when combined with TGF-ß 1

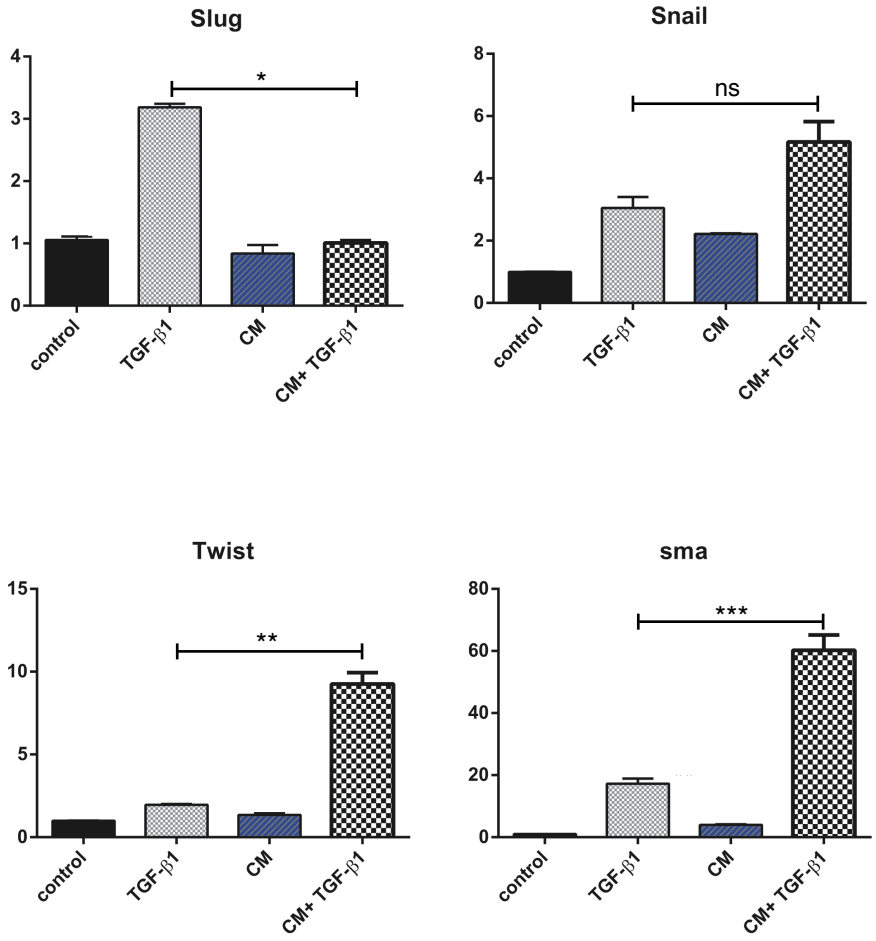

Supplementary Figure 2. Conditioned medium (CM) derived from Thioglycollate elicited peritoneal macrophages promote EndMT. qRT-PCR showing expression of EndMT marker genes in MCECs treated with TGF-ß1, CM, or both combined. P values show means + SEM from three technical replicates. Biological replicates are n=1.

References

1. Zeisberg M, Kalluri R. Cellular Mechanisms of Tissue Fibrosis. 1. Common and organ-specific mechanisms associated with tissue fibrosis. American Journal of Physiology - Cell Physiology. 2013;304(3):C216-C225. doi:10.1152/ajpcell.00328.2012.
2. Kapetanaki MG1, Mora AL, Rojas M. Influence of age on wound healing and fibrosis. J Pathol. 2013 Jan;229(2):310-22. doi: 10.1002/path.4122.
3. Biernacka A, Frangogiannis NG. Aging and Cardiac Fibrosis. Aging Dis. 2011;2:158–173.
4. Ping Kong, Panagiota Christia, and Nikolaos G Frangogiannis. The Pathogenesis of Cardiac Fibrosis. Cell Mol Life Sci. 2014 Feb; 71(4): 549–574.
5. Berk BC, Fujiwara K, Lehoux S. ECM remodeling in hypertensive heart disease. J Clin Invest. 2007;117:568–575.
6. Weber, K. T. Cardiac interstitium in health and disease: the fibrillar collagen network. J. Am. Coll. Cardiol. 13, 1637–1652 (1989).
7. Tania Rozario, Douglas W. DeSimone. The extracellular matrix in development and morphogenesis: A dynamic view. Dev Biol. 2010 May 1;341(1):126-40 1.
8. Zebrowski DC, Engel FB. The cardiomyocyte cell cycle in hypertrophy, tissue homeostasis, and regeneration. Rev Physiol Biochem Pharmacol 165: 67–96, 2013.
9. Borer JS, Truter S, Herrold EM, Falcone DJ, Pena M, Carter JN, Dumlao TF, Lee JA, Supino PG. Myocardial fibrosis in chronic aortic regurgitation: molecular and cellular responses to volume overload. Circulation. 2002;105:1837–1842.
10. Ashrafian H, McKenna WJ, Watkins H. Disease pathways and novel therapeutic targets in hypertrophic cardiomyopathy. Circ Res. 2011;109:86–96.
11. Kania G, Blyszczuk P, Eriksson U. Mechanisms of cardiac fibrosis in inflammatory heart disease. Trends Cardiovasc Med. 2009;19:247–252.
12. Asbun J, Villarreal FJ. The pathogenesis of myocardial fibrosis in the setting of diabetic cardiomyopathy. J Am Coll Cardiol. 2006;47:693–700.
13. Cavalera M, Wang J, Frangogiannis NG. Obesity, metabolic dysfunction, and cardiac fibrosis: pathophysiological pathways, molecular mechanisms, and therapeutic opportunities. Transl Res. 2014 Oct;164(4):323-35.
14. Frangogiannis NG. Fibroblast-Extracellular Matrix Interactions in Tissue Fibrosis. Curr Pathobiol Rep. 2016 Mar;4(1):11-18. Epub 2016 Feb 5.
15. Karl T. Weber, Yao Sun, Syamal K. Bhattacharya, Robert A. Ahokas and Ivan C. Gerling. Myofibroblast-mediated mechanisms of pathological remodelling of the heart. Nat Rev Cardiol. 2013 Jan;10(1):15-26.
16. Pinto AR, Ilinykh A, Ivey MJ, Kuwabara JT, D'Antoni ML, Debuque R, Chandran A, Wang L, Arora K, Rosenthal NA, Tallquist MD. Revisiting Cardiac Cellular Composition. Circ Res. 2016 Feb 5;118(3):400-9.
17. Baum J, Duffy HS. Fibroblasts and myofibroblasts: what are we talking about? J Cardiovasc Pharmacol. 2011 Apr;57(4):376-9. doi: 10.1097/FJC.0b013e3182116e39.

18. Von Gise A, Pu WT. Endocardial and epicardial epithelial to mesenchymal transitions in heart development and disease. Circulation research. 2012;110(12):1628-1645. doi:10.1161/CIRCRESAHA.111.259960.
19. Ali SR, Ranjbarvaziri S, Talkhabi M, Zhao P, Subat A, Hojjat A, Kamran P, Muller AMS, Volz KS, Tang ZY, Red-Horse K, Ardehali R. Developmental heterogeneity of cardiac fibroblasts does not predict pathological proliferation and activation. Circ Res. 2014;115:625–U681
20. Moore-Morris T, Guimaraes-Camboa N, Banerjee I, Zambon AC, Kisseleva T, Velayoudon A, Stallcup WB, Gu YS, Dalton ND, Cedenilla M, Gomez-Amaro R, Zhou B, Brenner DA, Peterson KL, Chen J, Evans SM. Resident fibroblast lineages mediate pressure overload-induced cardiac fibrosis. J Clin Invest. 2014;124:2921–2934.
21. Oliver G, Srinivasan RS. Endothelial cell plasticity: how to become and remain a lymphatic endothelial cell. Development (Cambridge, England). 2010;137(3):363-372. doi:10.1242/dev.035360.
22. Krenning G, Barauna VG, Krieger JE, Harmsen MC, Moonen J-RAJ. Endothelial Plasticity: Shifting Phenotypes through Force Feedback. Stem Cells International. 2016;2016:9762959. doi:10.1155/2016/9762959.
23. Davies PF, Civelek M, Fang Y, Guerraty MA, Passerini AG. Endothelial Heterogeneity Associated with Regional Athero-Susceptibility and Adaptation to Disturbed Blood Flow in Vivo. Seminars in thrombosis and hemostasis. 2010;36(3):10.1055/s-0030-1253449. doi:10.1055/s-0030-1253449.
24. Jiang Y-Z, Manduchi E, Jiménez JM, Davies PF. Endothelial epigenetics in biomechanical stress: Disturbed flow-mediated epigenomic plasticity in vivo and in vitro. Arteriosclerosis, thrombosis, and vascular biology. 2015;35(6):1317-1326. doi:10.1161/ATVBAHA.115.303427.
25. Koudstaal S, Jansen of Lorkeers SJ, Gaetani R, et al. Concise Review: Heart Regeneration and the Role of Cardiac Stem Cells. Stem Cells Translational Medicine. 2013;2(6):434-443. doi:10.5966/sctm.2013-0001.
26. Van Berlo JH, Kanisicak O, Maillet M, et al. c-kit+ Cells Minimally Contribute Cardiomyocytes to the Heart. Nature. 2014;509(7500):337-341. doi:10.1038/nature13309.
27. Piera-Velazquez S, Mendoza FA, Jimenez SA. Endothelial to Mesenchymal Transition (EndoMT) in the Pathogenesis of Human Fibrotic Diseases. Brenner DA, Kisseleva T, Fuxe J, eds. Journal of Clinical Medicine. 2016;5(4):45. doi:10.3390/jcm5040045.
28. Medici D. Endothelial-Mesenchymal Transition in Regenerative Medicine. Stem Cells International. 2016;2016:6962801. doi:10.1155/2016/6962801.
29. Dejana E, Hirschi KK, Simons M. The molecular basis of endothelial cell plasticity. Nature Communications. 2017;8:14361. doi:10.1038/ncomms14361.
30. Ubil E., Duan J., Pillai I. C. L., et al. Mesenchymal-endothelial transition contributes to cardiac neovascularization. *Nature*. 2014;514(7524):585–590. doi: 10.1038/nature13839.
31. Kovacic J. C., Mercader N., Torres M., Boehm M. & Fuster V. Epithelial-to-mesenchymal and endothelial-to-mesenchymal transition: from cardiovascular development to disease. Circulation 125, 1795–1808 (2012).
32. Nieto M.A. 2002. The Snail superfamily of zinc finger transcription factors. Nat. Rev. Mol. Cell Biol. 3: 155–166.

33. Medici D, Potenta S, Kalluri R. Transforming Growth Factor-β2 promotes Snail-mediated endothelial-mesenchymal transition through convergence of Smad-dependent and Smad-independent signaling. The Biochemical journal. 2011;437(3):515-520. doi:10.1042/BJ20101500.
34. Cooley BC, Nevado J, Mellad J, et al. TGF-β signaling mediates endothelial to mesenchymal transition (EndMT) during vein graft remodeling. Science translational medicine. 2014;6(227): 227ra34. doi:10.1126/scitranslmed.3006927.
35. Batlle E., Sancho, E., Franci, C., Dominguez, D., Monfar, M., Baulida, J., and Garcia De Herreros, A. 2000. The transcription factor Snail is a repressor of E-cadherin gene expression in epithelial tumor cells. Nat. Cell Biol. 2: 84–89.
36. Xu X, Tan X, Tampe B, Sanchez E, Zeisberg M, Zeisberg EM. Snail Is a Direct Target of Hypoxia-inducible Factor 1α (HIF1α) in Hypoxia-induced Endothelial to Mesenchymal Transition of Human Coronary Endothelial Cells. The Journal of Biological Chemistry. 2015;290(27):16653-16664. doi:10.1074/jbc.M115.636944.
37. Cano A., Pérez, M.A., Rodrigo, I., Locascio, A., Blanco, M.J., Del Barrio, M.G., Portillo, F., and Nieto, M.A. 2000. The transcription factor Snail controls epithelial-mesenchymal transitions by repressing E-cadherin expression. Nat. Cell Biol. 2: 76–83.
38. Yokohama K., Kamata, N., Fujimoto, R., Tsutsumi, S., Tomonari, M., Taki, M., Hosokawa, H., and Nagayama, M. 2003. Increased invasion and matrix metalloproteinase-2 expression by Snail-induced mesenchymal transition in squamous cell carcinomas. Int. J. Oncol. 22: 891–898.
39. Guaita S., Puig, I., Franci, C., Garrido, M., Domínguez, D., Batlle, E., Sancho, E., Dedhar, S., De Herreros, A.G., and Baulida, J. 2002. Snail induction of epithelial to mesenchymal transition in tumor cells is accompanied by MUC1 repression and ZEB1 expression. J. Biol. Chem. 277: 39209–39216.
40. Kajita M, McClinic KN, Wade PA. Aberrant Expression of the Transcription Factors Snail and Slug Alters the Response to Genotoxic Stress. Molecular and Cellular Biology. 2004;24(17): 7559-7566. doi:10.1128/MCB.24.17.7559-7566.2004.
41. Vega S, Morales AV, Ocaña OH, Valdés F, Fabregat I, Nieto MA. Snail blocks the cell cycle and confers resistance to cell death. Genes & Development. 2004;18(10):1131-1143. doi:10.1101/gad.294104.
42. Inai K, Norris RA, Hoffman S, Markwald RR, Sugi Y. BMP-2 induces cell migration and periostin expression during atrioventricular valvulogenesis. Developmental biology. 2008;315(2): 383-396. doi:10.1016/j.ydbio.2007.12.028.
43. Yang MH, et al. Direct regulation of TWIST by HIF-1α promotes metastasis. Nature Cell Biol. 2008;10:295–305.
44. Xu X, Friehs I, Hu TZ, et al. Endocardial Fibroelastosis is Caused by Aberrant Endothelial to Mesenchymal Transition. Circulation research. 2015;116(5):857-866. doi:10.1161/CIRCRESAHA.116.305629.
45. Roger R. Markwald, Timothy P. Fitzharris and Francis J. Manasek. Structural Development of Endocardial Cushions. The American Journal of Anatomy. 1976. 148: 85-120.

46. Timmerman LA, Grego-Bessa J, Raya A, et al. Notch promotes epithelial-mesenchymal transition during cardiac development and oncogenic transformation. Genes & Development. 2004;18(1):99-115. doi:10.1101/gad.276304.
47. Camenisch TD, Molin DG, Person A, Runyan RB, Gittenberger-de Groot AC, McDonald JA, Klewer SE. Temporal and distinct TGFbeta ligand requirements during mouse and avian endocardial cushion morphogenesis. Developmental Biology. 2002 Aug 1;248(1):170-81.
48. Lakkis M.M. and Epstein, J.A. 1998. Neurofibromin modulation of ras activity is required for normal endocardial-mesenchymal transformation in the developing heart. Development 125: 4359–4367.
49. Arciniegas E, Sutton AB, Allen TD, Schor AM. Transforming growth factor beta 1 promotes the differentiation of endothelial cells into smooth muscle-like cells in vitro. Journal of Cell Science. 1992 Oct;103 (Pt 2):521-9.
50. Arciniegas E, Ponce L, Hartt Y, Graterol A, Carlini RG. Intimal thickening involves transdifferentiation of embryonic endothelial cells. The Anatomical Record. 2000 Jan 1;258(1): 47-57.
51. Arciniegas, E., Neves, C. Y., Carrillo, L. M., Zambrano, E. A., and Ramirez, R. (2005). Endothelial–mesenchymal transition occurs during embryonic pulmonary artery development. Endothelium.12, 193–200.
52. Armulik A, Abramsson A, Betsholtz C. Endothelial/Pericyte Interactions. Circ Res. 2005;97:512–523.
53. Potenta S, Zeisberg E, Kalluri R. The role of endothelial-to-mesenchymal transition in cancer progression. British Journal of Cancer. 2008;99(9):1375-1379. doi:10.1038/sj.bjc.6604662.
54. Gerhardt H, Golding M, Fruttiger M, Ruhrberg C, Lundkvist A, Abramsson A, Jeltsch M, Mitchell C, Alitalo K, Shima D, Betsholtz C. VEGF guides angiogenic sprouting utilizing endothelial tip cell filopodia. J Cell Biol. 2003;161:1163–1177.
55. Editorial. Developing disease. Nature Cell Biology. 9, 983 (2007). doi:10.1038/ncb0907-983
56. Zeisberg EM, Tarnavski O, Zeisberg M, Dorfman AL, McMullen JR, Gustafsson E, et al. Endothelial-to-mesenchymal transition contributes to cardiac fibrosis. Nature Medicine. 2007;13:952–961.
57. Omonigho Aisagbonhi, Meena Rai, Sergey Ryzhov, Nick Atria, Igor Feoktistov, Antonis K. Hatzopoulos. Experimental myocardial infarction triggers canonical Wnt signaling and endothelial-to-mesenchymal transition. Disease Models & Mechanisms. 2011. 4: 469-483; doi: 10.1242/dmm.006510.
58. Widyantoro B, Emoto N, Nakayama K, Anggrahini DW, Adiarto S, Iwasa N, Yagi K, Miyagawa K, Rikitake Y, Suzuki T, Kisanuki YY, Yanagisawa M, Hirata K. Circulation. 2010 Jun 8;121(22): 2407-18. doi: 10.1161/CIRCULATIONAHA.110.938217
59. Tang R, Gao M, Wu M, Liu H, Zhang X, Liu B. High glucose mediates endothelial-to-chondrocyte transition in human aortic endothelial cells. Cardiovascular Diabetology. 2012;11:113. doi:10.1186/1475-2840-11-113.
60. Yan F, Zhang G, Feng M, et al. Glucagon-Like Peptide 1 Protects against Hyperglycemic-Induced Endothelial-to-Mesenchymal Transition and Improves Myocardial Dysfunction by Suppressing Poly(ADP-Ribose) Polymerase 1 Activity. Molecular Medicine. 2015;21(1):15-25. doi:10.2119/molmed.2014.00259.

61. Xiong J. To be EndMT or not to be, that is the question in pulmonary hypertension. Protein & Cell. 2015;6(8):547-550. doi:10.1007/s13238-015-0183-z.
62. Zeisberg EM, Potenta SE, Sugimoto H, Zeisberg M, Kalluri R. Fibroblasts in kidney fibrosis emerge via endothelial-to-mesenchymal transition. J Am Soc Nephrol. 2008;19:2282–2287.
63. Hashimoto N, Phan SH, Imaizumi K, Matsuo M, Nakashima H, Kawabe T, Shimokata K, Hasegawa Y. Endothelial-mesenchymal transition in bleomycin-induced pulmonary fibrosis. Am J Respir Cell Mol Biol. 2010;43:161–172. doi: 10.1165/rcmb.2009-0031OC.
64. Choi SH, Hong ZY, Nam JK, Jang J, Lee HJ, Yoo RJ, Lee YJ, Park S, Ji YH, Lee YS et al (2015) A hypoxia-induced vascular endothelial-to-mesenchymal transition in development of radiation-induced pulmonary fibrosis. Clin Cancer Res
65. Qiao L, Nishimura T, Shi L, Sessions D, Thrasher A, Trudell JR, Berry GJ, Pearl RG, Kao PN. Endothelial fate mapping in mice with pulmonary hypertension. Circulation. 2014;129:692–703. doi: 10.1161/CIRCULATIONAHA.113.003734.
66. Good RB, Gilbane AJ, Trinder SL, Denton CP, Coghlan G, Abraham DJ, Holmes AM (2015) Endothelial to mesenchymal transition contributes to endothelial dysfunction in pulmonary artery hypertension. Am J Pathol. 2015 Jul;185(7):1850-8. doi: 10.1016/j.ajpath.2015.03.019.
67. Ranchoux B, Antigny F, Rucker-Martin C, Hautefort A, Pechoux C, Bogaard HJ, Dorfmuller P, Remy S, Lecerf F, Plante S, et al. Endothelial-to-mesenchymal transition in pulmonary hypertension. Circulation. 2015;131:1006–1018. doi: 10.1161/CIRCULATIONAHA.114.008750.
68. Choi SH, Hong ZY, Nam JK, Jang J, Lee HJ, Yoo RJ, Lee YJ, Park S, Ji YH, Lee YS et al (2015) A hypoxia-induced vascular endothelial-to-mesenchymal transition in development of radiation-induced pulmonary fibrosis. Clin Cancer Res. 2015 Aug 15;21(16):3716-26. doi: 10.1158/1078-0432.CCR-14-3193.
69. Li J, Qu X, Bertram JF. Endothelial-myofibroblast transition contributes to the early development of diabetic renal interstitial fibrosis in streptozotocin-induced diabetic mice. Am J Pathol. 2009;175:1380–1388.
70. Rieder F, Kessler SP, West GA, et al. Inflammation-induced endothelial-to-mesenchymal transition: a novel mechanism of intestinal fibrosis. Am J Pathol. 2011;179:2660–2673.
71. Pei-Yu Chen, Lingfeng Qin, Nicolas Baeyens, Guangxin Li, Titilayo Afolabi, Madhusudhan Budatha, George Tellides, Martin A. Schwartz, Michael Simons.Endothelial-to-mesenchymal transition drives atherosclerosis progression. J Clin Invest. 2015;125(12):4514-4528. doi: 10.1172/JCI82719.
72. Evrard SM, Lecce L, Michelis KC, et al. Endothelial to mesenchymal transition is common in atherosclerotic lesions and is associated with plaque instability. Nature Communications. 2016;7:11853. doi:10.1038/ncomms11853.
73. Lloyd-Jones D, Adams RJ, Brown TM, Carnethon M, Dai S, De Simone G, Ferguson TB, Ford E, Furie K, Gillespie C, Go A, Greenlund K, Haase N, Hailpern S, Ho PM, Howard V, Kissela B, Kittner S, Lackland D, Lisabeth L, Marelli A, McDermott MM, Meigs J, Mozaffarian D, Mussolino M, Nichol G, Roger VL, Rosamond W, Sacco R, Sorlie P, Roger VL, Thom T, Wasserthiel-Smoller S, Wong ND, Wylie-Rosett J; American Heart Association Statistics Committee and Stroke Statistics Subcommittee. Heart disease and stroke statistics--2010 update: a report from the American Heart Association. Circulation. 2010 Feb 23;121(7):e46-e215. doi: 10.1161/CIRCULATIONAHA.109.192667.

74. Virmani R, Burke AP, Kolodgie FD, Farb A. Vulnerable plaque: the pathology of unstable coronary lesions. J Interv Cardiol. 2002;15:439–446.
75. Massagué J, Blain SW, Lo RS. TGF[beta] signaling in growth control, cancer, and heritable disorders. Cell. 2000;103:295–309. doi: 10.1016/S0092-8674(00)00121-5.
76. Tampe B, Tampe D, Müller CA, Sugimoto H, LeBleu V, Xu X, Müller GA, Zeisberg EM, Kalluri R, Zeisberg M. Tet3-mediated hydroxymethylation of epigenetically silenced genes contributes to bone morphogenic protein 7-induced reversal of kidney fibrosis. J Am Soc Nephrol. 2014 May;25(5):905-12. doi: 10.1681/ASN.2013070723.
77. Qiu X, Cheng JC, Zhao J, Chang HM, Leung PC. Transforming growth factor-β stimulates human ovarian cancer cell migration by up-regulating connexin43 expression via Smad2/3 signaling. Cell Signal. 2015 Oct;27(10):1956-62. doi: 10.1016/j.cellsig.2015.07.010
78. Kubiczkova L, Sedlarikova L, Hajek R, Sevcikova S. TGF-β – an excellent servant but a bad master. Journal of Translational Medicine. 2012;10:183. doi:10.1186/1479-5876-10-183.
79. Frangogiannis NG. Chemokines in the ischemic myocardium: from inflammation to fibrosis. Inflamm Res. 2004;53:585–595
80. Meyer A, Wang W, Qu J, et al. Platelet TGF-β1 contributions to plasma TGF-β1, cardiac fibrosis, and systolic dysfunction in a mouse model of pressure overload. Blood. 2012;119(4): 1064-1074. doi:10.1182/blood-2011-09-377648.
81. Khalil N. TGF-beta: from latent to active. Microbes Infect. 1999 Dec;1(15):1255-63.
82. Peter ten Dijke & Helen M. Arthur. Extracellular control of TGFß signalling in vascular development and disease. Nature Reviews Molecular Cell Biology 8, 857-869
83. Cheifetz S, Weatherbee JA, Tsang ML, Anderson JK, Mole JE, Lucas R, Massagué J. The transforming growth factor-beta system, a complex pattern of cross-reactive ligands and receptors. Cell. 1987;48:409–415. doi: 10.1016/0092-8674(87)90192-9.
84. Moustakas A, Heldin CH. The regulation of TGFβ signal transduction. Development. 2009;136:3699–3714.
85. Massagué J. TGFβ signalling in context. Nature reviews Molecular cell biology. 2012;13(10): 616-630. doi:10.1038/nrm3434.
86. Jennings JC1, Mohan S, Linkhart TA, Widstrom R, Baylink DJ. Comparison of the biological actions of TGF beta-1 and TGF beta-2: differential activity in endothelial cells. J Cell Physiol. 1988 Oct;137(1):167-72.
87. Goumans M-J, Valdimarsdottir G, Itoh S, Lebrin F, Larsson J, Mummery C, Karlsson S, ten Dijke P (2003) Activin receptor-like kinase (ALK)1 is an antagonistic mediator of lateral TGF-β/ ALK5 signaling. Mol Cell 12: 817–828
88. Goumans MJ1, Mummery C. Functional analysis of the TGFbeta receptor/Smad pathway through gene ablation in mice. Int J Dev Biol. 2000 Apr;44(3):253-65.
89. Van Meeteren LA, ten Dijke P. Regulation of endothelial cell plasticity by TGF-β. Cell and Tissue Research. 2012;347(1):177-186. doi:10.1007/s00441-011-1222-6.
90. Nomura-Kitabayashi A, Anderson GA, Sleep G, Mena J, Karabegovic A, Karamath S, Letarte M, Puri MC. Endoglin is dispensable for angiogenesis, but required for endocardial cushion formation in the midgestation mouse embryo. Dev Biol. 2009 Nov 1;335(1):66-77. doi: 10.1016/ j.ydbio.2009.08.016.

91. Martínez-Sanz E, Del Río A, Barrio C, et al. Alteration of medial-edge epithelium cell adhesion in two Tgf-β3 null mouse strains. Differentiation; Research in Biological Diversity. 2008;76(4): 417-430. doi:10.1111/j.1432-0436.2007.00226.x.
92. Kokudo T1, Suzuki Y, Yoshimatsu Y, Yamazaki T, Watabe T, Miyazono K. Snail is required for TGFbeta-induced endothelial-mesenchymal transition of embryonic stem cell-derived endothelial cells. J Cell Sci. 2008 Oct 15;121(Pt 20):3317-24. doi: 10.1242/jcs.028282.
93. Timmerman LA, Grego-Bessa J, Raya A, et al. Notch promotes epithelial-mesenchymal transition during cardiac development and oncogenic transformation. Genes & Development. 2004;18(1):99-115. doi:10.1101/gad.276304.
94. Gridley T. Notch signaling in vertebrate development and disease. Mol Cell Neurosci.1997;9(2): 103-8.
95. D'souza B, Miyamoto A, Weinmaster G. The many facets of Notch ligands. Oncogene. 2008;27(38):5148-5167. doi:10.1038/onc.2008.229.
96. LaVoie MJ, Selkoe DJ. The Notch ligands, Jagged and Delta, are sequentially processed by alpha-secretase and presenilin/gamma-secretase and release signaling fragments. J Biol Chem. 2003 Sep 5;278(36):34427-37.
97. Catherine A. Parr-Sturgess, David J. Rushton, Edward T. Parkin. Ectodomain shedding of the Notch ligand Jagged1 is mediated by ADAM17, but is not a lipid-raft-associated event
98. Katoh M, Katoh M. Integrative genomic analyses on HES/HEY family: Notch-independent HES1, HES3 transcription in undifferentiated ES cells, and Notch-dependent HES1, HES5, HEY1, HEY2, HEYL transcription in fetal tissues, adult tissues, or cancer. Int J Oncol. 2007 Aug;31(2):461-6.
99. Hatakeyama J, Bessho Y, Katoh K, Ookawara S, Fujioka M, Guillemot F et al. (2004). Hes genes regulate size, shape and histogenesis of the nervous system by control of the timing of neural stem cell differentiation. Development 131: 5539–5550.
100. Chang AC, Fu Y, Garside VC, Niessen K, Chang L, Fuller M, Setiadi A, Smrz J, Kyle A, Minchinton A, Marra M, Hoodless PA, Karsan A. Notch initiates the endothelial-to-mesenchymal transition in the atrioventricular canal through autocrine activation of soluble guanylyl cyclase. Dev Cell. 2011 Aug 16;21(2):288-300. doi: 10.1016/j.devcel.2011.06.022.
101. Fu Y, Chang ACY, Fournier M, Chang L, Niessen K, Karsan A. RUNX3 Maintains the Mesenchymal Phenotype after Termination of the Notch Signal. The Journal of Biological Chemistry. 2011;286(13):11803-11813. doi:10.1074/jbc.M111.222331.
102. Frías A, Lambies G, Viñas-Castells R, et al. A Switch in Akt Isoforms Is Required for Notch-Induced Snail1 Expression and Protection from Cell Death. Molecular and Cellular Biology. 2016;36(6):923-940. doi:10.1128/MCB.01074-15.
103. Chen H-F, Wu K-J. Endothelial Transdifferentiation of Tumor Cells Triggered by the Twist1-Jagged1-KLF4 Axis: Relationship between Cancer Stemness and Angiogenesis. Stem Cells International. 2016;2016:6439864. doi:10.1155/2016/6439864.
104. Cortney M Bouldin and David Kimelman. Taking a bite out of Wnts. Cell Research (2012) 22:1621–1623. doi:10.1038/cr.2012.104
105. Cárdenas-García M, González-Pérez PP, Montagna S, Cortés OS, Caballero EH. Modeling Intercellular Communication as a Survival Strategy of Cancer Cells: An In Silico Approach on a

Flexible Bioinformatics Framework. Bioinformatics and Biology Insights. 2016;10:5-18. doi: 10.4137/BBI.S38075.

106.Srivastava SP, Koya D, Kanasaki K. MicroRNAs in Kidney Fibrosis and Diabetic Nephropathy: Roles on EMT and EndMT. BioMed Research International. 2013;2013:125469. doi: 10.1155/2013/125469.

107.Howard S, Deroo T, Fujita Y, Itasaki N. A Positive Role of Cadherin in Wnt/β-Catenin Signalling during Epithelial-Mesenchymal Transition. Heisenberg C-P, ed. PLoS ONE. 2011;6(8):e23899. doi:10.1371/journal.pone.0023899.

108.Cheng S-L, Shao J-S, Behrmann A, Krchma K, Towler DA. Dkk1 and Msx2-Wnt7b Signaling Reciprocally Regulate The Endothelial-Mesenchymal Transition In Aortic Endothelial Cells. Arteriosclerosis, thrombosis, and vascular biology. 2013;33(7):10.1161/ATVBAHA.113.300647. doi:10.1161/ATVBAHA.113.300647.

109.Castellano E, Santos E. Functional Specificity of Ras Isoforms: So Similar but So Different. Santos E, ed. Genes & Cancer. 2011;2(3):216-231. doi:10.1177/1947601911408081.

110.Bechtel W, McGoohan S, Zeisberg EM, et al. Methylation determines fibroblast activation and fibrogenesis in the kidney. Nature medicine. 2010;16(5):544-550. doi:10.1038/nm.2135.

111.Xu X, Tan X, Tampe B, Nyamsuren G, Liu X, Maier LS, Sossalla S, Kalluri R, Zeisberg M, Hasenfuss G, Zeisberg EM. Epigenetic balance of aberrant Rasal1 promoter methylation and hydroxymethylation regulates cardiac fibrosis. Cardiovasc Res. 2015 Mar 1;105(3):279-91. doi: 10.1093/cvr/cvv015.

112.Zhou X, Chen X, Cai J, et al. Relaxin inhibits cardiac fibrosis and endothelial–mesenchymal transition via the Notch pathway. Drug Design, Development and Therapy. 2015;9:4599-4611. doi:10.2147/DDDT.S85399.

113.Xu X, Tan X, Hulshoff MS, Wilhelmi T, Zeisberg M, Zeisberg EM. Hypoxia-induced endothelial-mesenchymal transition is associated with RASAL1 promoter hypermethylation in human coronary endothelial cells. FEBS Lett. 2016 Apr;590(8):1222-33. doi: 10.1002/1873-3468.12158.

114.Frangogiannis NG. The immune system and cardiac repair. Pharmacological research : the official journal of the Italian Pharmacological Society. 2008;58(2):88-111. doi:10.1016/j.phrs. 2008.06.007.

115.Pinto MT, Covas DT, Kashima S, Rodrigues CO. Endothelial Mesenchymal Transition: Comparative Analysis of Different Induction Methods. Biological Procedures Online. 2016;18:10. doi:10.1186/s12575-016-0040-3.

116.Xu YP, He Q, Shen Z, Shu XL, Wang CH, Zhu JJ, Shi LP, Du LZ. MiR-126a-5p is involved in the hypoxia-induced endothelial-to-mesenchymal transition of neonatal pulmonary hypertension. Hypertens Res. 2017 Feb 2. doi: 10.1038/hr.2017.2.

117.Mahler GJ, Farrar EJ, Butcher JT. Inflammatory cytokines promote mesenchymal transformation in embryonic and adult valve endothelial cells. Arteriosclerosis, thrombosis, and vascular biology. 2013;33(1):121-130. doi:10.1161/ATVBAHA.112.300504.

118.Maleszewska M1, Moonen JR, Huijkman N, van de Sluis B, Krenning G, Harmsen MC. IL-1β and TGFβ2 synergistically induce endothelial to mesenchymal transition in an NFκB-dependent manner. Immunobiology. 2013 Apr;218(4):443-54. doi: 10.1016/j.imbio.2012.05.026.

119.Li L, Chen L, Zang J, Tang X, Liu Y, Zhang J, Bai L, Yin Q, Lu Y, Cheng J, Fu P, Liu F. C3a and C5a receptor antagonists ameliorate endothelial-myofibroblast transition via the Wnt/β-catenin signaling pathway in diabetic kidney disease. Metabolism. 2015 May;64(5):597-610. doi: 10.1016/j.metabol.2015.01.014

120.Pérez L, Muñoz-Durango N, Riedel CA, Echeverría C, Kalergis AM, Cabello-Verrugio C, Simon F.Endothelial-to-mesenchymal transition: Cytokine-mediated pathways that determine endothelial fibrosis under inflammatory conditions. Cytokine Growth Factor Rev. 2017 Feb; 33:41-54. doi: 10.1016/j.cytogfr.2016.09.002.

121.Víctor Delgado Cuevas. Transcriptional profile of human anti-inflammatory macrophages under homeostatic, activating and pathological conditions. Doctoral Thesis. Madrid 2016.

122.Okabe, Y., and Medzhitov, R. (2016). Tissue biology perspective on macrophages. Nature immunology 17, 9-17.

123.Chovatiya, R., and Medzhitov, R. (2014). Stress, in ammation, and defense of homeostasis. Molecular cell 54, 281-288.

124.Wynn, T.A., Chawla, A., and Pollard, J.W. (2013). Macrophage biology in development, homeostasis and disease. Nature 496, 445-455.

125.van Furth, R., Cohn, Z.A., Hirsch, J.G., Humphrey, J.H., Spector, W.G., and Langevoort, H.L. (1972). The mononuclear phagocyte system: a new classi cation of macrophages, monocytes, and their precursor cells. Bulletin of the World Health Organization 46, 845-852.

126.Epelman, S., Lavine, K.J., Beaudin, A.E., Sojka, D.K., Carrero, J.A., Calderon, B., Brija, T., Gautier, E.L., Ivanov, S., Satpathy, A.T., et al. (2014). Embryonic and adult-derived resident cardiac macrophages are maintained through distinct mechanisms at steady state and during in ammation. Immunity 40, 91-104.

127.Calderon, B., Carrero, J.A., Ferris, S.T., Sojka, D.K., Moore, L., Epelman, S., Murphy, K.M., Yokoyama, W.M., Randolph, G.J., and Unanue, E.R. (2015). The pancreas anatomy conditions the origin and properties of resident macrophages. The Journal of experimental medicine 212, 1497-1512.

128.Bain, C.C., Bravo-Blas, A., Scott, C.L., Gomez Perdiguero, E., Geissmann, F., Henri, S., Malissen, B., Osborne, L.C., Artis, D., and Mowat, A.M. (2014). Constant replenishment from circulating monocytes maintains the macrophage pool in the intestine of adult mice. Nature immunology 15, 929-937.

129.Tamoutounour, S., Guilliams, M., Montanana Sanchis, F., Liu, H., Terhorst, D., Malosse, C., Pollet, E., Ardouin, L., Luche, H., Sanchez, C., et al. (2013). Origins and functional specialization of macrophages and of conventional and monocyte-derived dendritic cells in mouse skin. Immunity 39, 925-938.

130.A. Cumano, I. Godin. Ontogeny of the hematopoietic system Annu. Rev. Immunol. 25,745 (2007).

131.S. H. Orkin, L. I. Zon. Hematopoiesis: an evolving paradigm for stem cell biology. Cell. 132, 631 (2008).

132.Serbina, N.V., Jia, T., Hohl, T.M., and Pamer, E.G. (2008). Monocyte-mediated defense against microbial pathogens. Annual review of immunology 26, 421-452.

133.Lavin, Y., Winter, D., Blecher-Gonen, R., David, E., Keren-Shaul, H., Merad, M., Jung, S., and Amit, I. (2014). Tissue-resident macrophage enhancer landscapes are shaped by the local microenvironment. Cell 159, 1312-1326.

134.Okabe, Y., and Medzhitov, R. (2016). Tissue biology perspective on macrophages. Nature immunology 17, 9-17.

135.Mosser, D.M., and Edwards, J.P. (2008). Exploring the full spectrum of macrophage activation. Nature reviews 8, 958-969.

136.Kawai, T., and Akira, S. (2010). The role of pattern-recognition receptors in innate immunity: update on Toll-like receptors. Nature immunology 11, 373-384.

137.Wynn, T.A., and Vannella, K.M. (2016). Macrophages in Tissue Repair, Regeneration, and Fibrosis. Immunity 44, 450-462.

138.Batista, F.D., and Harwood, N.E. (2009). The who, how and where of antigen presentation to B cells. Nature reviews 9, 15-27.

139.Hume, D.A. (2008). Macrophages as APC and the dendritic cell myth. J Immunol 181, 5829-5835.

140.Jantsch, J., Binger, K.J., Muller, D.N., and Titze, J. (2014). Macrophages in homeostatic immune function. Front Physiol 5, 146.

141.Murray, P.J., Allen, J.E., Biswas, S.K., Fisher, E.A., Gilroy, D.W., Goerdt, S., Gordon, S., Hamilton, J.A., Ivashkiv, L.B., Lawrence, T., et al. (2014). Macrophage activation and polarization: nomenclature and experimental guidelines. Immunity 41, 14-20.

142.Martinez, F.O., and Gordon, S. (2014). The M1 and M2 paradigm of macrophage activation: time for reassessment. F1000prime reports 6, 13.

143.Sica, A., and Mantovani, A. (2012). Macrophage plasticity and polarization: in vivo veritas. J Clin Invest 122, 787-795.

144.Cohen HB, Mosser DM. Cardiac macrophages: how to mend a broken heart. Immunity. 2014 Jan 16;40(1):3-5. doi: 10.1016/j.immuni.2013.12.005.

145.Embryonic and Adult-Derived Resident Cardiac Macrophages Are Maintained through Distinct Mechanisms at Steady State and during Inflammation. Immunity. 2014;40:91–104.

146.Lavine KJ, Epelman S, Uchida K, et al. Distinct macrophage lineages contribute to disparate patterns of cardiac recovery and remodeling in the neonatal and adult heart. Proceedings of the National Academy of Sciences of the United States of America. 2014;111(45):16029-16034. doi:10.1073/pnas.1406508111.

147.Raschke WC, et al. Functional macrophage cell lines transformed by Abelson leukemia virus. Cell 15: 261-267, 1978.

148.Burgess, M. L., Terracio, L, Hirozane, T., Borg, T. K. (2002) Differential integrin expression by cardiac fibroblasts from hypertensive and exercise-trained rat hearts. Cardiovasc Pathol 11(2): 78-87

149.Gey GO, et al. Tissue culture studies of the proliferative capacity of cervical carcinoma and normal epithelium. Cancer Res. 12: 264-265, 1952

150.Characterization of a renal tubular epithelial cell line which secretes the autologous target antigen of autoimmune experimental interstitial nephritis. *The Journal of Cell Biology*. 1988;107(4):1359-1368.

151.S Burattini, P Ferri, M Battistelli, R Curci, F Luchetti, E Falcieri. C2C12murine myoblasts as a model of skeletal muscle development: morpho-functional characterization. European Journal of Histochemistry. 2004; vol. 48;3:223-234.

152.Barbieri SS, Weksler BB. Tobacco smoke cooperates with interleukin-1beta to alter beta-catenin trafficking in vascular endothelium resulting in increased permeability and induction of cyclooxygenase-2 expression in vitro and in vivo. FASEB J. 2007 Jun;21(8):1831-43

153.Zhang X, Goncalves R, Mosser DM. The Isolation and Characterization of Murine Macrophages. *Current protocols in immunology / edited by John E Coligan . [et al]*. 2008;CHAPTER:Unit-14.1. doi:10.1002/0471142735.im1401s83.

154.Manabe Y, Miyatake S, Takagi M, et al. Characterization of an Acute Muscle Contraction Model Using Cultured C2C12 Myotubes. Randeva HS, ed. *PLoS ONE*. 2012;7(12):e52592. doi: 10.1371/journal.pone.0052592.

155.Król M, Pawłowski KM, Szyszko K, et al. The gene expression profiles of canine mammary cancer cells grown with carcinoma-associated fibroblasts (CAFs) as a co-culture *in vitro*. *BMC Veterinary Research*. 2012;8:35. doi:10.1186/1746-6148-8-35.

156.Mark W.M. Schellings, Davy Vanhoutte, Geert C. van Almen, Melissa Swinnen, Joost J.G. Leenders, Nard Kubben, Rick E.W. van Leeuwen, Leo Hofstra, Stephane Heymans, Yigal M. Pinto. Syndecan-1 Amplifies Angiotensin II–Induced Cardiac Fibrosis. Hypertension. 2010;55:249-256

157.Ge S, Hertel B, Koltsova EK, et al. Increased Atherosclerotic Lesion Formation and Vascular Leukocyte Accumulation in Renal Impairment are Mediated by Interleukin 17A. *Circulation research*. 2013;113(8):10.1161/CIRCRESAHA.113.301934. doi:10.1161/CIRCRESAHA.113.301934.

158.Faxon DP, Gibbons RJ, Chronos NA, Gurbel PA, Sheehan F. The effect of blockade of the CD11/ CD18 integrin receptor on infarct size in patients with acute myocardial infarction treated with direct angioplasty: the results of the HALT-MI study. J Am Coll Cardiol 2002;40:1199–1204.

159.Attarwala H. TGN1412: From Discovery to Disaster. *Journal of Young Pharmacists : JYP*. 2010;2(3):332-336. doi:10.4103/0975-1483.66810.

160.Lee WW, Marinelli B, van der Laan AM, Sena BF, Gorbatov R, Leuschner F, et al. PET/MRI of inflammation in myocardial infarction. J Am Coll Cardiol. 2012;59:153–163.

161.Cojocaru E1, Trandafirescu M, Leon M, Cotuţiu C, Foia L. Rom J. Morphol Embryol. 2012;53(1):61-6. Immunohistochemical expression of anti-CD68 antibody in atherosclerotic plaque.

162.Micklem K., Rigney E., Cordell J., Simmons D., Stross P., Turley H., Seed B., Mason D. 1989. A human macrophage-associated antigen (CD68) detected by six different monoclonal antibodies. Br. J. Haematol. 73: 6–11

163.Human CD68 promoter GFP transgenic mice allow analysis of monocyte to macrophage differentiation in vivo. Blood. 2014;124(15):e33-e44. doi:10.1182/blood-2014-04-568691.

164.Barone-Rochette G1, Piérard S, Seldrum S, de Meester de Ravenstein C, Melchior J, Maes F, Pouleur AC, Vancraeynest D, Pasquet A, Vanoverschelde JL, Gerber BL. Aortic valve area, stroke volume, left ventricular hypertrophy, remodeling, and fibrosis in aortic stenosis assessed by cardiac magnetic resonance imaging: comparison between high and low gradient and normal and low flow aortic stenosis. Circ Cardiovasc Imaging. 2013 Nov;6(6):1009-17

165.Milano AD1, Faggian G, Dodonov M, Golia G, Tomezzoli A, Bortolotti U, Mazzucco A. Prognostic value of myocardial fibrosis in patients with severe aortic valve stenosis. J Thorac Cardiovasc Surg. 2012 Oct;144(4):830-7.

166. Tahara N, Kudo H, Takemiya K, Koga M, Yamamoto T, Imaizumi T. Pressure-independent effects of angiotensin II on hypertensive myocardial fibrosis. Hypertension. 2004;43:499–503.

167.Mryanda J Sopel, Nicole L Rosin, Timothy DG Lee and Jean-Francois Legare. Myocardial fibrosis in response to Angiotensin II is preceded by the recruitment of mesenchymal progenitor cells. Laboratory Investigation (2011) 91,565–578

168. Kim S, Iwao H. Molecular and cellular mechanisms of angiotensin II-mediated cardiovascular and renal diseases. Pharmacol Rev. 2000 Mar;52(1):11-34.

169.Pinto AR, Paolicelli R, Salimova E, et al. An Abundant Tissue Macrophage Population in the Adult Murine Heart with a Distinct Alternatively-Activated Macrophage Profile. Boone DL, ed. PLoS ONE. 2012;7(5):e36814. doi:10.1371/journal.pone.0036814.

170.Weisheit C, Zhang Y, Faron A, et al. Ly6Clow and Not Ly6Chigh Macrophages Accumulate First in the Heart in a Model of Murine Pressure-Overload. Frangogiannis N, ed. PLoS ONE. 2014;9(11):e112710. doi:10.1371/journal.pone.0112710.

171.Ying X, Lee K, Li N, Corbett D, Mendoza L, Frangogiannis NG. Characterization of the Inflammatory and Fibrotic Response in a Mouse Model of Cardiac Pressure Overload. Histochemistry and cell biology. 2009;131(4):471-481. doi:10.1007/s00418-008-0541-5.

172.Kathryn J. Moore and Ira Tabas. The Cellular Biology of Macrophages in Atherosclerosis

173.Tabas I, García-Cardeña G, Owens GK. Recent insights into the cellular biology of atherosclerosis. *The Journal of Cell Biology*. 2015;209(1):13-22. doi:10.1083/jcb.201412052.

174.Jawien J. The role of an experimental model of atherosclerosis: apoE-knockout mice in developing new drugs against atherogenesis. Curr Pharm Biotechnol. 2012 Oct;13(13):2435-9.

175.Hamilton, J.A. (2008). Colony-stimulating factors in inflammation and autoimmunity. Nature reviews 8, 533-544.

176.Fleetwood, A.J., Lawrence, T., Hamilton, J.A., and Cook, A.D. (2007). Granulocyte-macrophage colony-stimulating factor (CSF) and macrophage CSF-dependent macrophage phenotypes display differences in cytokine profiles and transcription factor activities: implications for CSF blockade in in ammation. J Immunol 178, 5245-5252.

177.Lacey, D.C., Achuthan, A., Fleetwood, A.J., Dinh, H., Roiniotis, J., Scholz, G.M., Chang, M.W., Beckman, S.K., Cook, A.D., and Hamilton, J.A. (2012). Defining GM-CSF- and Macrophage-CSF- Dependent Macrophage Responses by In Vitro Models. J Immunol 188, 5752-5765.

178.Hulsmans M, Sam F, Nahrendorf M. Monocyte and Macrophage Contributions to Cardiac Remodeling. Journal of molecular and cellular cardiology. 2016;93:149-155. doi:10.1016/j.yjmcc.2015.11.015.

179.Lech M, Anders HJ. Macrophages and fibrosis: How resident and infiltrating mononuclear phagocytes orchestrate all phases of tissue injury and repair. Biochim Biophys Acta. 2013 Jul; 1832(7):989-97.

180.Król M, Pawłowski KM, Majchrzak K, Gajewska M, Majewska A, Motyl T. Global gene expression profiles of canine macrophages and canine mammary cancer cells grown as a co-culture in vitro. BMC Veterinary Research. 2012;8:16. doi:10.1186/1746-6148-8-16.

181.McMahon DK, Anderson PA, Nassar R, Bunting JB, Saba Z, Oakeley AE, Malouf NN. C2C12 cells: biophysical, biochemical, and immunocytochemical properties. Am J Physiol. 1994 Jun; 266(6 Pt 1):C1795-802.

182.Kataoka Y, Matsumura I, Ezoe S, Nakata S, Takigawa E, Sato Y, Kawasaki A, Yokota T, Nakajima K, Felsani A, Kanakura Y. Reciprocal inhibition between MyoD and STAT3 in the regulation of growth and differentiation of myoblasts. J Biol Chem. 2003 Nov 7;278(45): 44178-87

183.Lawson MA, Purslow PP. Differentiation of myoblasts in serum-free media: effects of modified media are cell line-specific. Cells Tissues Organs. 2000;167(2-3):130-7.

184.Quintar A, McArdle S, Wolf D, Marki A, Ehinger E, Vassallo M, Miller JF, Mikulski Z, Ley K2, Buscher K3.Endothelial Protective Monocyte Patrolling in Large Arteries Intensified by Western Diet and Atherosclerosis. Circ Res. 2017 Mar 16. pii: CIRCRESAHA.117.310739.

185.Hulsmans M, Sam F, Nahrendorf M. Monocyte and Macrophage Contributions to Cardiac Remodeling. Journal of molecular and cellular cardiology. 2016;93:149-155. doi:10.1016/ j.yjmcc.2015.11.015.

186.Good DW, George T, Watts BA. Toll-like Receptor 2 Is Required for LPS-induced Toll-like Receptor 4 Signaling and Inhibition of Ion Transport in Renal Thick Ascending Limb. *The Journal of Biological Chemistry*. 2012;287(24):20208-20220. doi:10.1074/jbc.M111.336255.

187.Frantz S, Kobzik L, Kim YD, Fukazawa R, Medzhitov R, Lee RT, Kelly RA. Toll4 (TLR4) expression in cardiac myocytes in normal and failing myocardium. J Clin Invest 1999;104:271–280.

188.Oyama J, Blais C Jr, Liu X, Pu M, Kobzik L, Kelly RA, Bourcier T. Reduced myocardial ischemia- reperfusion injury in toll-like receptor 4-deficient mice. Circulation 2004;109:784–789.

189.Riad A, Jager S, Sobirey M, Escher F, Yaulema-Riss A, Westermann D, Karatas A, Heimesaat MM, Bereswill S, Dragun D, et al. Toll-like receptor-4 modulates survival by induction of left ventricular remodeling after myocardial infarction in mice. J Immunol 2008;180:6954–6961.

190.Shishido T, Nozaki N, Yamaguchi S, Shibata Y, Nitobe J, Miyamoto T, Takahashi H, Arimoto T, Maeda K, Yamakawa M, et al. Toll-like receptor-2 modulates ventricular remodeling after myocardial infarction. Circulation 2003;108:2905–2910.

191.Hjortnaes J, Shapero K, Goettsch C, et al. Valvular Interstitial Cells Suppress Calcification of Valvular Endothelial Cells. *Atherosclerosis*. 2015;242(1):251-260. doi:10.1016/j.atherosclerosis. 2015.07.008.

192.Li X-F, Wang Y, Zheng D-D, et al. M1 macrophages promote aortic valve calcification mediated by microRNA-214/TWIST1 pathway in valvular interstitial cells. *American Journal of Translational Research*. 2016;8(12):5773-5783.

193.Urbina P, Singla DK. BMP-7 attenuates adverse cardiac remodeling mediated through M2 macrophages in prediabetic cardiomyopathy. *American Journal of Physiology - Heart and Circulatory Physiology*. 2014;307(5):H762-H772. doi:10.1152/ajpheart.00367.2014.

194.Bornfeldt KE. 2013 Russell Ross Memorial Lecture in Vascular Biology: Cellular and Molecular Mechanisms of Diabetes-Accelerated Atherosclerosis. *Arteriosclerosis, thrombosis, and vascular biology*. 2014;34(4):705-714. doi:10.1161/ATVBAHA.113.301928.

195.Masters SL, Dunne A, Subramanian SL, et al. Activation of the Nlrp3 inflammasome by islet amyloid polypeptide provides a mechanism for enhanced IL-1β in type 2 diabetes. *Nature immunology*. 2010;11(10):897-904. doi:10.1038/ni.1935.

196.Fettelschoss A, Kistowska M, LeibundGut-Landmann S, et al. Inflammasome activation and IL-1β target IL-1α for secretion as opposed to surface expression. *Proceedings of the National Academy of Sciences of the United States of America*. 2011;108(44):18055-18060. doi: 10.1073/pnas.1109176108.

197.Foldi J, Chung AY, Xu H, et al. Autoamplification of Notch signaling in macrophages by TLR-induced and RBP-J-dependent induction of Jagged1. *Journal of immunology (Baltimore, Md : 1950)*. 2010;185(9):5023-5031. doi:10.4049/jimmunol.1001544.

198.Rutz S1, Mordmüller B, Sakano S, Scheffold A. Notch ligands Delta-like1, Delta-like4 and Jagged1 differentially regulate activation of peripheral T helper cells. Eur J Immunol. 2005 Aug; 35(8):2443-51.

199.Kaikita K, Hayasaki T, Okuma T, Kuziel WA, Ogawa H, Takeya M. Targeted deletion of CC chemokine receptor 2 attenuates left ventricular remodeling after experimental myocardial infarction. Am J Pathol 2004;165:439–447.

200.Gu L, Tseng SC, Rollins BJ. Monocyte chemoattractant protein-1. Chem Immunol 1999;72:7–29.

201.Kaikita K, Hayasaki T, Okuma T, Kuziel WA, Ogawa H, Takeya M. Targeted deletion of CC chemokine receptor 2 attenuates left ventricular remodeling after experimental myocardial infarction. Am J Pathol 2004;165:439–447.

202.Salcedo R, Ponce ML, Young HA, Wasserman K, Ward JM, Kleinman HK, Oppenheim JJ, Murphy WJ. Human endothelial cells express CCR2 and respond to MCP-1: direct role of MCP-1 in angiogenesis and tumor progression. Blood 2000;96:34–40.

203.Elena Sierra-Filardi, Concha Nieto, Ángeles Domínguez-Soto, Rubén Barroso, Paloma Sánchez-Mateos, Amaya Puig-Kroger, María López-Bravo, Jorge Joven, Carlos Ardavín, José L. Rodríguez-Fernández, Carmen Sánchez-Torres, Mario Mellado and Ángel L. Corbí. CCL2 Shapes Macrophage Polarization by GM-CSF and M-CSF: Identification of CCL2/CCR2-Dependent Gene Expression Profile. J Immunol. April 15, 2014, 192 (8) 3858-3867; DOI: https://doi.org/10.4049/jimmunol.1302821

204.Ashida N, Arai H, Yamasaki M, Kita T. Distinct signaling pathways for MCP-1-dependent integrin activation and chemotaxis. J Biol Chem. 2001;276:16555–16560.

205. Ushach I, Zlotnik A. Biological role of granulocyte macrophage colony-stimulating factor (GM-CSF) and macrophage colony-stimulating factor (M-CSF) on cells of the myeloid lineage. J Leukoc Biol. 2016 Sep;100(3):481-9. doi: 10.1189/jlb.3RU0316-144R.

206.Boudina S, Abel ED. Diabetic cardiomyopathy, causes and effects. *Reviews in endocrine & metabolic disorders*. 2010;11(1):31-39. doi:10.1007/s11154-010-9131-7.

207.Howard S, Deroo T, Fujita Y, Itasaki N. A Positive Role of Cadherin in Wnt/β-Catenin Signalling during Epithelial-Mesenchymal Transition. Heisenberg C-P, ed. *PLoS ONE*. 2011;6(8):e23899. doi:10.1371/journal.pone.0023899.

208.Maretto S, Cordenonsi M, Dupont S, Braghetta P, Broccoli V, et al. Mapping Wnt/beta-catenin signaling during mouse development and in colorectal tumors. Proc Natl Acad Sci U S A. 2003;100:3299–3304.

209.Chapman DL, Papaioannou VE. Three neural tubes in mouse embryos with mutations in the T-box gene Tbx6. Nature. 1998;391:695–697.

210.Yoshikawa Y, Fujimori T, McMahon AP, Takada S. Evidence that absence of Wnt-3a signaling promotes neuralization instead of paraxial mesoderm development in the mouse. Dev Biol. 1997;183:234–242.

211.Dawkins E, Small DH. Insights into the physiological function of the β-amyloid precursor protein: beyond Alzheimer's disease. *Journal of Neurochemistry*. 2014;129(5):756-769. doi: 10.1111/jnc.12675.

212.Fre S, Pallavi SK, Huyghe M, et al. Notch and Wnt signals cooperatively control cell proliferation and tumorigenesis in the intestine. *Proceedings of the National Academy of Sciences of the United States of America*. 2009;106(15):6309-6314. doi:10.1073/pnas. 0900427106.

213.Steinbach, E.C., and Plevy, S.E. (2014). The role of macrophages and dendritic cells in the initiation of in ammation in IBD. In ammatory bowel diseases 20, 166-175.

214.Udalova, I.A., Mantovani, A., and Feldmann, M. (2016). Macrophage heterogeneity in the context of rheumatoid arthritis. Nat Rev Rheumatol 12, 472-485.

215.Heppner, F.L., Ransohoff, R.M., and Becher, B. (2015). Immune attack: the role of in ammation in Alzheimer disease. Nature reviews Neuroscience 16, 358-372.

216.Lang, R.et al. (2002) Shaping gene expression in activated and resting primary macrophages by IL-10. J. Immunol. 169, 2253–2263

217.Riley JK, Takeda K, Akira S, Schreiber RD. Interleukin-10 receptor signaling through the JAK-STAT pathway. Requirement for two distinct receptor-derived signals for anti-inflammatory action. J Biol Chem. 1999 Jun 4;274(23):16513-21.

218.Leach HG, Chrobak I, Han R, Trojanowska M. Endothelial Cells Recruit Macrophages and Contribute to a Fibrotic Milieu in Bleomycin Lung Injury. *American Journal of Respiratory Cell and Molecular Biology*. 2013;49(6):1093-1101. doi:10.1165/rcmb.2013-0152OC.

219.Carlin LM, Stamatiades EG, Auffray C, et al. *Nr4a1*-Dependent Ly6C^{low} Monocytes Monitor Endothelial Cells and Orchestrate Their Disposal. *Cell*. 2013;153(2):362-375. doi:10.1016/j.cell. 2013.03.010.

220.Brissette M-J, Lepage S, Lamonde A-S, et al. MFG-E8 Released by Apoptotic Endothelial Cells Triggers Anti-Inflammatory Macrophage Reprogramming. Fritz JH, ed. *PLoS ONE*. 2012;7(4):e36368. doi:10.1371/journal.pone.0036368.

221.Rollins BJ. Monocyte chemoattractant protein 1: a potential regulator of monocyte recruitment in inflammatory disease. Mol Med Today 1996;2:198–204.

222.Gu L, Tseng SC, Rollins BJ. Monocyte chemoattractant protein-1. Chem Immunol 1999;72:7–29.

223.Salcedo R, Ponce ML, Young HA, Wasserman K, Ward JM, Kleinman HK, Oppenheim JJ, Murphy WJ. Human endothelial cells express CCR2 and respond to MCP-1: direct role of MCP-1 in angiogenesis and tumor progression. Blood 2000;96:34–40.

224.Kaikita K, Hayasaki T, Okuma T, Kuziel WA, Ogawa H, Takeya M. Targeted deletion of CC chemokine receptor 2 attenuates left ventricular remodeling after experimental myocardial infarction. Am J Pathol 2004;165:439–447.

225.Dobaczewski M, Frangogiannis NG. Chemokines and cardiac fibrosis. *Frontiers in bioscience (Scholar edition)*. 2009;1:391-405.